TR91124
3 JANUARY 1992

MICROWAVE vs OPTICAL CROSSLINK STUDY

FINAL REPORT

PREPARED FOR:

NASA LEWIS RESEARCH CENTER
CLEVELAND, OHIO

PREPARED UNDER:

CONTRACT NUMBER: NAS3-25091

PREPARED BY:

PAULMAN W. KWONG
RONALD C. BRUNO
and
ROBERT G. MARSHALEK
(BALL AEROSPACE)

STANFORD TELECOM®
1761 Business Center Drive ■ Reston, VA 22090 ■ 703/438/8000

TR91124
3 JANUARY 1992

MICROWAVE vs OPTICAL CROSSLINK STUDY

FINAL REPORT

PREPARED FOR:

NASA LEWIS RESEARCH CENTER
CLEVELAND, OHIO

PREPARED UNDER:

CONTRACT NUMBER: NAS3-25091

PREPARED BY:

PAULMAN W. KWONG
RONALD C. BRUNO
and
ROBERT G. MARSHALEK
(BALL AEROSPACE)

STANFORD TELECOM®

1761 Business Center Drive ■ Reston, VA 22090 ■ 703/438/8000

TABLE OF CONTENTS

TABLE OF CONTENTS (Cont'd)

LIST OF EXHIBITS

TABLE OF CONTENTS (Cont'd)

EXHIBIT (Cont'd) **PAGE**

SECTION 1: INTRODUCTION

The intersatellite links (ISLs) at geostationary orbit is currently a missing link in commercial satellite services. Prior studies [1] - [2] have found that potential application of ISLs to domestic, regional, and global satellites will provide more cost-effective services than the non-ISLs systems (i.e., multiple-hop systems). In addition, ISLs can improve and expand the existing satellite services in several aspects. For example, ISLs can conserve the scarce spectrum allocated for fixed satellite services (FSS) by avoiding multiple hopping of the relay stations. ISLs can also conserve prime orbit slot by effectively expanding the geostationary arc. As a result of the coverage extension by using ISLs more users will have direct access to the satellite network, thus providing reduced signal propagation delay and improved signal quality.

Given the potential benefits of ISLs system, it is of interest to determine the appropriate implementations for some potential ISL architectures. Summary of the selected ISL network architectures as supplied by NASA are listed in Exhibit 1-1. The projected high data rate requirements (> 400 Mbps) suggest that high frequency RF or optical implementations are natural approaches. Both RF and optical systems have their own merits and weaknesses which make the choice between them dependent on the specific application. Due to its relatively mature technology base, the implementation risk associated with RF (at least for 32 GHz) is lower than that of the optical ISLs. However, the relatively large antenna size required by RF ISLs payload may cause real-estate problems on the host spacecraft. In addition, because of the frequency sharing (for duplex multiple channels communications) within the limited bandwidth allocated, RF ISLs are more susceptible to inter-system and inter-channel interferences. On the other hand, optical ISLs can offer interference-free transmission and compact sized payload. However, the extremely narrow beam widths (on the order of 10 μrad) associated with optical ISLs impose very stringent pointing, acquisition, and tracking requirements on the system. Even if the RF and optical systems are considered separately, questions still remain as to selection of RF frequency, direct versus coherent optical detection etc. in implementing an ISL for a particular network architecture. These and other issues are the subject of this study.

No.	ISL Architecture	ISL Nominal Range (Degree)	ISL Payload Capacity (Mbps)	Orbit Locations
1	CONUS - 4 Zone Coverage CONUS 1 - CONUS 2 CONUS 2 - CONUS 3 CONUS 3 - CONUS 4	 30 30 30	 7600 10300 20500	49 W TO 143 W
2	CONUS - Europe	50	600	58 W, 8 W
3	ITU Region 1-2-3 Region 1 - Region 2 Region 2 - Region 3 Region 3 - Region 1	 125 125 110	 1400 400 500	 15 E, 110 W 110 W, 125 E 125 E, 15 E

Exhibit 1-1: Selected ISL Network Architectures

1.1 STUDY OBJECTIVE, SCOPE, AND APPROACH

The objective of this study is to investigate and compare RF and optical ISL systems in order to determine the role of each in advanced satellite communication systems. Specifically, six different RF and optical ISL approaches:

- RF at 32 GHz (PSK, uncoded).
- RF at 60 GHz (PSK, uncoded).
- Optical Direct Detection QPPM.
- Optical Direct Detection Subcarrier Intensity Modulation.
- Optical Heterodyne Detection QFSK.
- Optical Homodyne Detection BPSK.

are analyzed and evaluated in order to determine which ISL implementation is best suited for each of the three architectures listed in Exhibit 1-1. Suitability is based on factors such as: ISL payload weight, size, power, cost, pointing/acquisition/tracking (PAT) subsystem requirements, and technological risks. The tasks approach and their relationship are delineated in Exhibit 1-2. Parametric link budget analyses, with technology assessment inputs, and performance requirements are developed. Key system performance issues, such as spatial acquisition and tracking for optical systems, are examined. Weight/size/power estimates of the ISL reference payloads are then generated from various data bases or algorithms. ISL payloads are then optimized in terms of minimum mass (i.e., aperture) and power for a given implementation and architecture. After establishing a set of criteria based on the input budget analyses, weight/size/power estimates and technology assessments, the six implementations are evaluated and a preferred approach is selected for each of the three ISL architectures.

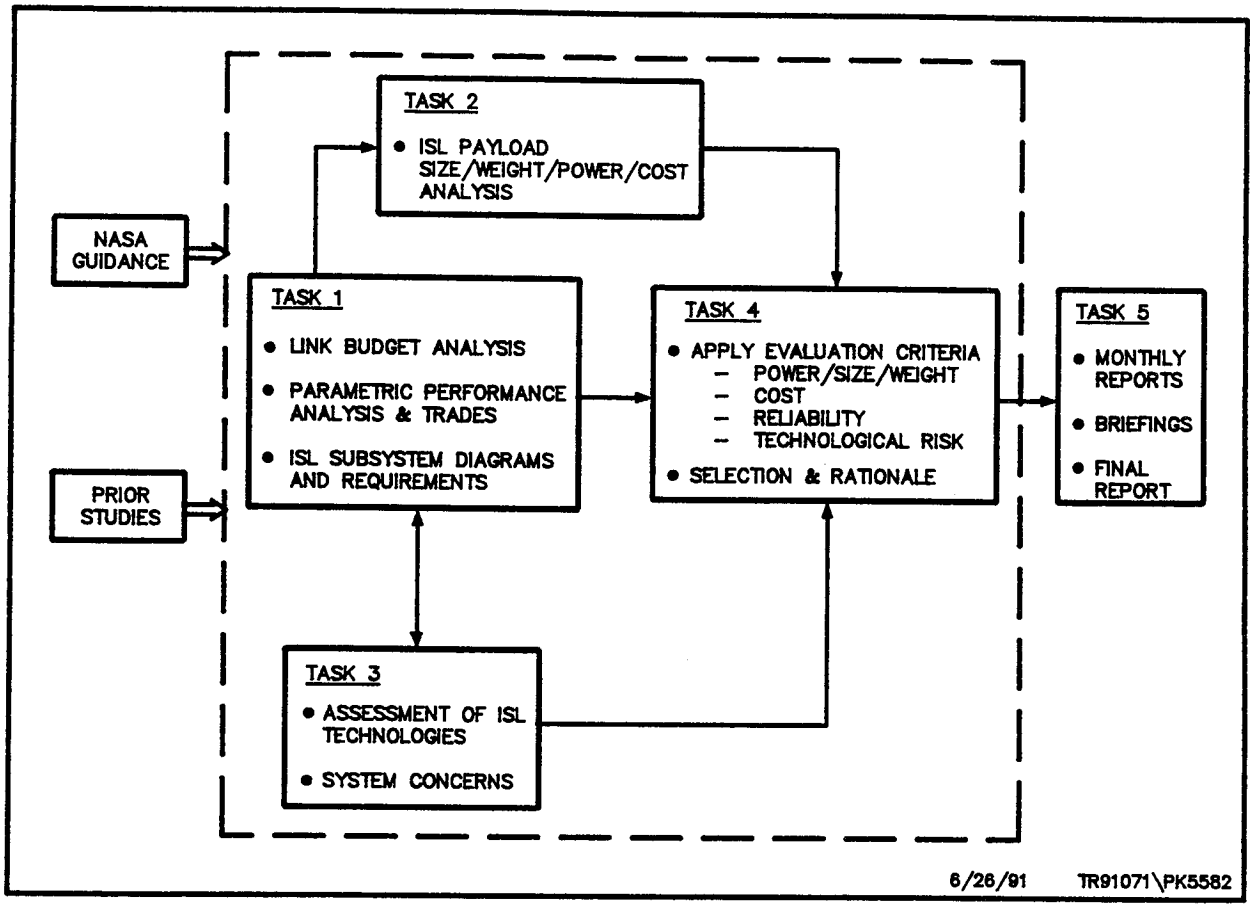

Exhibit 1–2: Task Relationships and Deliverables

1.2 RESULTS SUMMARY AND CONCLUSIONS

The key results of this study are:

- Description of ISL RF and optical implementations:
  - system block diagrams.
  - link budgets.
- Assessment of key components technology for both RF and optical implementations.
- Assessment of key system performance objectives.
- Identification and optimization of key system parameters based on link budget analysis and technology inputs.
  - Estimation of RF and optical payload weight/size/power/cost.
- Evaluation of RF and optical implementations for each of the three ISL architectures.

1.2.1 Description of ISL RF and Optical Implementations

Link budget analysis shown that 5 Gbps envelope data rates per satellite is probably the upper-limit given the technology constraint of key components of both RF and optical implementations. Multiple-channel operation is required in order to accommodate the envelope data rate which ranges from 1.8 Gbps to 5 Gbps (for architecture 1 and 3.) For RF systems, 5 channels and 2 channels (1 Gbps per channel) are required in architecture 1 and 3, respectively. For optical system, as many as 8 channels are needed in architecture 1 in order to make up the lower data rate (625 Mbps) per channel assumed in the implementations. In this study, the RF systems are given higher single-channel data rates mainly because RF technology is more mature than its optical counterpart. However, this assumption is subjected to change when the free-space lasercom technology becomes more mature in the future. In fact, optical systems have the potential of operating at very high data rate (> 1 Gbps) due to its extremely wide bandwidth capacity. The limiting factor are the components technology and the complexity of the systems.

Based on the above envelope data rates assumption, ranges of interest for key systems link parameters have been defined through link budget analysis as shown in Exhibit 1-3.

In multiple-channel operation, frequency division multiplexing (FDM) and wavelength division multiplexing (WDM) are assumed for RF and optical systems, respectively. For the 32-GHz system, spectrum limitation of multiple-channel requires higher order PSK modulation. In general, multiple-channel operation greatly increases the complexity of the systems. Among all the RF and optical implementations, the optical homodyne BPSK system with multiple-channel operation is probably the most challenging to implement due to the limited tunability of Nd:YAG laser. Substantial R&D effort must be taken in order to come up with innovative design for the multiple-channel Nd:YAG homodyne system. Other high power laser sources should also be explored.

ISL Architecture	Implementation	Required Transmit Power (W)	Required Aperture (m)
1	RF	86-114	1.5-1.75
2		16-21	1.5-1.75
3		24-28	3-3.25
1	Optical	.8-8	.08-.29
2		.15-1	.09-.31
3		.3-3	.14-.41

Exhibit 1-3: Ranges of Interest for Key System Link Parameters

1.2.2 Technology Assessment

Technology assessment of major components for both RF and optical systems are summarized in Exhibit 1-4. In general, the RF technology is more mature than the optical technology assuming a technology cut-off date of year 1997. In the commercial arena, 32-GHz technology is probably more mature than the 60-GHz technology. However, certain 60-GHz components have been developed by NASA or the military to an advanced level. One example is the 75-watts 60-GHz TWTA being developed by Hughes and NASA LeRC.

Most of the state-of-the-art optical components are developed either by the various existing lasercom programs (NASA FSDD, MIT-LL LITE, and ESA SILEX) or by the commercial sector. Due to lack of flight experience, very few of these components are actually space qualified. Without performing test and evaluation in space, the technology risk is relatively high for lasercom systems, especially for multiple-channel implementations. However, this picture may change in the next 5-10 years as the various lasercom programs become more mature.

MAJOR COMPONENTS	TECHNOLOGY MATURITY	POTENTIAL TECHNOLOGY GAP
HPA • TWTA • SSPA	• TWTA CAN PROVIDE 100-200 W OF OUTPUT POWER BY YEAR 1997 • CASCADED SSPA CAN GENERATE 10's W OF OUTPUT POWER	• NO GAPS FOR TWTA TECHNOLOGY • SSPA OUTPUT POWER IS NOT ENOUGH FOR ARCHITECTURE 3
RF ANTENNA	• 2-3 m HIGH GAIN 60 GHz ANTENNA IS ANTICIPATED BY YEAR 1997	• NONE FOR ANTENNAS ≤ 3 m
TELESCOPE	• QUALITY TELESCOPE W/RMS WAVEFRONT DISTORTION = WAVELENGTH/10 IS AVAILABLE	• NONE FOR < 20 cm DIAMETER
LASER XMITTER • AlGaAs DIODE AND ARRAYS • Nd:YAG	• SINGLE AlGaAs DIODE HAS OUTPUT POWER OF APPROX. 150 mW • AlGaAs DIODE ARRAYS CAN BE EXPECTED TO GENERATE MORE THAN 1 WATT BY 1997 • Nd:YAG MAY GENERATE A FEW WATTS W/5-10% EFFICIENCY	• HIGH POWER AlGaAs DIODE WITH NARROW LINEWIDTH (< 1 MHz) IS NOT AVAILABLE – REQUIRED FOR HETERODYNE SCHEME
EXTERNAL MODULATOR	• ELECTRO-OPTIC AND WAVEGUIDE MODULATORS W/< 2 dB INSERTION LOSS AND 1 GHz BANDWIDTH ARE COMMERCIALLY AVAILABLE	• CURRENT E-O MODULATORS HAVE LOW SIGNAL POWER CAPABILITY (<300 mW)
POINTING ACQUISITION AND TRACKING SYSTEM	• SUB-MICRORADIAN TRACKING SYSTEMS HAVE BEEN DESIGNED BUT NOT SPACE QUALIFIED	• FLIGHT TEST EXPERIENCE NOT AVAILABLE FOR LASERCOM SYSTEM BUT PRECISION TRACKING ON BOARD OTHER SYSTEMS (I.E., HUBBLE TELESCOPE) HAVE BEEN DEMONSTRATED
PHOTODETECTOR	• QUALITY DETECTORS W/HIGH QUANTUM EFFICIENCY ARE AVAILABLE	• NONE
OPTICAL FREQUENCY & PHASE TRACKERS	• UNDER DEVELOPMENT BY MIT-LL AND OTHER EUROPEAN LABS	• FLIGHT TEST EXPERIENCE NOT AVAILABLE

Exhibit 1-4: Technology Assessment

1.2.3 Assessment of Key System Objectives

Three major system issues were considered in this study:

1. Spatial Acquisition for optical systems problem: ISL platform attitude uncertainty (few μrad) > 5 μrad transmit beamwidth of 20 cm telescope; initial acquisition scenario required for reduced initial pointing uncertainty; acquisition should be robust and quick (< 1 minute.)

2. Spatial tracking for optical systems problem: ISL platform jitter (approximately 10 μrad rms) > 5 μrad transmit beamwidth of 20 cm telescope thereby resulting in a fading channel with degraded BER; spatial tracking control system required; tracking must be robust and should be eliminate major fading channel effects.

3. Phase noise in carrier for coherent optical and high frequency RF systems problem: phase noise can seriously degrade BER of coherent systems; transmitter with low phase noise are required.

Spatial Acquisition

Prior study [3] had identified an efficient acquisition scheme which proceeds as follow:

- Receiver FOV encompasses initial pointing uncertainty.
- Transmitter broadens beam to a few hundred mrad and scans its pointing uncertainty FOV.
- receiver detects transmit beam and responds with similar beacons.

Successful completion of this acquisition scenario in < 1 minute requires a minimum power collected by the receiver aperture. For example, for a ISL GEO-GEO separation of 40,000 km, and receiver aperture of 20 cm, the required transmit power for acquisition is roughly 30 mW with 6 dB margin. This level of transmit power can be easily provided by the same laser used in communication mode.

Spatial Pointing/Tracking

Spatial pointing/tracking error mainly comes from two sources: 1) relative motion and on-board mechanical vibration of platform, and 2) tracking sensor noise. In the presence of tracking error, higher transmit power is required to achieve the same BER performance (as the jitter-free case). Well-designed servo tracking system can be expected to reduce the tracking error of about 11 μrad (based on LANDSAT data) to 0.5-1 μrad. Although an optimum transmitter gain (or aperture size) can be selected to minimize the required transmitter power for the desired BER given certain off-point jitter and bias, fading channel analysis indicates that a smaller (than optimal) aperture is desirable in order to avoid significant fading.

Phase Noise

Phase noise in semiconductor lasers has two effects on signal quality of coherent optical system: signal attenuation or suppression, and crosstalk (signal distortions.) The combined effect contributes to SNR reduction, and consequently, BER degradation. Laser linewidth of 1-10 MHz is desirable for QFSK heterodyne system operating between 100 Mbps and 1 Gbps in order to limit phase noise degradation to < 0.5 dB. For the homodyne BPSK system using Nd:YAG laser which has line width ≤ 1 KHz, the impact of phase noise is negligible when the system is operating at 100 Kbps or above.

Phase noise in RF systems are typically caused by the instability of various oscillators used to generate carrier and mixing frequencies, and thermal noise. For a well-designed tracking loop (e.g., phase-locked-loop) operating at reasonable bandwidth, RMS phase error of a few degrees can be expected. As a result, < 1 dB additional power is typically required to maintain 10^{-6} BER as compared to zero phase error system.

1.2.4 Definition and Optimization of ISL RF and Optical Payloads

With inputs from the data bases developed in the ATDRSS Phase A Definition studies (for RF payload) and various lasercom programs (for optical payload), weight/size/power estimation were performed. Detailed results are presented in APPENDIX B, and the range of interest of these estimates are listed in Exhibit 1-5.

Payload mass and power models were developed using COMSAT and Ball Aerospace antenna mass model and other parametric results. Based on these models, antenna/telescope size can be selected to minimize the payload mass and power. Preliminary results indicated that antenna size of 1.25 - 2.5 meters minimizes the payload mass of the 32-GHz and 60-GHz systems for all architectures (assuming that appropriate transmitters are available.) A larger aperture (than this range) involves higher technological risks while smaller apertures tend to increase payload mass rapidly.

Similarly, optimization results for the DD/QPPM system indicated that 16 - 20 cm aperture tends to minimize payload mass of architectures 1 and 2 while payload mass of architecture 3 is optimized at around 27 cm. Aperture size larger than 20 cm involves higher technological risks and a demanding PAT subsystem.

With optimized link parameters and payload weight/size/power as inputs, cost estimation was performed by Ball Aerospace in the following procedures:

- Identify cost drivers and risk factors.
- Identify and apply parametric cost models to RF and optical implementations.
- Provide round-figure cost estimates for single-channel, 30-degree RF and optical links.
- Provide relative normalized cost estimates for all other links.

The major issues associated with ISL payload cost estimation are:

- Cost estimates generated by parametric models have low confidence level (especially for optical systems) due to limited flight experience.
- Reliability concern can have a great impact on final cost.

ISL Architec-ture	Implementation	Weight (lb)	Aperture Size (m)	Power (w)
1	RF	171 -407	1.5 - 1.75	126 - 500
2		165 - 182	1.5 - 1.75	136 - 151
3		246 - 380	3 - 3.25	239 - 430
1	Optical	164 - 900	0.08 - 0.29	133 - 445
2		163 - 244	0.09 - 0.31	120 - 171
3		165 - 500	0.14 - 0.41	145 - 418

Exhibit 1-5: Range of Interest for Payload Envelope Parameters

Key conclusions on cost estimation are:

- In general, given the technology cut-off date of 1997, the RF implementations (32 GHz and 60 GHz) are more cost-effective than their optical counterparts. The difference is mainly driven by relative technical maturity.

- Multiple-channel high data rate operation significantly increases technological risks and payload weight/size/power, and consequently, cost in both RF and optical systems.

- Cost estimates should only be viewed as qualitative trend indicators.

1.2.5 Evaluation of ISL Implementations

With inputs from link budget analysis, technology assessment, weight/size/power/cost estimations, and system optimizations, number score are assigned to each evaluation criteria for all implementations in each architecture. Based on the results presented in Section 7, the following observations can be made:

- In general, RF systems perform better than optical systems in all 3 ISL architectures.
  - The difference is driven mainly by technical maturity.
  - However, 32-GHz multiple-channel operation requires high order PSK modulation which results in highly complex system.
- For long crosslink with single or few channels, heterodyne QFSK system and DD/QPPM system both look like viable alternative to RF systems.
- Optical homodyne BPSK system is the least favorable implementation due to high technology risk in its key components (1997 is too early for homodyne).
- Successful demonstration of the European test-bed program may reduce the risk.
  - Homodyne system potentially can deliver great benefits in a later date.

SECTION 2: DESCRIPTION OF ISL ALTERNATIVES

The six ISL implementation considered are defined in Exhibit 2-1a. Each of the six RF and optical ISL implementations has its own distinctive features which are summarized in Exhibit 2-1b. For the two RF systems (32 GHz and 60 GHz), the implementations are similar. Both systems require relatively large antenna sizes (1 - 3 m) and high transmit power as compared to optical systems. However, the relatively large transmit beam widths (3 - 6 μrad) of these systems imply a less demanding PAT subsystem. Both RF systems are applicable to regenerative (baseband) and non-regenerative (IF) signals. On the other hand, the four optical implementations have some common features as well as major differences. All four systems require only modest antenna (telescope) apertures (10 - 30 cm) and low transmit power. These optical implementations also have very low cross-system interference. However, the narrow transmit beam widths (5 - 10 μrad common to these systems) impose a rather stringent PAT subsystem requirement (e.g., tracking in the sub-microradian range.) Both Direct Detection PPM and Subcarrier Intensity Modulation (SIM) are noncoherent schemes which detect energy directly on the detectors. In other words, these approaches do not carry any frequency/phase information on the optical carrier. On the other hand, the heterodyne FSK and homodyne PSK systems are coherent schemes which modulate the frequency or phase of the optical carrier by the input data. The data is recovered by mixing the carrier (with a optical local oscillator) to either IF or baseband prior to detection by a PIN diode. Among the four optical systems, SIM is the only analog non-regenerative implementation. The homodyne BPSK system uses diode-pumped Nd:YAG laser (wavelength = 1064 nm) as transmitter. The other three optical systems use AlGaAs laser diode (wavelength = 860 nm) as transmitter.

Simplified block diagrams for each of the six implementations are presented in Exhibit 2-2 to 2-6. The diagrams are composed of individual modules which are at a level suitable for weight/size/power estimations. It should be emphasized that the configurations shown in these figures do not represent the optimal nor the only possible designs of RF and optical implementations. They simply represent reference system designs which are in line with those state-of-the-art RF and optical implementations (e.g., optical DD-PPM system under development by NASA GODDARD.) Each block diagram will be briefly described below.

Note that all block diagrams depict multiple-channel systems which reflect an approach to accommodate the high envelope data rates (> 1.8 Gbps) required by ISL architectures 1 and 3 . It will be shown later that the allowable number of channels is limited by the bandwidth allocated and technology constraints. Frequency division multiplexing (FDM) and wavelength division multiplexing (WDM) are assumed for RF and optical multiple-channel systems, respectively.

- RF System
  - 60 GHz:
    - Uncoded data or IF waveform modulates RF carrier by shifting it to one of 4 phases (i.e., QPSK)
  - 32 GHz:
    - Uncoded QPSK modulation for single-channel operation
    - Higher order modulation for multiple-channel operation
- Optical System
  - Direct Detection quaternary pulse position modulation (DD/QPPM):
    - Input data switches laser diode (LD) on during 1 of 4 time slots
    - Direct energy detection of baseband optical signals noncoherently
  - Direct detection subcarrier intensity modulation (DD/SIM):
    - Analog MOD/DEMOD of IF waveform signal noncoherently
    - Optional FM on subcarrier for SNR improvement
  - Heterodyne quaternary frequency shift keying (HET/QFSK):
    - Frequency modulated data on optical carrier
    - Mixed to IF at receiver and demodulated to baseband
  - Homodyne binary phase shift keying (HOM/BPSK):
    - Phase modulated data on optical carrier
    - Mixed to baseband at receiver

Exhibit 2-1a: Alternative Crosslink Systems Considered

<table>
<tr><td rowspan="4">Unique Features</td><td rowspan="2">60-GHz</td><td rowspan="2">• Sufficient spectrum available to support multiple-channel system</td><td>DD/QPPM</td><td>• Simplest optical implementation</td></tr>
<tr><td>DD/SIM</td><td>• The only non-regen (i.e., bent-pipe) optical implementation)</td></tr>
<tr><td rowspan="2">32-GHz</td><td rowspan="2">• Spectrum limitation of multiple channel system requires higher order PSK modulation (e.g., 8 PSK)</td><td>HET/QFSK</td><td>• Requires narrow line width laser diode for phase noise reduction</td></tr>
<tr><td>HOM/BPSK</td><td>• Requires external modulator
• The only optical scheme using Nd:YAG laser</td></tr>
<tr><td>Common Features</td><td colspan="2">• Large XMIT beam width (3-6 μrad) → relatively easy pats
• Relatively large antenna size (1-3m)
• High xmit output power system
• Potential cross-system interference
• Applicable to regen and nongen
• Frequency division multiplexing (FDM) is assumed for multiple-channel implementations
• Duplex communication by dual frequency polarization</td><td colspan="2">• Small antenna (telescope) size (10-30 cm)
• Narrow xmit beam width (5-10 μrad) → demanding pats
• Low xmit output power system → XMTER output power not a major driver for system prime power
• Very low cross-system interference
• Wavelength division multiplexing (WDM) is assumed for multiple-channel implementations
• Duplex communication by using different wavelength each way.</td></tr>
</table>

Exhibit 2-1b: Key Distinguishing Features of Alternative XL Systems

In order to ensure reliable communication between the satellite terminals, it is important to identify performance requirement issues for key components/subsystems. Summary of these performance issues for RF antenna, high power amplifier and low noise amplifier are listed in Exhibit 2-2. Performance issues for key optical components are listed in Exhibit 2-3. Specific performance parameters will be identified in the subsequent sections (i.e., link budget analyses and technology assessment) of this report. The choice of parameters will have direct impact on the ISL payload definition.

Components/Subsystems	Performance Requirements Issues
High Power Amplifier	• Output Power • Reliability • Efficiency • Phase Noise • Bandwidth
Low Noise Amplifier	• Noise Figure • Bandwidth • Gain • Reliability
Antenna	• Gain • Loss • Ruggedness

Exhibit 2-2: Performance Requirement Issues for RF Systems

Components/Subsystems	Performance Requirement Issues		
	Direct Detection*	Heterodyne**	Homodyne**
AlGaAs Laser Diode Xmitter	• Output Power • Efficiency • Reliability	• Output Power • Linewidth • Efficiency • Reliability	NA
Nd:YAG Laser Xmitter	NA	NA	• Output Power • Linewidth • Efficiency • Reliability
APD	• Quantum Efficiency • Noise Figure	NA	NA
Current Driver	• Current Capability • Bandwidth	NA	NA
External Modulator	NA	NA	• Bandwidth • Insertion Loss • Input Power
Tracking/Pointing System	Sub-Microradian Performance		

* Digital and Waveform SIM

** Digital Only

Exhibit 2-3: Performance Requirement Issues for Optical Systems

2.1 RF ISL COMMUNICATION TRANSCEIVER (32 GHZ AND 60 GHZ)

The implementations for both 32 GHz and 60 GHz systems are similar and therefore only one block diagram is presented. As shown in Exhibit 2-4, modulated baseband signal or IF waveform is upconverted to the carrier frequency, bandpass filtered, amplified by the HPA and transmitted through the high gain antenna. On the receiver side, the signal is detected by the low noise amplifier and then down mixed back to IF and demodulated (in the case of regenerative system) to baseband. In this system, uncoded QPSK signal is assumed in order to conserve bandwidth and to avoid code-driven complexity and speed. The pointing of the antenna is accomplished by the automatic control of a gimbal system.

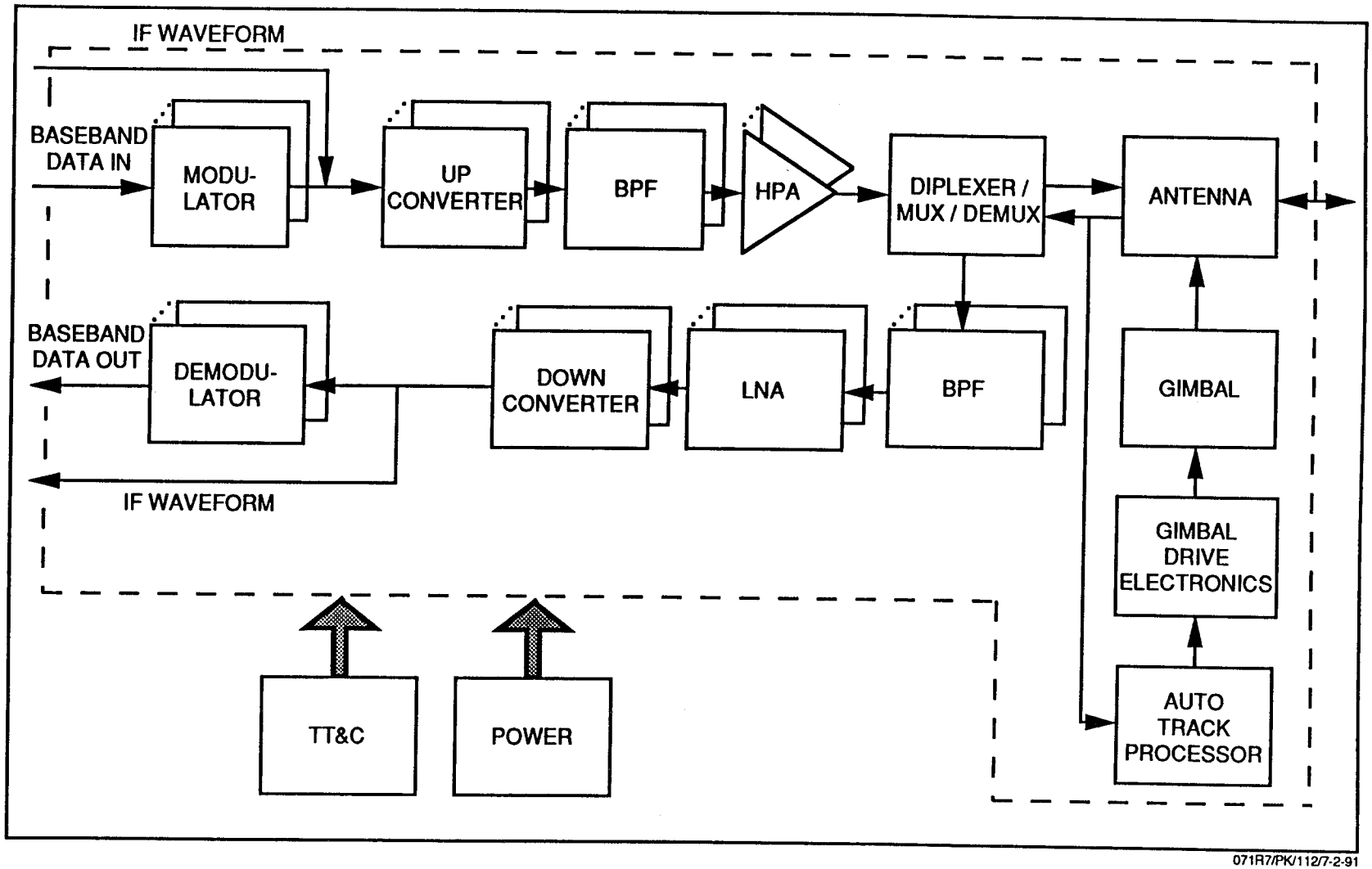

Exhibit 2-4: RF ISL Communication Transceiver

2.2 PULSE POSITION MODULATION/DIRECT DETECTION LASERCOM TRANSCEIVER

The operation of this type of lasercom system is well known and has been discussed in great details by many authors [4] - [6]. Ground and flight demonstration systems are being developed by both NASA GSFC (FSDD programs) and ESA (SILEX program.) Japan is also developing a DD/BPPM system for future flight testing. Upon completion of spatial acquisition, communication begins with the input of baseband data which control the timing of the current pulses sent by the laser driver. For example, for BPPM, a "1" is represented by sending a pulse at the first time slot and a "0" is a pulse at the second slot. In response to these current fluctuations, the laser transmitter outputs optical pulses (i.e., pulse position modulation) accordingly. The resulting laser beam is then collimated and transmit through the telescope to the cooperating terminal. The received signal is optically bandpass filtered and is detected by a photodetector and preamplifier. The baseband data is finally recovered by the PPM demodulator. One key element in this (and other) optical implementation is the pointing/acquisition/tracking control subsystem. As mention above, due to the narrow beam width (5 - 10 urad) of optical system, the PAT function is very demanding. The performance requirement of PAT subsystem will be assessed in Section 5.

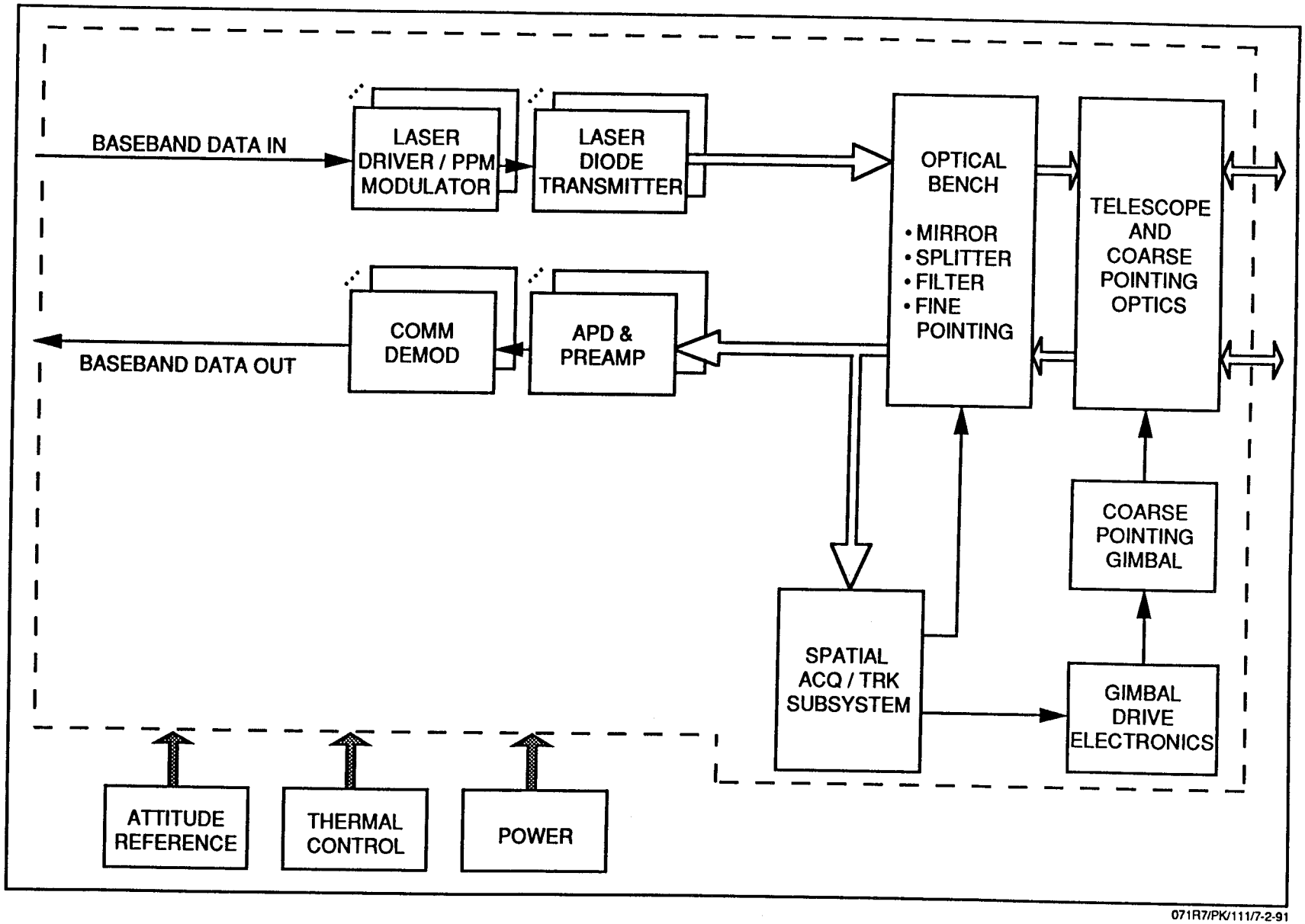

Exhibit 2-5: Laser Diode Based Direct Detection Lasercomm Transceiver

2.3 SUBCARRIER INTENSITY MODULATION/DIRECT DETECTION LASERCOM TRANSCEIVER

As shown in Exhibit 2-6, the configuration of this system is almost identical to that of the DD/PPM system except that the input/output data are IF waveforms instead of baseband signal. This implementation eliminates the need for modulation/demodulation of input/output data. As a result, the SIM transceiver structure is simpler than the other three optical implementations. However, for high and variable data rate applications, the performance of DD/SIM system is typically 12 dB worse than that of DD/PPM system (FM on subcarrier may improve performance by ~ 5.5 dB but at the expense of a more complex system.) In other words, if all other parameters are the same for both systems, DD/SIM will need transmit/receive antenna size four times that of DD/PPM. Consequently, the PATs requirements become very stringent due to the resulting narrow beam width (which is inversely proportional to antenna size.) Since antenna and PATs are the main drivers for weight/size/power/cost of optical systems, DD/SIM implementation is probably not suitable for the high data rate ISL applications considered herein.

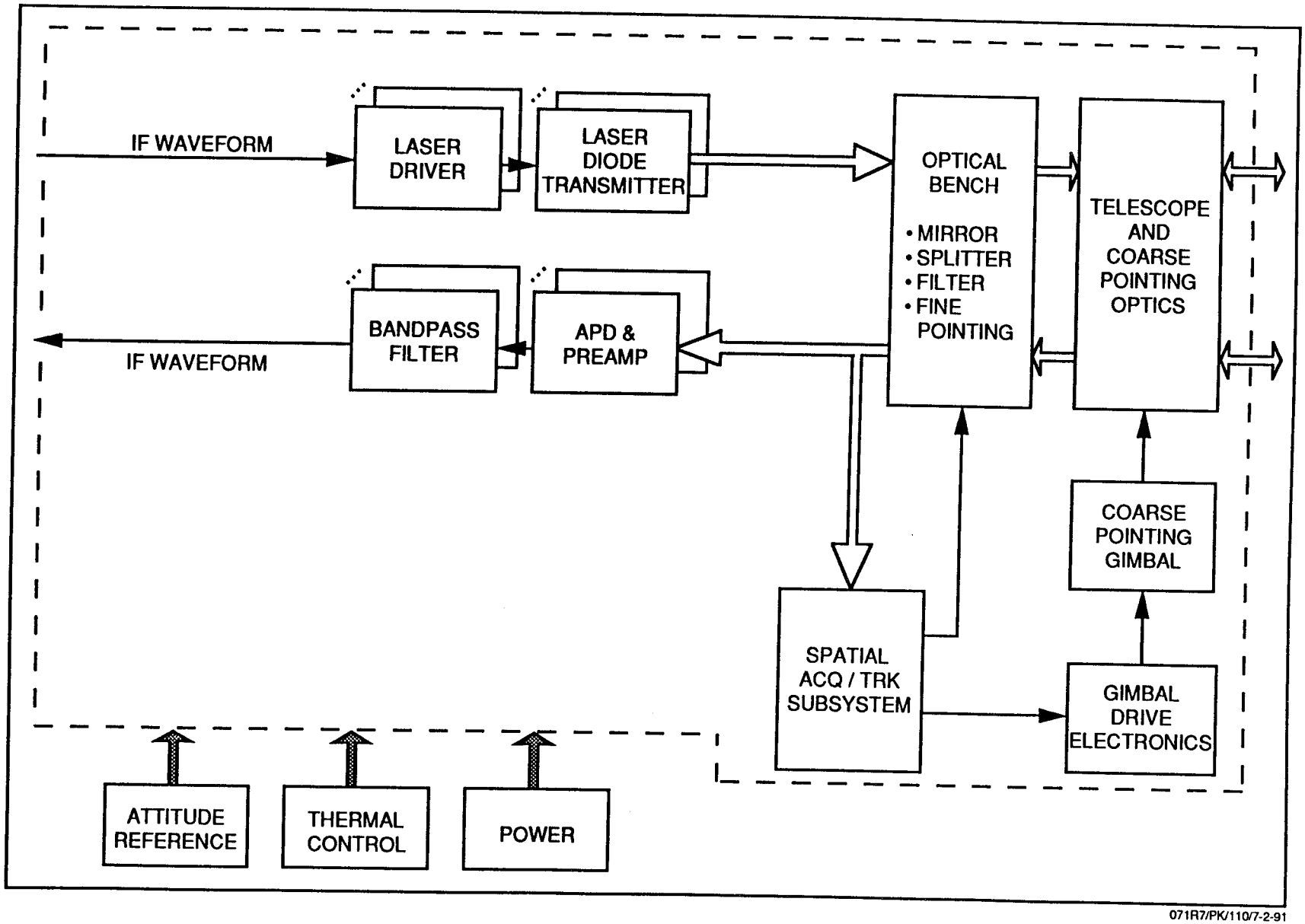

Exhibit 2-6: Subcarrier Intensity Modulation / Direct Detection Lasercomm Transceiver

2.4 HETERODYNE DETECTION LASERCOM TRANSCEIVER

Heterodyne FSK system similar to the one depicted in Exhibit 2-7 has been developed by MIT-Lincoln Laboratory [7]. In this implementation, the optical carrier (laser transmitter output) is frequency modulated by the input data through a FSK mod/equalize current driver. On the receiver side, the received laser beam is mixed with an optical local oscillator to IF prior to photodetection. The resulting (electrical) signal is then bandpass filtered and demodulated for data recovery. To maintain IF stability, the receiver LO laser must be frequency tracked with the incoming signal by using a Frequency Locked Loop (FLL). The PAT subsystem is similar to the one employed in the direct detection systems.

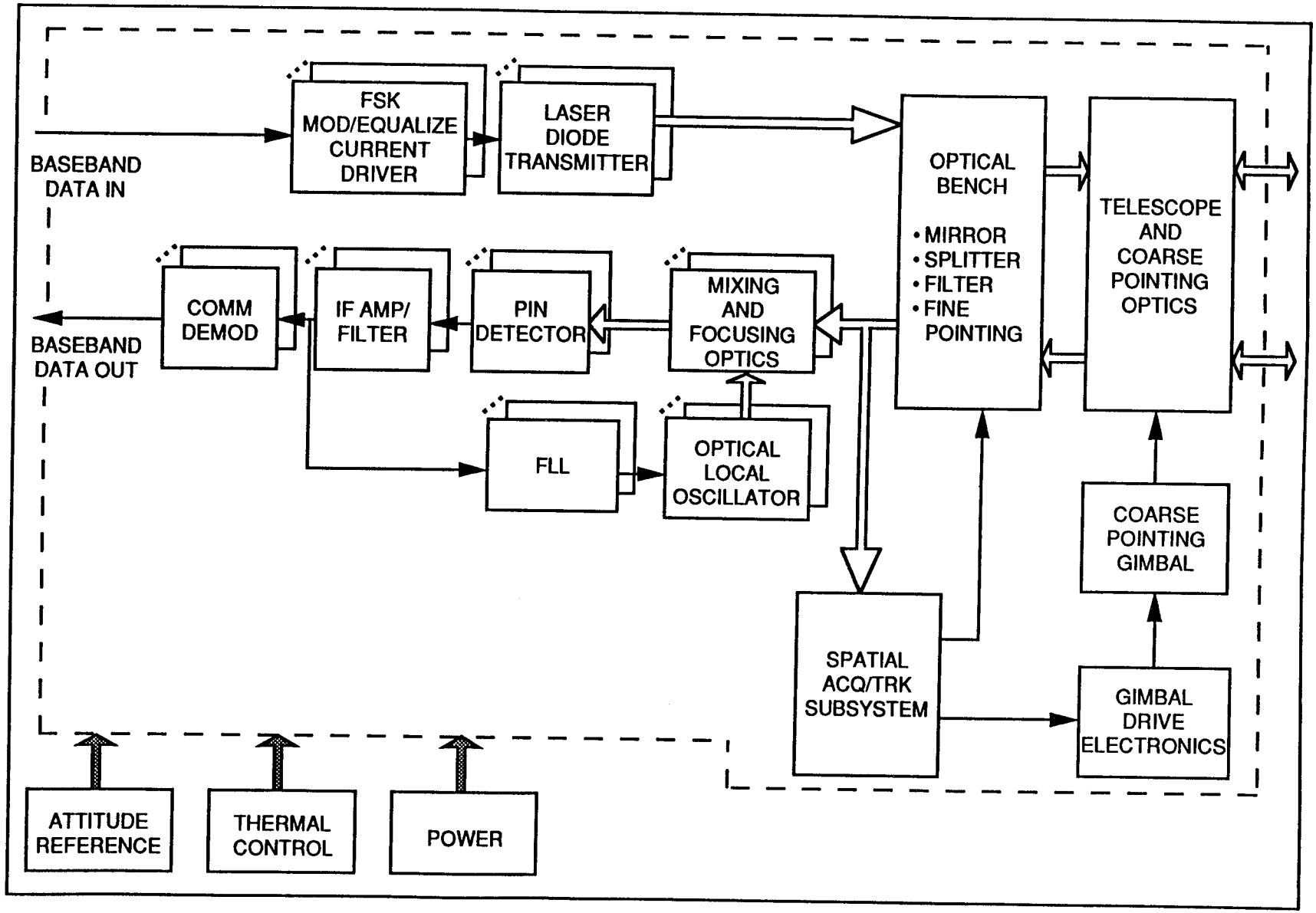

Exhibit 2-7: Laser Diode Based Heterodyne Detection Lasercomm Transceiver

2.5 HOMODYNE DETECTION LASERCOM TRANSCEIVER

Single-channel ISL homodyne BPSK test-bed system similar to the one considered for ISL architecture 2 is under development by the Europeans [8]. However, in order to accommodate the high envelope data rates of architectures 1 and 3, a multiple-channel system is assumed in Exhibit 2-8. As shown in the block diagram, the diode-pumped Nd:YAG laser is phase modulated by the input data through an external modulator. The homodyne detection process is similar to that of the heterodyne except that the received laser beam is down mixed to baseband directly in this case. The phase of the optical LO is locked onto that of the incoming signal by using a phase locked loop (PLL).

Although a multiple-channel system is illustrated in the figure, it will be discussed later that the actual implementation of this system is very difficult due to the limited tunability of the Nd:YAG laser transmitter. Substantial R&D effort is required in order to reduce the technology risk of the multiple-channel implementation.

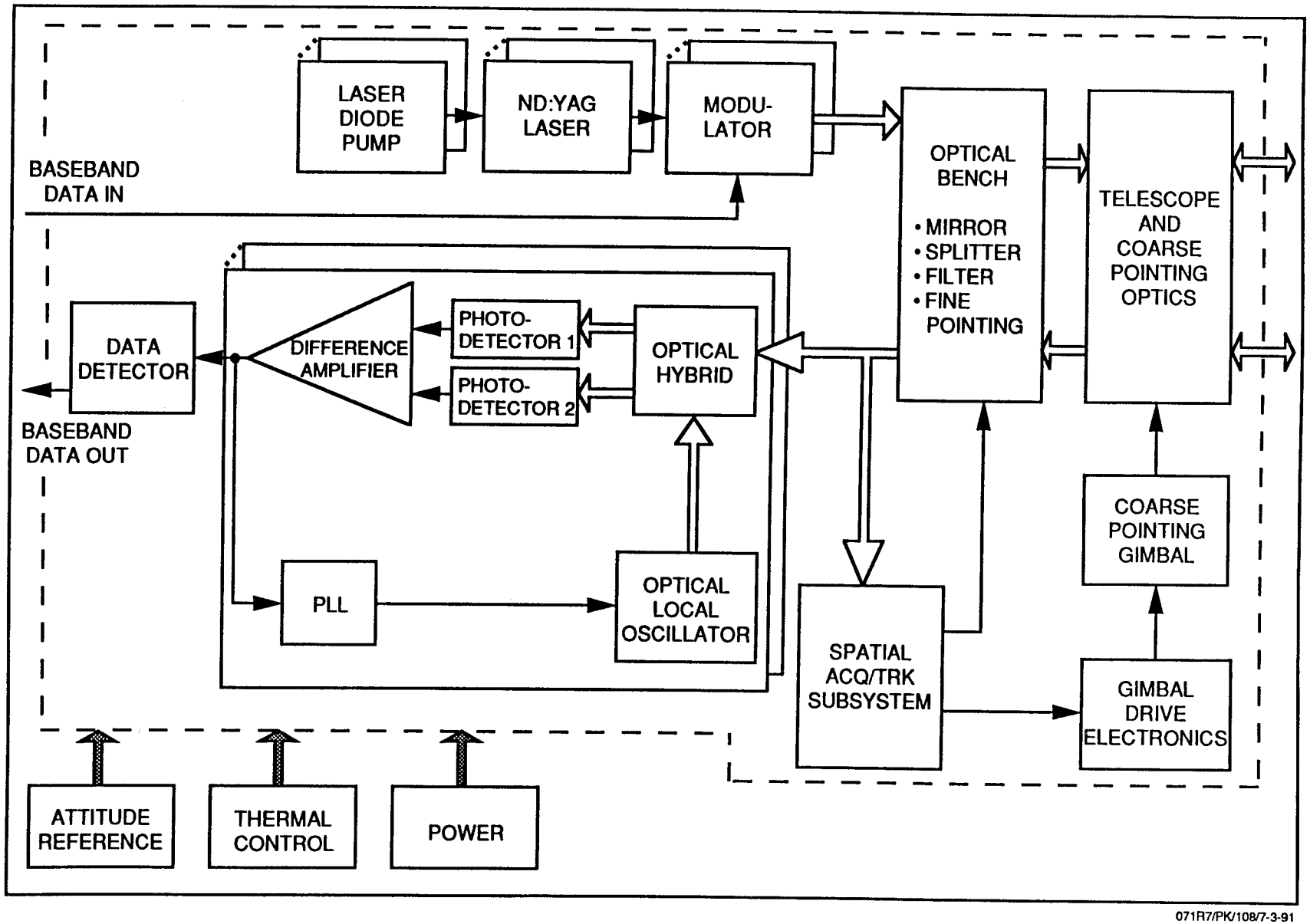

Exhibit 2-8: Nd:YAG BPSK Homodyne Detection Lasercomm Transceiver

SECTION 3: PARAMETRIC LINK ANALYSIS

Reference link budgets as well as parametric curves are developed to provide a point of departure for transmit power versus aperture trades. These link budgets also established an initial performance goals that guide the technology assessments of key components and provided inputs for identifying system-wide issues (e.g., PAT). Specific link budgets, and the equations which generate them are presented in Appendix A. In this section, focus will be on the parametric results of transmit power versus aperture trades.

There are several key assumptions for RF and optical link analyses. For RF systems, uncoded QPSK modulation is assumed in order to conserve bandwidth and to avoid code-driven complexity and speed. For direct detection optical systems, BPPM or QPPM yield best performance given AlGaAs laser diode's peak and average power constraints. In addition, AlGaAs peak and power constraints eliminate On-Off Keying (OOK) as an implementation option. For coherent heterodyne system, 2-FSK or 4-FSK implementation is assumed and is consistent with the MIT-LL design. Heterodyne PSK is not considered due to its severe phase noise problem and complexity.

In order to provide a more realistic definition for the ISL payload, channelization is performed on the envelope data rate requirement of the three ISL architectures. The results are presented in Exhibit 3-1. The channelization is based on the following assumptions:

- 5 Gbps is the maximum trunk capacity for a commercial satellite.
- 1 Gbps is the highest achievable channel data rate for RF systems, and 625 Mbps is the maximum realizable channel data rate for optical systems.

Salient parameters of RF and optical systems for generating link budgets and parametric curves are given in the link budgets in Appendix A.

Based on the above assumptions and parameters, parametric curves of the six alternative implementations for ISL architecture one, two, and three are developed and presented in Exhibit 3-2, 3-3, and 3-4, respectively. From these curves, key trade space items for optical and RF implementations can be identified and are summarized in Exhibit 3-5. The trades among the six alternative implementations need further refinement with technology inputs and other considerations such as cost and mass minimization. Such detail payload definition will be performed in Section 6.

ISL Architecture	Envelope Data Rate Requirement	Channelization*	
		RF	Optical
1	7.6 Gbps	5 x 1 Gbps	8 x 625 Mbps
	10.3 Gbps	5 x 1 Gbps	8 x 625 Mbps
	20.5 Gbps	5 x 1 Gbps	8 x 625 Mbps
2	600 Mbps	1 x 625 Mbps	1 x 625 Mbps
3	1.4 Gbps	2 x 1 Gbps	3 x 625 Mbps
	400 Mbps	1 x 1 Gbps	1 x 625 Mbps
	500 Mbps	1 x 1 Gbps	1 x 625 Mbps

* Assume 5 Gbps is the maximum trunk capacity per satellite

Exhibit 3-1: Channelization of ISL Envelope Data Rate Requirement

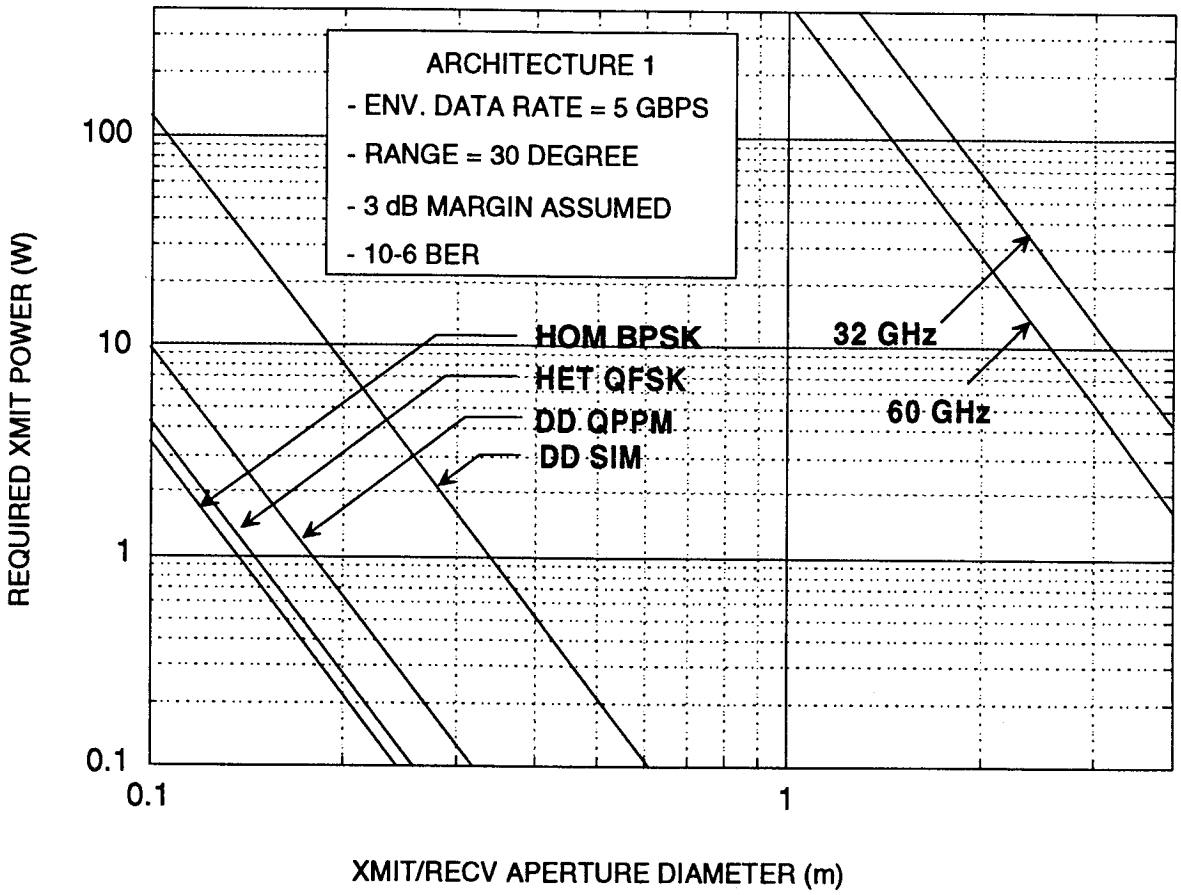

Exhibit 3-2: Required Power vs Antenna Size for Arch. 1

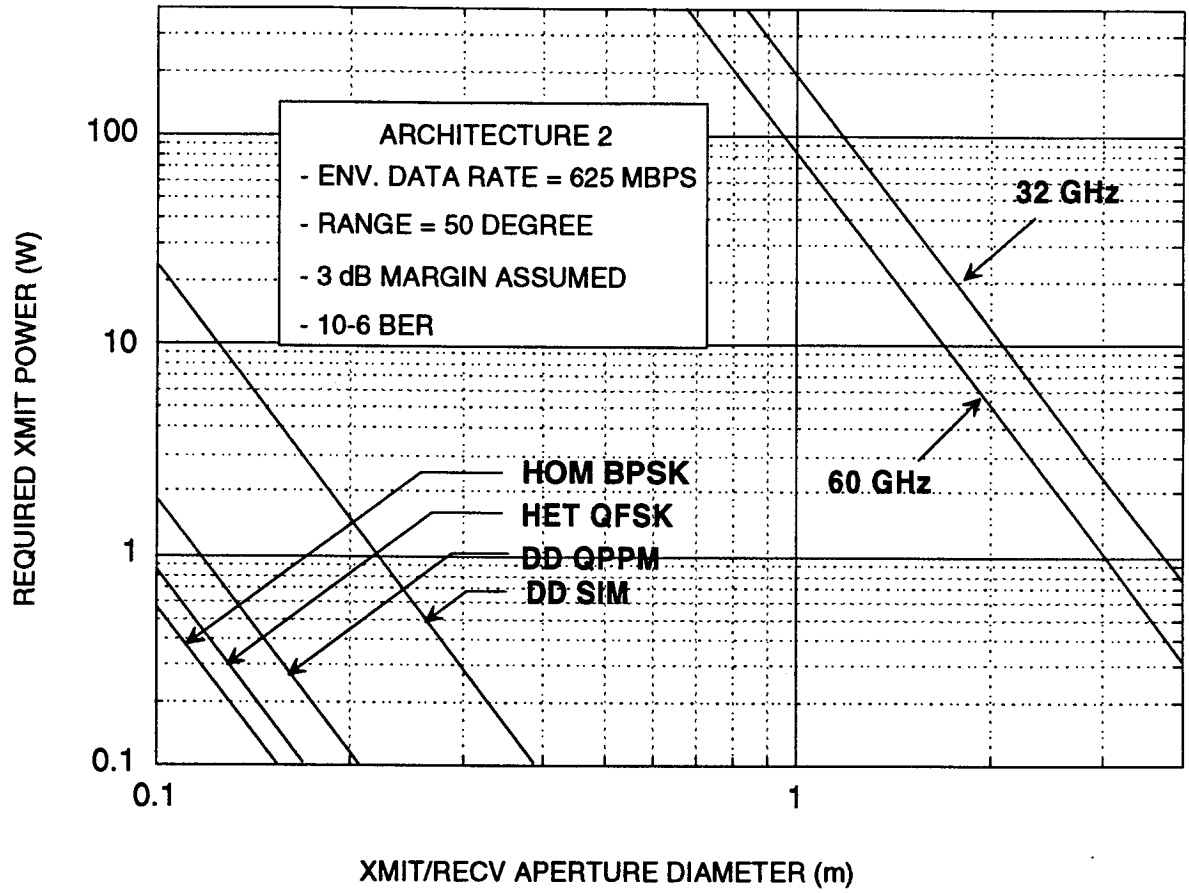

Exhibit 3-3: Required Power vs Antenna Size for Arch. 2

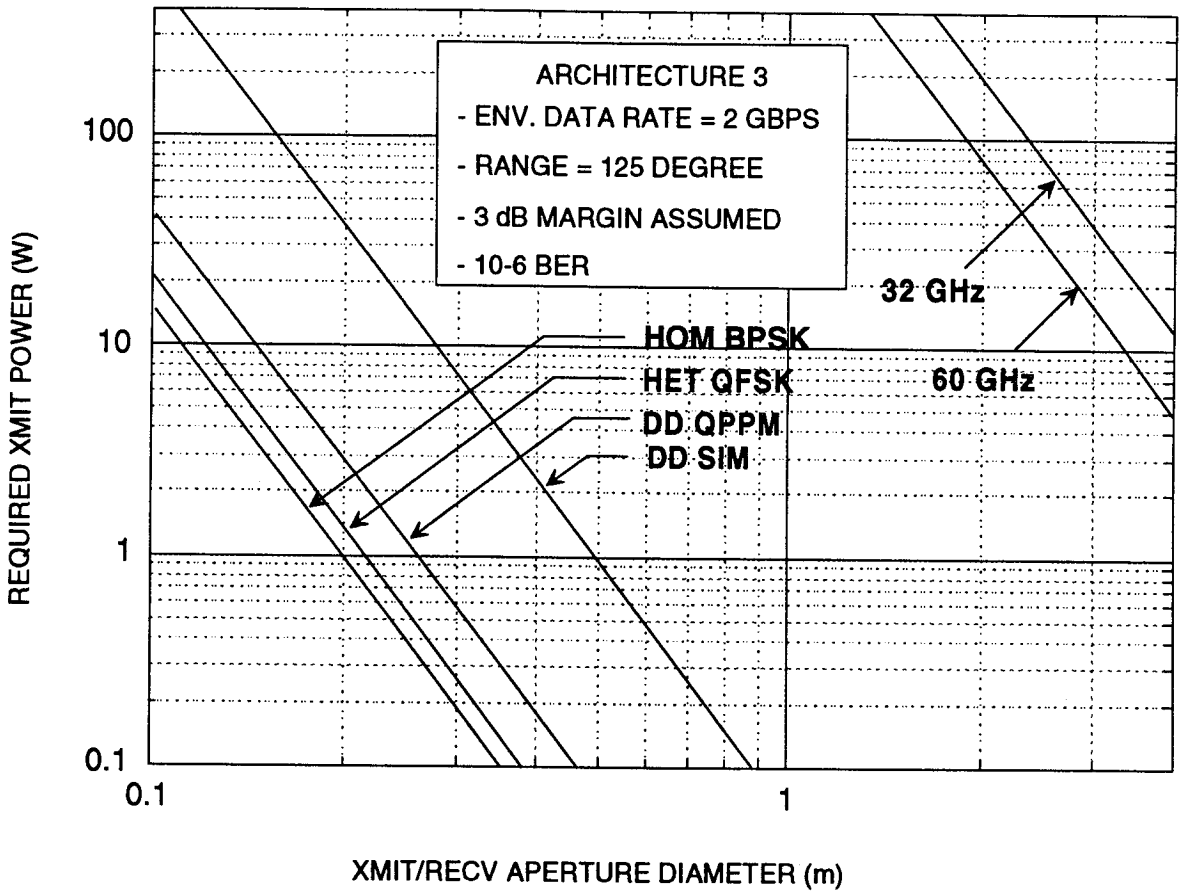

Exhibit 3-4: Required Power vs Antenna Size for Arch. 3

- Optical Implementations: Key trade space items include XMIT/RCV Aperture, XMIT Power and overall RCVR sensitivity
  - Analog SIM Requires ≈ 15 times (12 dB) more power than DD/PPM
    - ♦ FM on subcarrier can have ≈ 5.5 dB improvement at the expense of a more complex system
  - Multiple channels needed to overcome component limitations relative to bandwidth and available coherent power
  - Improvements/Uncertainties in the performance of key components (Diode or Nd:YAG phase noise, APD noise figure) tend to blur the performance differences between DD, HET and HOM
- RF Implementations: Key trade space items include XMIT/RCV aperture and XMIT power
  - Multiple channels needed to overcome component limitation

Exhibit 3-5: Key Trade Space of Parametric Analysis

SECTION 4: TECHNOLOGY ASSESSMENT OF KEY COMPONENTS

Technology needs are driven by channel power requirement of the specified ISL implementations. Technology assessment includes current and projected (year 1997) status of key components technology. The availability, efficiency, and reliability of technologies will also be assessed. The following major RF and optical components are examined:

- RF (32 GHz and 60 GHz).
  - HPA (TWTA and solid state power amplifier).
  - LNA.
  - 60 GHz antenna.
- Optical.
  - Laser transmitter (AlGaAs single LD & array and Nd:YAG).
  - External modulator.
  - Photodetector.

Each of these components will be briefly discussed below.

4.1 HPA

RF power can be amplified by using either the traditional Travelling Wave Tube Amplifier (TWTA) or the Solid State Power Amplifier (SSPA). These two different kinds of power amplifiers are discussed separately below.

The two most common circuits used in TWTA design are: coupled cavity and helix. In general, helix TWT is lighter , more power efficient and with higher bandwidth than coupled cavity TWT while the latter device offers an order of magnitude higher output power. In terms of output power, the upper limit for helix technology is probably around 100 Watts due to its lower thermal dissipation capability. For ISL applications considered herein, the channel power requirement can be met by both types of TWTs. Information relevant to TWTAs operating at 32 GHz and 60 GHz are given in Exhibit 4-1 and a level of readiness chart of various TWTAs is presented in Exhibit 4-2. Further details concerning TWT design can be found in reference [9].

Presently, at operating frequencies above 30 GHz, IMPATT and Gunn devices are the two dominant types of solid-state devices for RF power amplification. However, the rapid advance in high electron mobility transistors (HEMTs) and GaAs heterojunction bipolar transistors (HBTs) technology may put them in a position to replace the IMPATT and Gunn devices in the next few years [10]. Another mature technology for generating RF power is GaAs metal semiconductor field-effect transistor (MESFET) and its monolithic microwave integrated circuit (MMIC) implementation. These devices can typically generate output power up to about 1 W with 10-50% efficiency at 32 GHz and 10-100 mW with 10-20% efficiency at 60 GHz. The power performance of GaAs FET devices tend to roll off rapidly at frequencies above 30 GHz. On the other hand, single IMPATT CW and multi-stage amplifiers are capable of generating a few watts and 10-25 watts of output power, respectively. Typical efficiency of IMPATT device is 20%. Although HBT devices have high power density capability, they also have some technological problems to be overcome and therefore they are not being considered here. HEMT devices and pseudomorphic HEMT (PHEMT, HEMT with an extra InGaAs layer) devices are capable of high power density (e.g., 0.8 W/mm for PHEMT) with 30-40% efficiency at frequencies above 30 GHz. In addition to higher efficiency, HEMT devices are also more reliable than IMPATT and Gunn diodes. As manufacturing techniques keep improving, HEMT may eventually replace IMPATT and Gunn devices as the preferred power source operating at high frequencies. Comments on SSPA operating at 32 GHz and 60 GHz are summarized in Exhibit 4-3.

Given the relatively low power capability of SSPA, it appears that single device SSPA does not meet the channel power requirement of most of the ISL network architectures. Either power combining of multiple SSPAs must be implemented or TWTAs must be used in these ISL applications. In order to keep the system design simple, TWTA is adopted as the power source for the RF implementations in all three ISL architectures.

POWER AMPLIFIER ALTERNATIVES	32 GHz	60 GHz
• TWTA – HELIX TYPE – COUPLED CAVITY	• 2–PHASE DEVELOPMENT OF HELIX TWT BY W/J: – 7W (PHASE 1) – 15W (PHASE 2) • HUGHES HAS DEMONSTRATED 11.5W HELIX TYPE TWT • UPPER LIMIT FOR HELIX TECHNOLOGY IS PROBABLY 60W • MAY INCREASE OUTPUT POWER TO 100W BY USING COUPLED CAVITY TECHNIQUE • EFFICIENCY IS APPROX. 50% FOR HELIX TWT AND 40% FOR COUPLED CAVITY TWT	• 66W COUPLED CAVITY TWT DEMONSTRATED BY W/J • COUPLED CAVITY WITH OUTPUT POWER 50–200W ARE UNDER DEVELOPMENT BY NASA, HUGHES AND TRW. • HELIX TWT MAY GENERATE UP TO 20W AT 60 GHZ • EFFICIENCY IS 40% FOR HELIX TWT AND 25% FOR COUPLED CAVITY
	• HELIX TWT IS LIGHTER THAN COUPLED CAVITY TWT WHILE THE LATTER DEVICE OFFERS HIGHER POWER	

06/27/91 TR91071\PK7896

Exhibit 4–1: RF HPA Technology Status

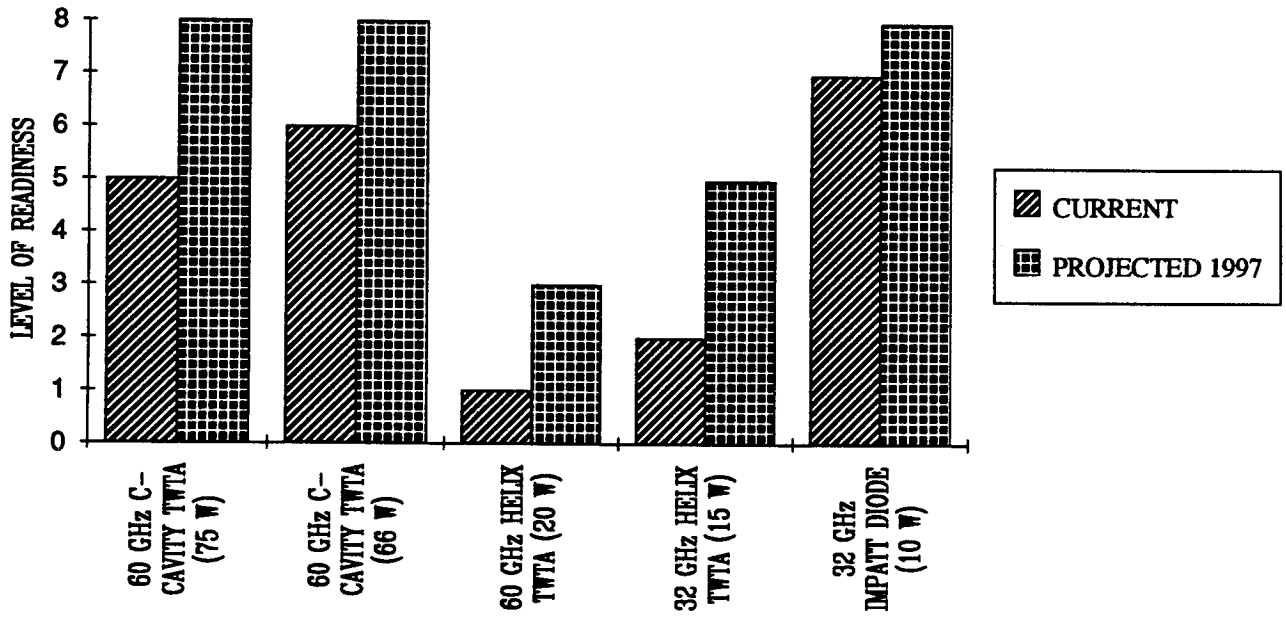

Exhibit 4-2: HPA Level of Readiness

POWER AMPLIFIER ALTERNATIVES	32 GHz	60 GHz
• SSPA – GaAs MESFET'S (metal semiconductor field–effect transistor) – GaAs MMIC'S – GaAs HBT'S (heterojunction bipolar transistor) – GaAs HEMT'S (high electron mobility transistor) – GUNN DEVICES (or transferred electron devices) – IMPATT DEVICES (IMPact Avalanche Transit Time)	• SINGLE IMPATT CW AMPLIFIER CAN GENERATE 3W WITH 20% EFFICIENCY • HUGHES MULTI–STAGE IMPATT AMPLIFIER IS CAPABLE OF GENERATING 25W POWER • 1W GaAs FET WITH 25% EFFICIENCY IS UNDER RESEARCH	• 1.5W SINGLE IMPATT DIODE IS AVAILABLE • 10W MULTI–STAGE IMPATT AMPLIFIER IS COMMERCIALLY AVAILABLE (NOT SPACE QUALIFIED) • 1W GaAs FET IS PROJECTED (YEAR 1995–2000) BUT SPACE QUALIFIED AT 60 GHZ IS UNCERTAIN

- BJT'S DOMINATE AT FREQUENCIES BELOW 5 GHZ
- GaAs MESFET'S ARE ATTRACTIVE UP TO 20–30 GHZ
- GUNN AND IMPATT DEVICES DOMINATE AT HIGHER FREQUENCIES – BUT RELIABILITY IS A PROBLEM FOR SPACE USE
- HBT'S AND HEMT'S ARE LIKELY CANDIDATES TO REPLACE GUNN AND IMPATT'S AT FREQUENCIES OF 10–100 GHZ

07/17/91 TR91071\PK7895

Exhibit 4–3: RF Solid State HPA Technology Status

4.2 LNA

GaAs FET and HEMT are the two dominant technologies used in LNA design. Both technologies have demonstrated relatively low noise figures, high gains, and wide band wide bandwidths. GaAs FET and HEMT devices are typically employed in a discrete component amplifier. With MMIC implementation of these devices, further reduction in weight, size, and power are envisioned. In addition to GaAsAl, several other kinds of HEMTs such as: Ti/Pt/Au "T" gate, InP, and InGaAs pseudo-morphic are also under development. The gain and noise figure of all these devices are listed in Exhibit 4-4. The performance projection curves for three selected LNA devices are plotted in Exhibit 4-5. These curves depict the gain and noise figure of the LNA devices over the frequency range of 18 GHz - 94 GHz. As shown in the exhibit, the gain decreases and the noise figure increases as the frequency increases. As shown, the HEMT devices are projected to perform better than the FETs. The level of readiness of selected LNAs are shown in Exhibit 4-6. The FETs are probably slightly more mature than the HEMTs. However, further advances in HEMT technology may change the picture in 5-10 years.

LOW NOISE AMPLIFIER (LNA) ALTERNATIVES	32 GHz		60 GHz	
	GAIN(dB)	NOISE FIGURE (dB)	GAIN(dB)	NOISE FIGURE (dB)
• GaAs MESFET	20	3.5	25	4
• GaAlAs HEMT	15	3.5	23	3.8
• Ti/Pt/Au "T" GATE HEMT	–	–	6	1.8
• InGaAs PSEUDO–MORPHIC HEMT	–	–	8	1.4
• MMIC GaAs FET	7.5	3.5	26	9.5

- GaAs MESFET AND HEMT DEMONSTRATED LOW NOISE FIGURES, HIGH GAINS, AND WIDE BGAINS, ANDWIDTHS
- FURTHER IMPROVEMENT ENVISIONED FOR GaAs MESFET AND HEMT
  - 2 TO 3 dB NOISE FIGURE DEVICE MAY BE AVAILABLE BY 1997
- PSEUDO–MORPHIC HEMT OFFERS EVEN LOWER NOISE FIGURE BUT WITH SMALLER GAIN

Exhibit 4–4: RF LNA Technology: Status Overview

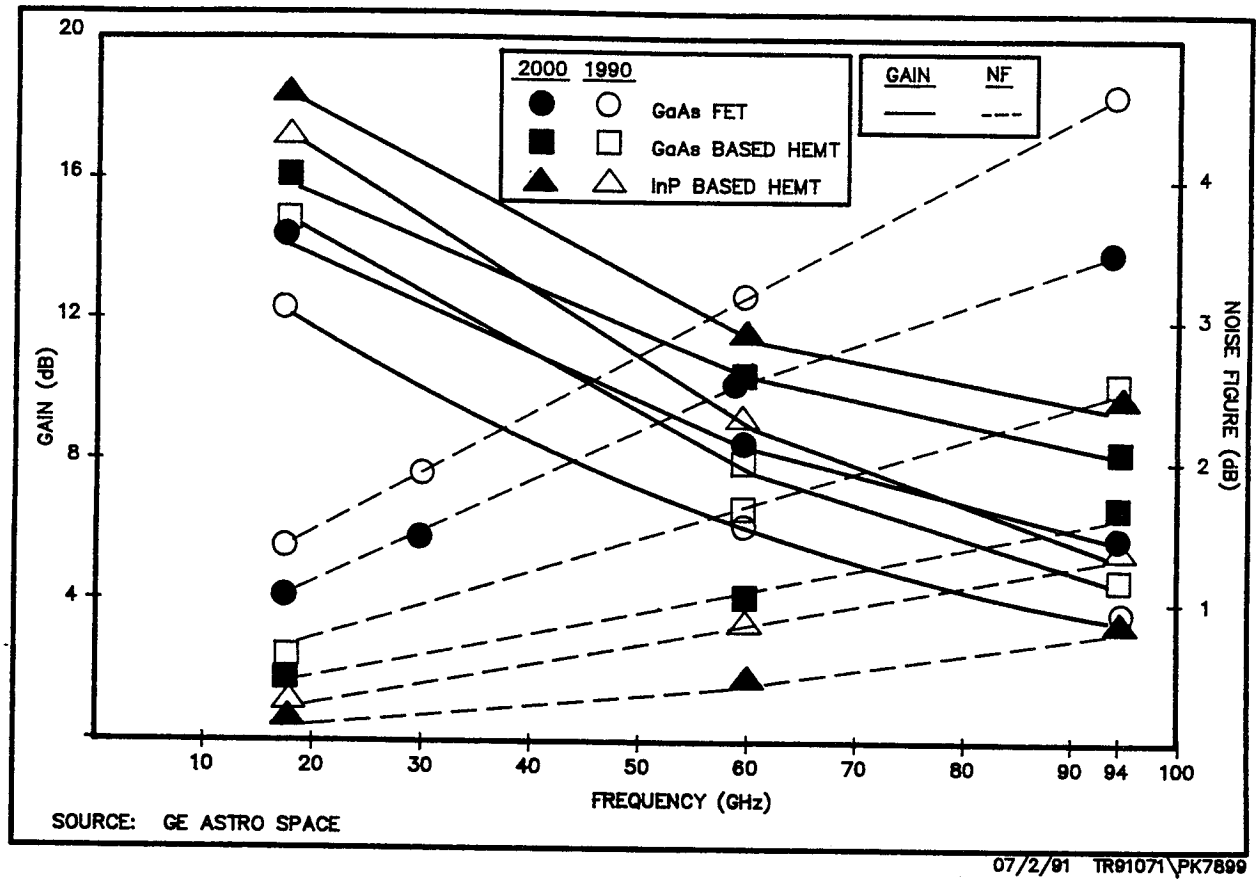

Exhibit 4–5: Low Noise Receiver Device Performance Projections

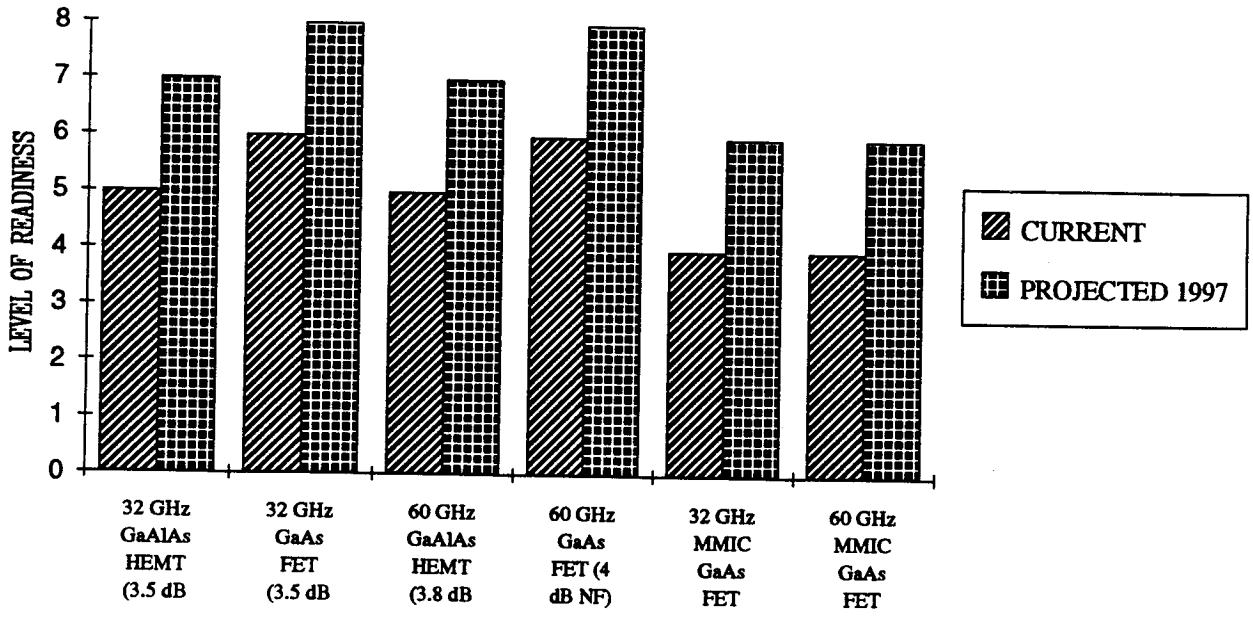

Exhibit 4-6: LNA Level of Readiness

4.3 60 GHZ ANTENNA

Antennas to support GEO-GEO crosslink at 60 GHz have been described in prior studies [11] - [12]. For best efficiency, dual axis gimbal drive parabolic dish antenna with shaped reflector is the leading candidate for the applications considered herein.

The technology for antenna with solid reflector up to 4 m in diameter and operating at 60 GHz is currently existed. Solid parabolic dish antenna with > 50% end-to-end efficiency and surface accuracies < 1 mil across a 2.7 m diameter can be expected by 1997. In order to minimize the weight, the trend in reflector design is to use composite materials with sufficient rigidity. Other design details such as antenna feed, polarizer, beam waveguide, and autotracker can be found in the above references. In summary, the 60 GHz antenna technology is projected to meet the performance requirements as determined by the link budget analysis and other end-to-end analysis.

4.4 LASER TRANSMITTERS

The laser transmitters considered in this study are:

- Semiconductor AlGaAs single laser diode and array (wavelength = 860 nm).
- Diode-pumped Nd:YAG (wavelength = 1064 nm).

Each kind of lasers has its own distinctive features.

Without getting into the details of specific laser structure, the state-of-the-art single AlGaAs laser diode (wavelength = 860 nm) can generate up to 150 mW of peak power. This kind of laser is both peak and average power limited. The best peak to average power ratio achievable to date is approximately 4:1. Therefore for direct detection PPM applications, the highest allowable PPM order is 4. AlGaAs LD has relatively high efficiency (up to 50%) as compared to Nd:YAG (< 10%). AlGaAs LD can also be internally/externally modulated at the rates of 100 MHz - 2 GHz. One drawback of AlGaAs LD is its large spectral linewidth (frequency fluctuation) which is on the order of 50 - 100 MHz. For heterodyne FSK detection, such linewidth contributes to phase noise problem and leads to performance degradation. The impact of phase noise on system performance will be discussed in section 5.

AlGaAs LD arrays have similar characteristics as the single LD such as: high efficiency (up to 50%), high bandwidth and low peak to average ratio. Single substrate diode arrays hold promise of generating a few watts of output power in 5-10 years.

A key feature of Nd:YAG laser is its high power capability. Nd:YAG with a few watts of CW output power is commercially available. Higher power Nd:YAG is under development in laboratory. However, as compared to AlGaAs LD, the end-to-end efficiency of Nd:YAG is relatively low (only 5-10% at 1064 nm). Another disadvantage of Nd:YAG laser (at 1064 nm) is its narrow tuning range which makes duplex multiple-channel implementation extremely difficult if not impossible. In addition, because of its relatively limited direct modulation capability, an external modulator is required for the homodyne PSK implementation. Despite these shortcomings, Nd:YAG lasers typically have very narrow linewidth (10-100 KHz) which makes them suitable for heterodyne or homodyne detection.

4.5 EXTERNAL MODULATOR

As mentioned above, an external modulator is required for the homodyne PSK implementation. Electro-optic (guided wave) modulators made of either $LiNbO_3$ or $LiTaO_3$ crystals are typically used for high bandwidth laser communication. The index of refraction of the crystal can be controlled by an applied external voltage. Due to electro-optic effect, the phase of the input signal is delayed by an amount which is proportional to the applied voltage. Binary phase modulation is achieved by switching the voltage between two values (i.e., BPSK). The switching voltage for electro-optic modulator is on the order of tens of volts which allows the modulator to operate at fairly high speed. However, the current $LiNbO_3$ modulators (operating at 1064 nm) do not have the capability to handle more than 100 mW of CW power [13], [14]. For the GEO_GEO crosslinks using high CW power (300 mW to 1 W) Nd:YAG laser transmitter, innovative modulator design is required or the transmit power must be substantially reduced. High bandwidth modulator with high CW power capability is probably one of the key components that introduces major technology risks and complexity to the homodyne implementation.

4.6 PHOTODETECTOR

There are many types of photodetectors available commercially. Among them are photomultipliers, pyroelectric detectors, and semiconductor-based photodiodes, photoconductors, and phototransistors [15]. Photomultipliers (PMTs) are capable of very high gain and low noise. However, it has very low quantum efficiency (< 1%), large size, and low reliability. Therefore PMTs are not suitable for the crosslink applications. For optical implementations considered herein, semiconductor-based PIN diodes and avalanche photodiodes (APD) are used because of their high quantum efficiency, small size, and high reliability. Current state-of-the-art PIN and APD diodes are predominantly made of silicon; although other materials such as germanium and GaAs are also being used. The silicon based photodetectors have peak response at wavelength around 900 nm which matches well with the operating wavelengths of the ISL optical implementations except the homodyne PSK scheme. The quantum efficiency for silicon photodetector is 80-90% at 850 nm but rolls off rapidly to 40% at 1064 nm. InGaAs APD at 1060 nm has high quantum efficiency (80-90%) but undesirably high excess noise factor. Key features of selected detectors are listed in Exhibit 4-7 . The estimated level of readiness for several photodetectors are depicted in Exhibit 4-8 . Note that the projected level of readiness will depend on the opportunity to perform space qualification on the detectors. Therefore the projection has some degree of uncertainty due to the lack of existing flight programs (excluding secret military programs, if any.)

DETECTOR TYPE	DETECTOR GAIN	QUANTUM EFFICIENCY	EXCESS NOISE FACTOR *	RELIABILITY	REMARKS
Si–APD @ 0.85 μm	UP TO 300	80–90%	2.8	HIGH	• RCA "SLIK" APD SPECIFICATION • APPLICABLE TO DIRECT DETECTION
Si–APD @ 1.064 μm	UP TO 300	40%	2.8	HIGH	• APPLICABLE TO Nd: YAG DIRECT DETECTION SYSTEM
InGaAs APD @ 1.064 μm	UP TO 50	80–90%	5.5	HIGH	• VERY HIGH K (UNDESIRABLE)
Si PIN @ 0.85 μm	UNITY	60–90%	1	HIGH	• TRADE OFF BETWEEN BW AND QUANTUM EFFICIENCY
Si PIN @ 1.064 μm	UNITY	40%	1	HIGH	• APPLICABLE TO Nd: YAG PSK HOMODYNE SYSTEM
AlGaAs PIN @ 0.85 μm	UNITY	85%	1	HIGH	• APPLICABLE TO HETERODYNE SYSTEM • MIT–LL CUSTOM MADE DEVICE
PMT @ 1.064 μm	10^5 TO 10^6	< 1%	1	MODERATE TO LOW	• LOW QE AND RELIABILITY MAKES PMT UNSATISFACTORY

* OPTIMIZED GAIN

07/01/91 TR91071\PK2152

Exhibit 4–7: Photo–Detector Technology Status

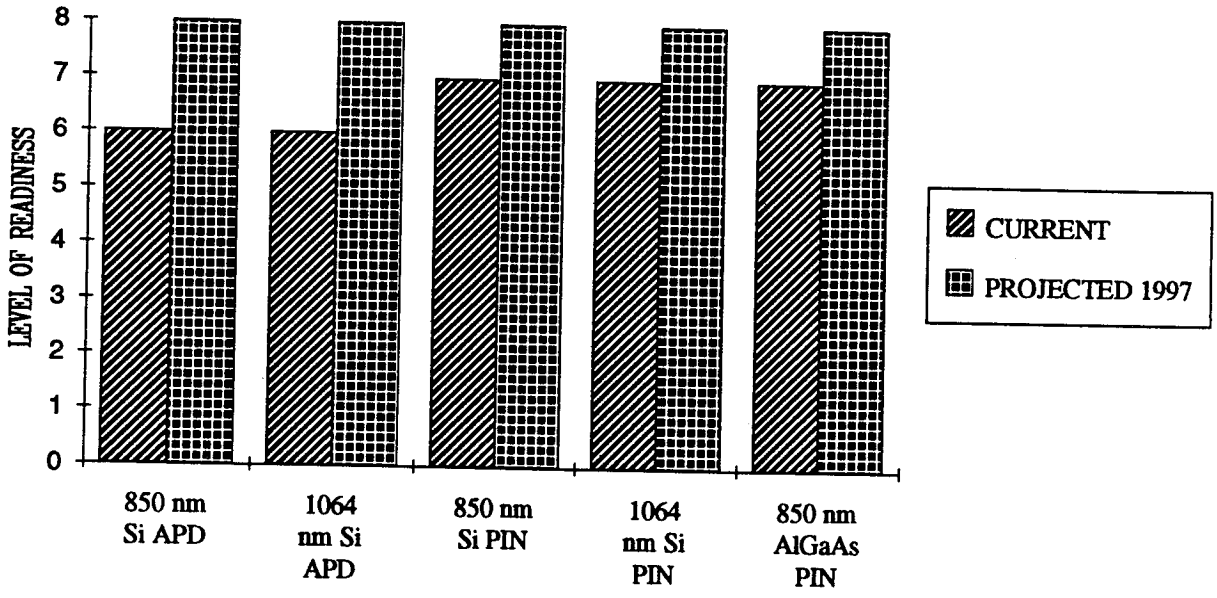

Exhibit 4-8: Photo-Detectors Level of Readiness

SECTION 5: ASSESSMENT OF KEY SYSTEM PERFORMANCE OBJECTIVES

There are several key system performance issues need to be addressed:

- Spatial acquisition for optical systems.
- Spatial tracking for optical systems.
- Phase noise in carrier for coherent optical and high frequency RF systems. Each of these issues will be briefly discussed below.

5.1 SPATIAL ACQUISITION FOR OPTICAL SYSTEMS

Typical ISL platform has attitude uncertainty of a few mrad which is much greater than the 5 μrad beam width of a 20 cm telescope. Before actual communication is possible, the initial pointing uncertainty must be reduced. Suitable acquisition scenario should be adopted in order to ensure a robust and quick (< 1 minute) spatial acquisition. Many scenarios have been explored for GEO-GEO ISL systems in prior studies [3], [16]. In the application considered herein, the most efficient acquisition scenario for optical ISL is as follow:

- The receiver FOV encompasses initial pointing uncertainty.
- The transmitter broadens beam to a few hundred μrad and scans its pointing uncertainty FOV.
- The receiver detects transmit beam and responds with similar beacons.

Without getting into the details of applicable detector type and post-detection processing method which can be found in references [3], [16], it can be simply stated that successful completion of this acquisition scenario in < 1 minute requires a minimum power collected by the receiver aperture. For example, for a transmit beamwidth of 300 μrad, this power is exceeded when $P_T A_R / R^2 > 0.3$ pW where P_T = transmit power, A_R = receiver aperture and R = the transmitter-receiver range. Thus, for R = 40,000 km, A_R = 20 cm, the required P_T for acquisition is approximately 30 mW with 6 dB margin. This power level can be easily met by the same laser transmitter for communication purposes.

5.2 POINTING/TRACKING ERROR IMPACT ON SYSTEM PERFORMANCE

Upon completion of spatial acquisition, cooperative pointing and tracking must be initiated and maintained before communication can take place between the ISL terminals. In general, on-board autotracking receivers track the spatial position of a target (beacon) and use this as a reference position for transmitter line-of-sight (LOS) pointing. However, relative motion and on-board mechanical vibration of platform tend to introduce pointing/tracking error of approximately 11 μrad (based on LANDSAT data) to the system. Using a well designed servo system with sufficient wide bandwidth (1000 Hz typical), the platform jitter can be suppressed to 0.5 - 1 μrad (RMS value) which is about 1/10th of the transmitter beam width. In addition to off-point jitter, there is also an off-point bias which is associated with the point ahead mechanism. The combined effect of off-point jitter and bias will have significant impact on the system BER performance. The system instantaneous BER is a function of P_T and $G_T(\theta)$ where P_T = transmitter laser power, G_T = transmitter gain function, and θ = composite offpoint angle with variance σ^2 and bias b [3]. In the presence of tracking error, higher transmit power is required to achieve the same BER performance as the ideal case (i.e., $\sigma = b = 0$). For example, 0.6 dB power degradation is expected for a direct-detection system with $\sigma D/l = bD/\lambda = 0.1$ where D = transmitter aperture diameter, and λ = optical wavelength. For a coherent heterodyne or homodyne system, however, spatial tracking errors not only affect the LOS pointing accuracy of the transmitter, but also tracking accuracy of the local oscillator (LO) at the receiver [5]. Thus the misalignment between the received signal and the LO imposed additional power penalty on the system.

Prior study [5] has shown that given certain offpoint σ and b, an optimum transmitter gain (or aperture size) can be selected to minimize the required transmit power for the desired BER (e.g., 10^{-6}). This fact is illustrated in Exhibit 5-1. However, fading channel analysis indicates that an transmitter aperture size smaller than the optimal aperture is desirable in order to avoid significant fading [3]. Two BER probability distribution charts are presented in Exhibits 5-2 and 5-3: one for BPPM system with a 20 cm aperture, and another one with an optimized 26.5 cm aperture, respectively. As shown in the exhibits, the system with the larger optimized aperture has BER distribution skewed toward the higher BER (10^{-3} to 10^{-1}) area while the system with suboptimal aperture has distribution concentrated at 10^{-7} to 10^{-4} section even though both systems have 10^{-6} average BER. In other words, a suboptimal smaller aperture is probably more desirable for optical system operating in fading channel. In addition, high quality large aperture telescopes (> 20 cm) can be very costly and difficult to manufacture.

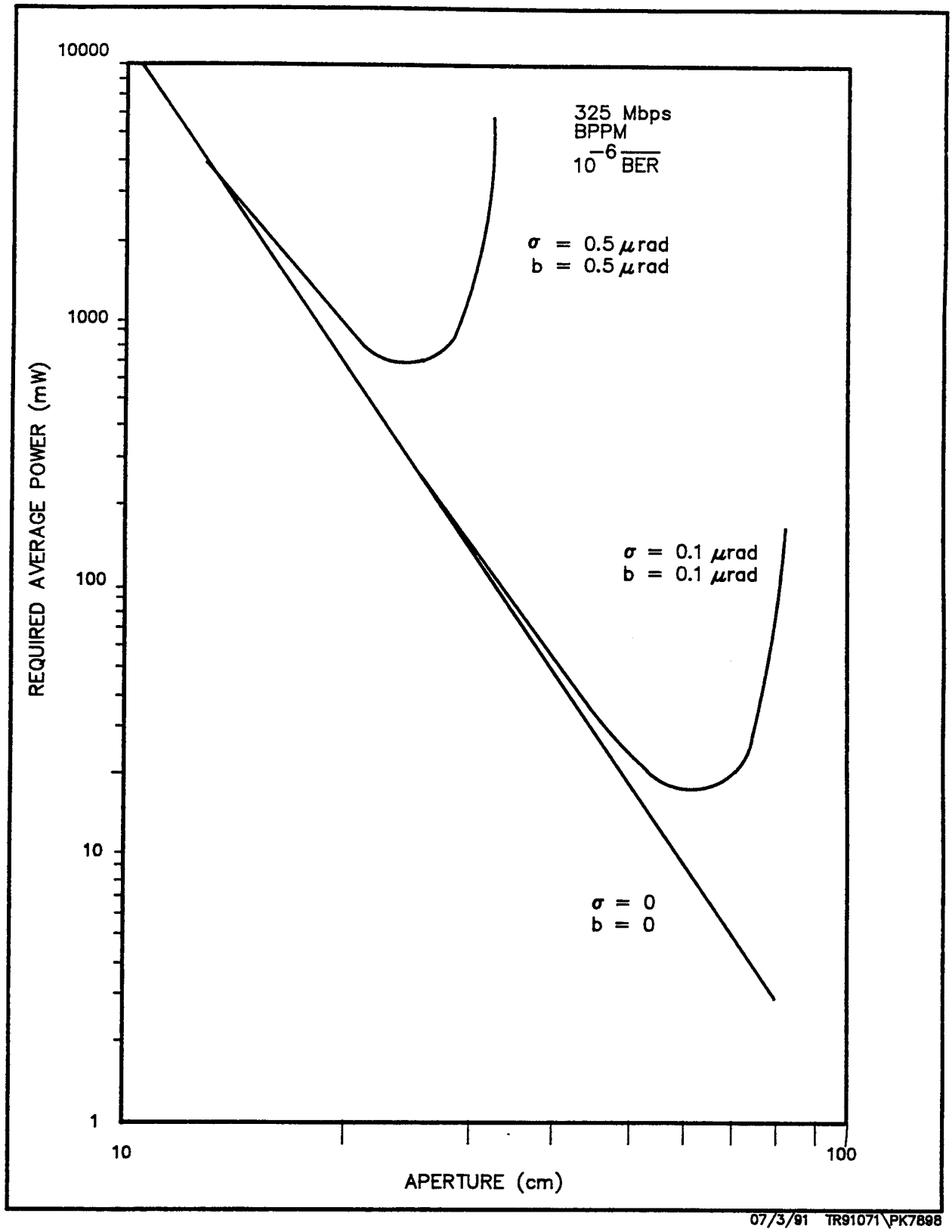

Exhibit 5–1: Geo–Geo Link: Power and Aperture Trade Off

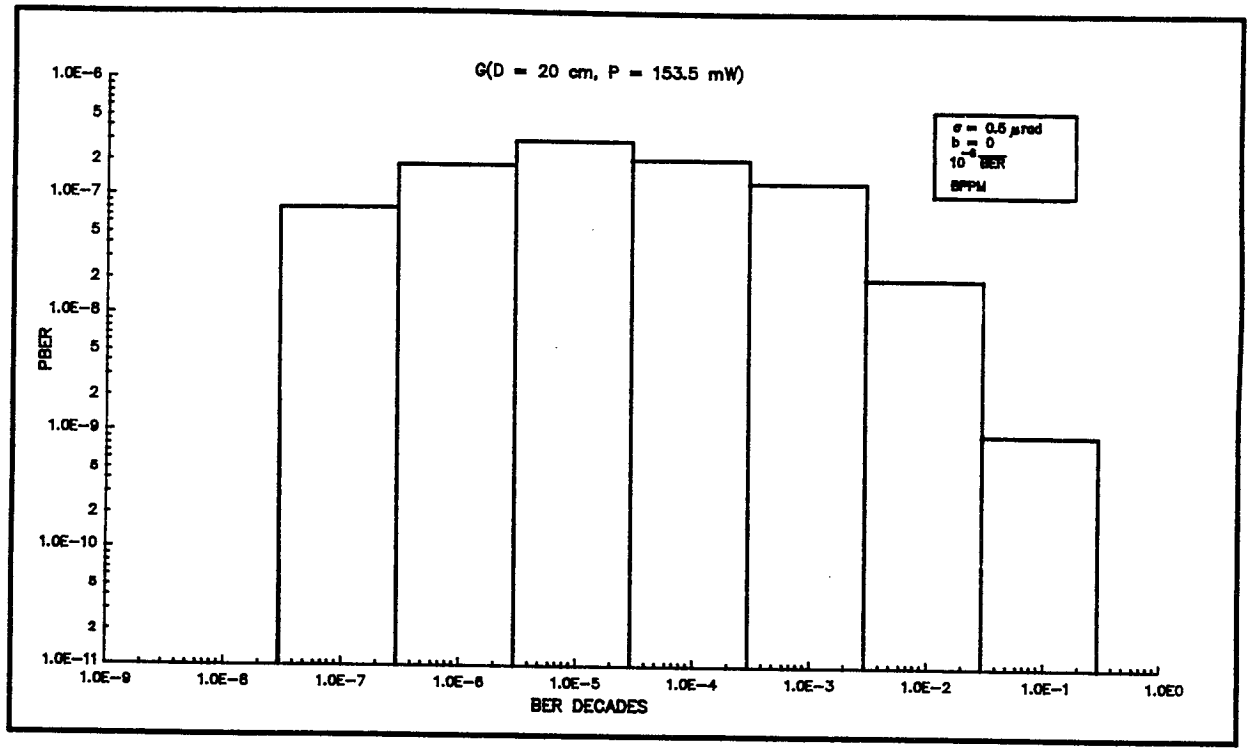

Exhibit 5–2: BER Probability Distribution: Suboptimal Aperture

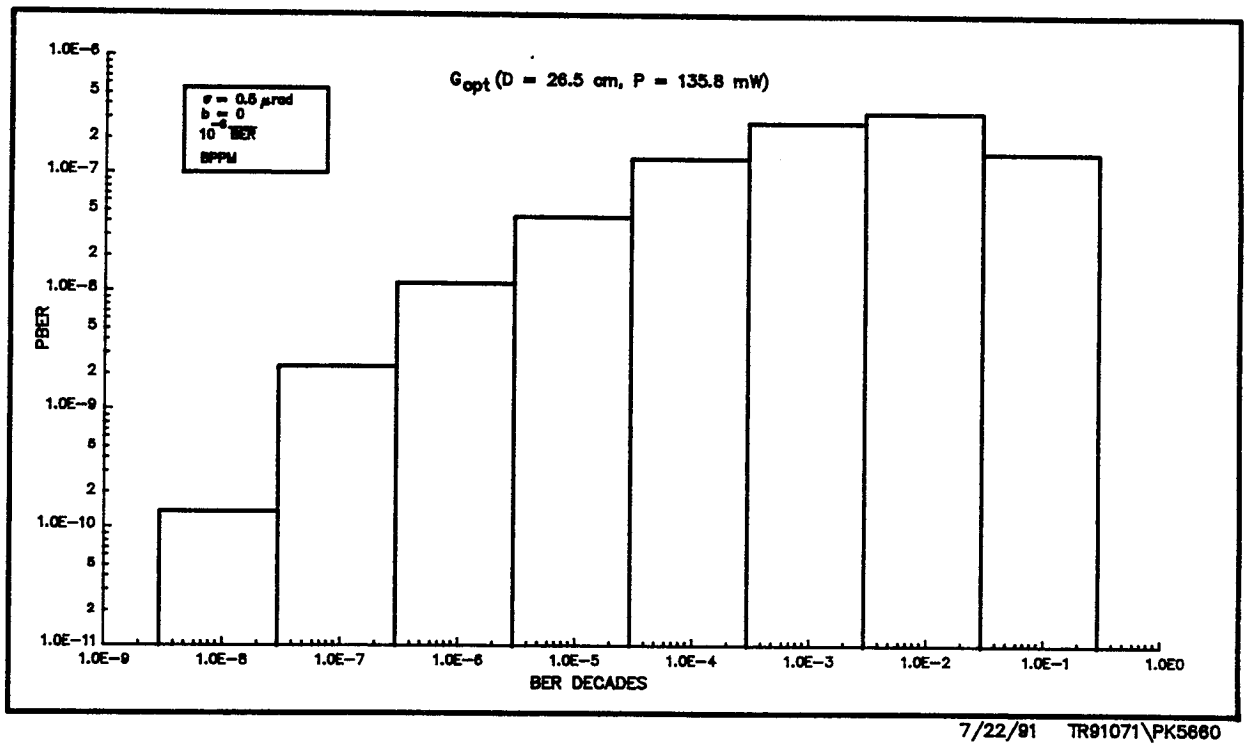

Exhibit 5–3: BER Probability Distribution: Optimal Aperture

5.3 PHASE NOISE ANALYSIS SUMMARY (COHERENT OPTICAL SYSTEM)

Phase/frequency noise in semiconductor lasers is the result of spontaneous emission of photons in the laser cavity. This noise causes spectral spreading (non-zero 3 dB linewidth) of the output signal. Basically, there are two effects of phase noise on signal quality [17]:

- Signal attenuation or suppression.
- Crosstalk (signal distortions).

The combined effect contributes to signal-to-noise (SNR) reduction, and consequently, BER degradation. Exhibit 5-4 illustrated the phase noise impact on an optical QFSK heterodyne system using envelop detection. Bit error rate is plotted against detected photons/bit (in dB) parameterized by various linewidth (normalized by data rate). The normalized tone spacing in this case is 1. For 300 Mbps and 10^{-6} BER, laser linewidth of 9 MHz will impose approximately 3 dB power penalty on the system. System operating at higher data rate with same linewidth will have smaller power penalty. Linewidth of 1 - 10 MHz is probably desirable for QFSK heterodyne system operating between 100 Mbps and 1 Gbps in order to limit phase noise degradation to < 0.5 dB. For homodyne BPSK system using Nd:YAG laser which has narrow linewidth (< 1 KHz typical), the impact of phase noise is very small when the system is operating at 100 Kbps or above.

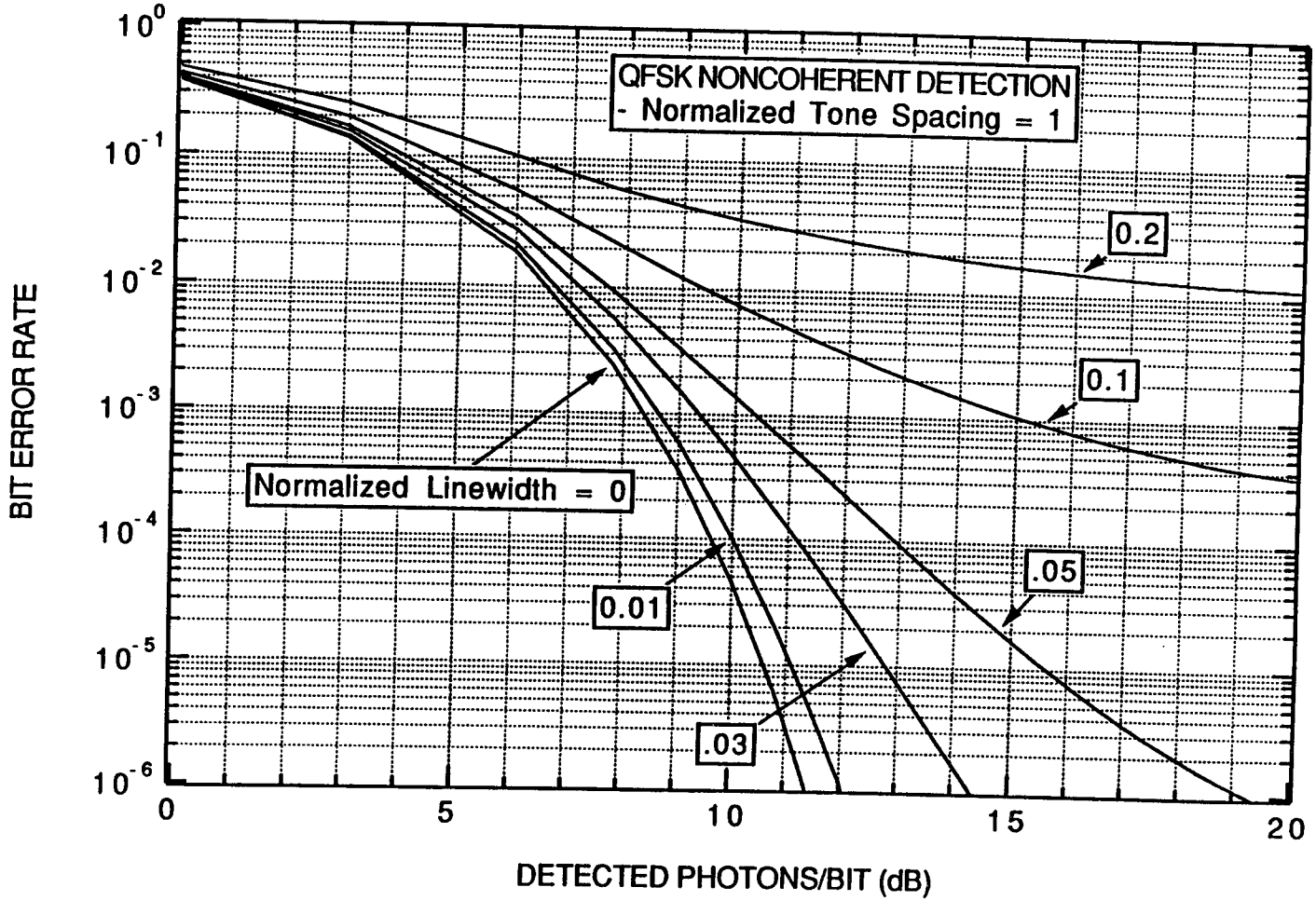

Exhibit 5-4: Phase Noise Impact on Optical QFSK Heterodyne System

5.4 PHASE NOISE ANALYSIS SUMMARY (RF SYSTEM)

The sources of phase noise in RF system are:

- The instability of various oscillators used to generate carrier and mixing frequencies.
- Thermal noise (additive white gaussian noise).

For coherent QPSK system, a phase-locked loop (PLL) is usually employed in carrier recovery and data detection. The operation and performance of PLL have been analyzed extensively in many references [18] - [20], and will not be repeated here. In summary, the residue phase error in the tracking loop degrades the BER performance and leads to cycle slip or loss of lock in extreme cases. RMS phase error is usually a quantity of interest for the system designer and is a function of loop bandwidth and E_b/N_0 of the signal. For a well-designed tracking loop operating at reasonable loop bandwidth, RMS phase error of a few degrees can be expected. As a result, < 1 dB additional power is typically required to maintain 10^{-6} BER as compared to zero phase error system.

SECTION 6: ISL PAYLOAD DEFINITION

Before a comparison and evaluation of the RF and optical alternative implementations can be performed, a more refined definition of the ISL reference payloads is required. The approach to ISL definition is delineated in Exhibit 6-1. With inputs from link budget studies and data bases of component weight/size/power, initial performance parameters and weight/size/power/cost estimates of all six implementations for each ISL network architectures are developed and are presented in Appendix B. Payload mass and power models for RF and optical systems are developed. Spacecraft bus mass model (which has dependencies on prime power) is also constructed. By using these models, ISL aperture versus power trades can be conducted with the goal of achieving mass minimization. However, it should be emphasized that other important factors such as technology risk and cost must also be considered in order to produce a more useful system optimization.

Implementations with optimized parameters are then tabulated for further comparison and evaluation in Section 7.

Each key steps of ISL payload definition are briefly discussed below.

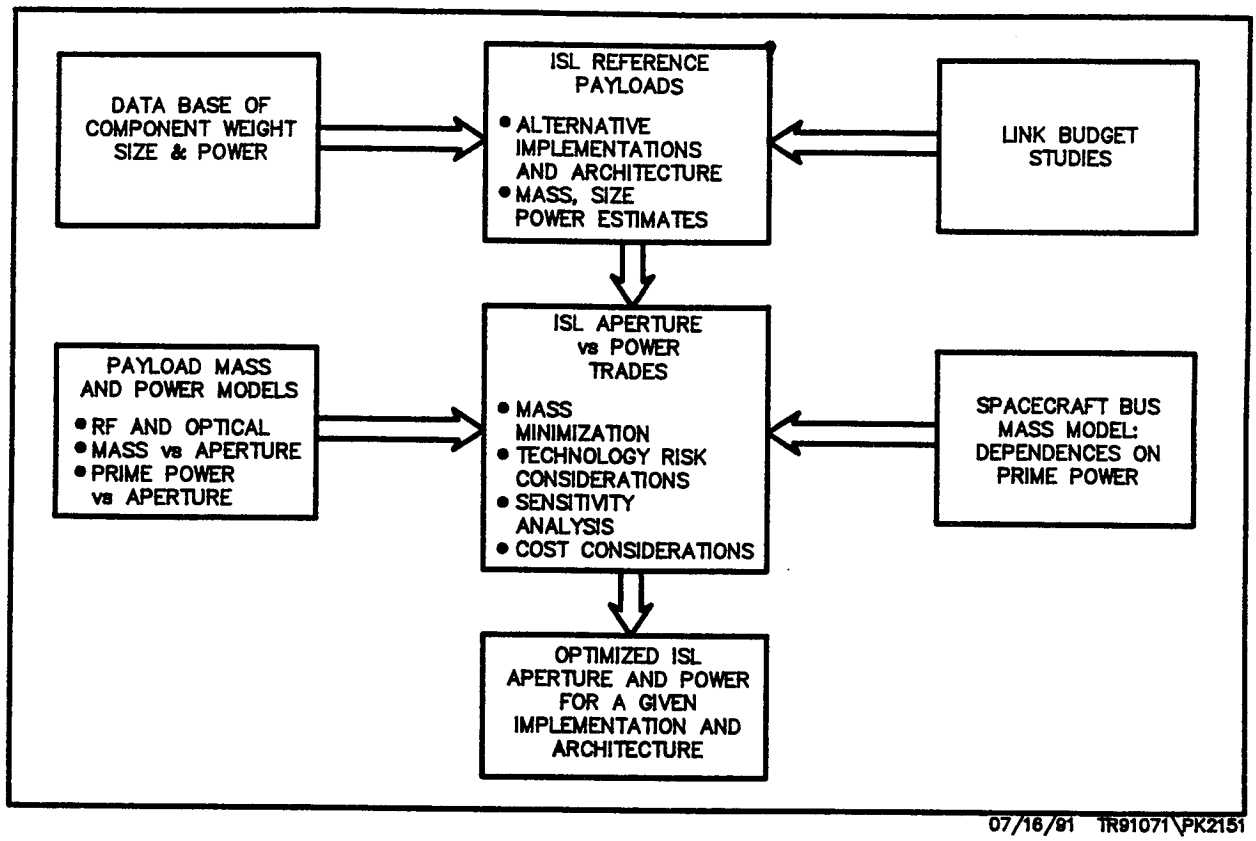

Exhibit 6–1: Approach to ISL Definition and Optimization

6.1 DATABASES OF WEIGHT/SIZE/POWER ESTIMATION

For each ISL implementation, the system can be subdivided into functional blocks according to the block diagrams and performance requirements presented in Section 2 and APPENDIX B, respectively. The weight/size/power of all subsystems/components are then estimated with input from the following data bases:

- RF payload data bases - ATDRSS phase A definition studies (developed by Ford Aerospace, General Electric, Hughes Corporation, TRW, and Lockheed Corporation).
- Optical payload data bases - various GSFC lasercom programs and MIT Lincoln laboratory LITE program.

Based on these informations, the weight/size/power estimates generated are believed to be more in line with state-of-the-art RF and optical technologies. The results are tabulated and presented in Appendix B.

6.2 ISL PAYLOAD MASS MODELS AND OPTIMIZATION (RF AND OPTICAL)

Prior study [1] has shown that ISL payload mass is a function of antenna diameter, payload power, and spacecraft bus mass (which depends on prime power.) The payload power in turn is a function of antenna diameter, and transmit power. For RF systems, payload mass (M_{ISL}) and power (P_{ISL}) can be represented by:

$$M_{ISL} = 1.75N_{TWTA}P_{RF}0.227 + (3.3D^{2.2} + 14) + 0.08P_{ISL} + 23 \text{ (in Kg)};$$
$$P_{ISL} = 17 + 3.4D^{2.2} + N_{TWTA}P_{RF}/E + 11 \text{ (in Watts)};$$

where N_{TWTA} = number of TWTAs used, D = antenna diameter, P_{RF} = RF power required to close the link, i.e., D^4P_{RF} = constant, and E = power efficiency in fraction. Note that this model is applicable to both 32 GHz and 60 GHz systems. However, the D^4P_{RF} product which is derived from the link budget will be different for each system, as it is reflecting their different system characteristics. Given these models, a RF antenna size can be selected to minimize the payload mass and power. Examples of payload mass optimizations for 32 GHz and 60 GHz are presented in Exhibit 6-2 and 6-3, respectively. In these cases, optimizations are performed for ISL architecture 1 with 5 channels, and a data rate of 1 Gbps per channel. The total data rate of 5 Gbps is considered to be a reasonable trunk capacity for a future generation commercial satellite. These preliminary results indicated that antenna size of 1.25 - 2.5 m minimizes the payload mass of the 32 GHz and 60 GHz systems for all architectures (assuming that appropriate transmitters are available.) A larger aperture (than this range) involves higher technological risk while smaller apertures tend to increase payload mass rapidly.

Similarly, for the optical systems, ISL payload mass (M_{ISL}) and power (P_{ISL}) can be represented by:

$$M_{ISL} = (1.1 + 200D^{1.7}) + 20 + 15P_{OP}1.3 + 0.08P_{ISL};$$
$$P_{ISL} = (1.25 + 20P_{OP}/E) + (40 + 20D^{1.3}) + (10 + 6X10^{-3}R_b);$$

where P_{OP} is laser output power in watts, E is the laser efficiency in fraction, R_b is data rate in Mbps, and D^4P_{OP} = constant. Optimization curve for architecture 2 using DD/PPM implementation is shown in Exhibit 6-4. Initial optimization results indicated that 16-20 cm aperture tends to minimize payload mass of architectures 1 and 2 while payload mass of architecture 3 is optimized at around 27 cm. Aperture size larger than 20 cm involves much higher technological risk and a demanding PAT subsystem. For DD/SIM and Homodyne BPSK systems, other factors such as technology risk, complexity, and cost tend to make them undesirable implementations; and therefore mass optimization is not performed for these systems. In addition, for all optical system, the aperture size is probably one of the key drivers for cost.

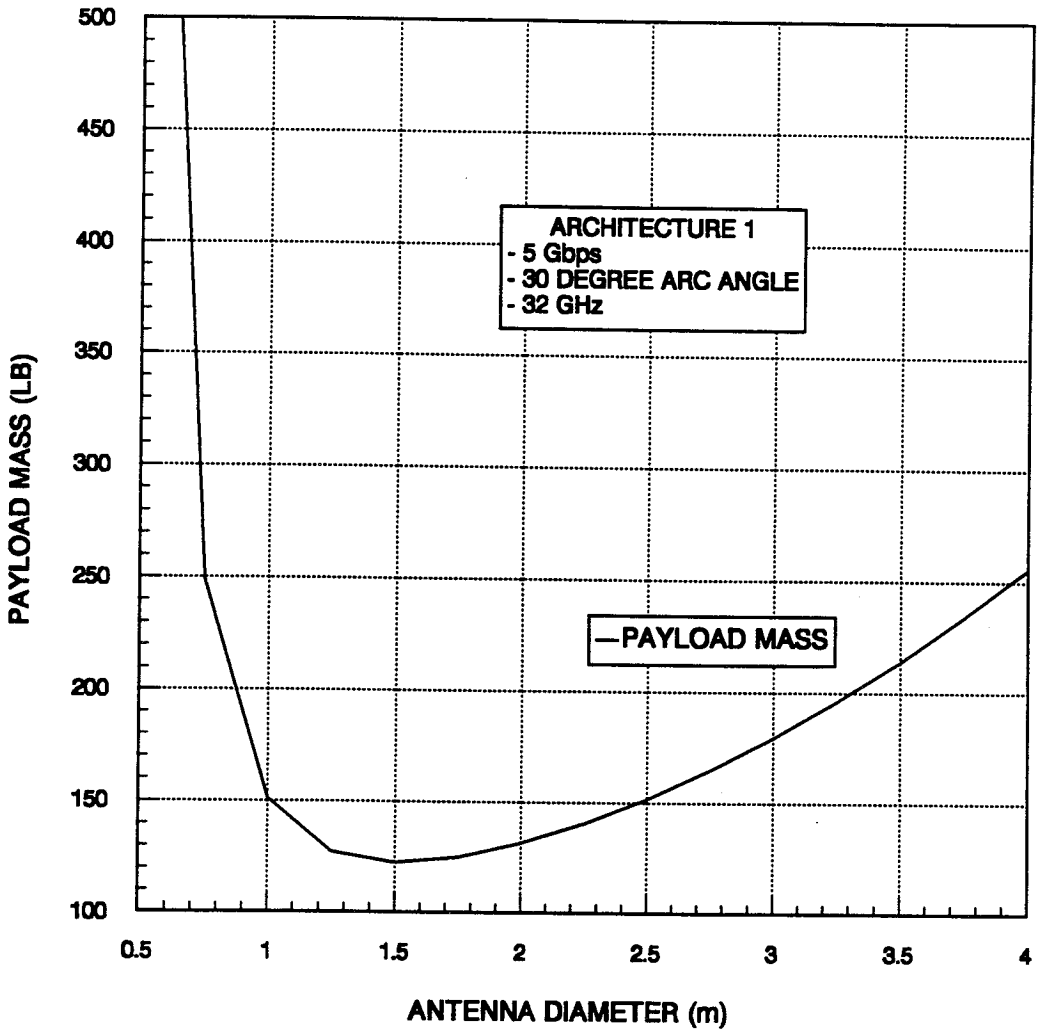

Exhibit 6-2: Optimization of RF (32 GHz) Payload Mass

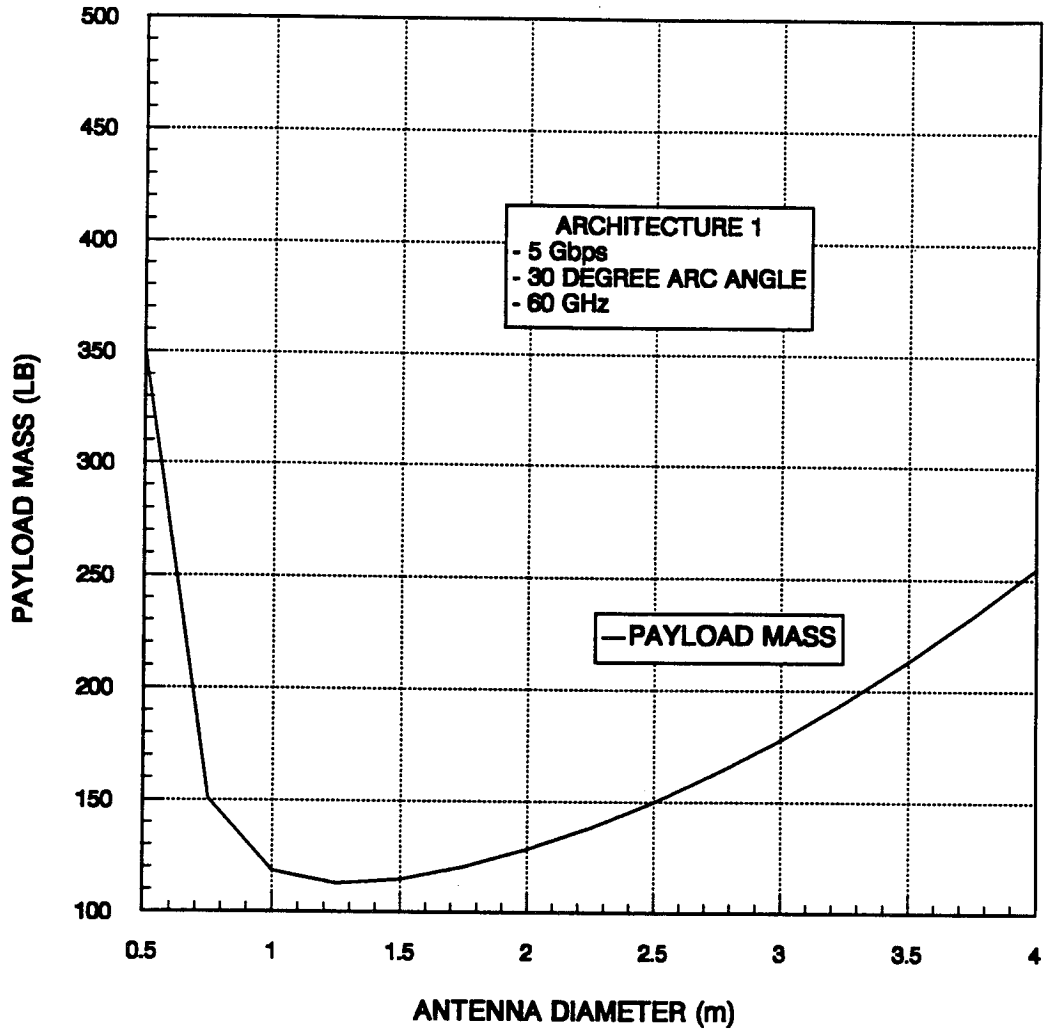

Exhibit 6-3: Optimization of RF (60 GHz) Payload Mass

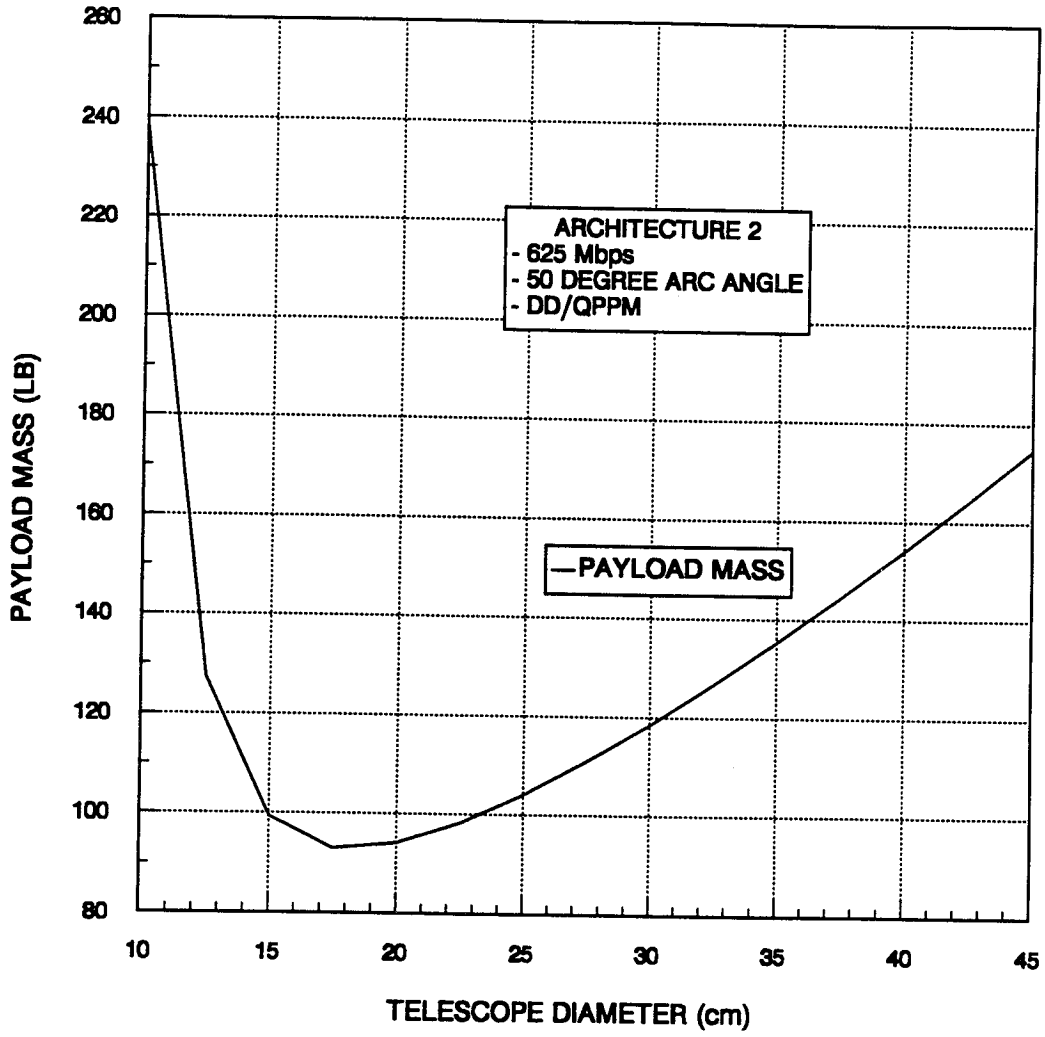

Exhibit 6-4: Optimization of Optical Payload Mass

Therefore, the most reasonable design approach may be the one using the highest available transmitter power in order to minimize the aperture size. For this reason and the fact that the heterodyne QFSK system requires narrow linewidth LD which has relatively low transmit power, mass optimization is not performed in this case.

6.3 ISL PAYLOAD COST ESTIMATION

This section outlines the methodology used to estimate the payload cost of the six RF and optical implementations for all three ISL architectures. Key cost drivers for each system were identified. Payload cost estimates were then generated and the results are presented below.

The process actually began when the design parameters are selected and optimized in order to minimize technological risk and payload weight/size/power. Based on these parameters, major cost drivers are then identified. By applying these key parameters to existing RF and optical cost models [1], [21], [22], cost estimates are generated. The models divide the payload into its antenna and repeater subsystems, and estimate both non-recurring and recurring cost elements for each. Total payload cost is given by the sum of these cost elements and the estimated cost of program management and engineering support. Although the models generate very specific cost figures, these estimates tend to have large statistical variation due to the lack of substantial flight experience (for high frequency and optical crosslink systems). The models are therefore viewed as somewhat qualitative, and are used to assess cost variations with changes in aperture, transmitter power, and payload prime power. The approach is therefore to use the models to calculate payload costs for all systems, and then to normalize the results to the single-channel, 30-degree 32-GHz RF and DD/QPPM optical links. Independent cost estimates are then determined for the RF and optical normalization systems.

Accurate cost estimates for the normalization systems are difficult to determine, and a best-effort approach was used. The calculated payload costs were supplemented with cost data from relevant in-house and customer-funded programs, and informal discussion with crosslink community contacts. This provided approximate cost ranges for the RF and optical payloads. Two key factors were considered while determining the independent cost estimates. First, using previous data for payload cost estimates is risky at best, because many former and on-going programs have experienced delays and cost increases as a result of technological developments that were needed "on the fly". Second, certain cost factors, such as space qualification and reliability impact, can only be roughly estimated because of the lack of heritage. The uncertainty in these factors is larger for optical technologies than for RF technologies.

Finally, cost estimates were obtained both with and without consideration of relative technology risks between the various systems. The estimates that include risk give realistic representations of expected payload costs, and those without risk indicate how cost can be reduced via dedicated technological developments. The latter estimates also indicate the trends that are anticipated when implementation difficulties are not critical, and cost is based solely on such spacecraft burdens as payload weight and prime power.

Summary of the costing methodology is presented in Exhibit 6-5.

- Identify cost drivers and associated risk factors based on a 1997 technology cut-off. Summarize key parameters for all architectures and implementations described in Part II. Designs strive to reduce cost by minimizing required technical developments.

- Apply existing parametric models to RF and optical implementations. Divide into non-recurring design and engineering cost elements, and recurring fabrication, integration, and test cost elements.

- Normalize payload cost estimates to the single-channel, 30-deg separation links (1000 Mbps for RF, 625 Mbps for optical). Independently estimate RF and optical payload costs both with and without relative technological risk between the various implementations.

- Provide high-level, round-figure cost estimates for the single-channel, 30-deg RF and optical links. Estimates based on parametric predictions, in-house and customer-funded development programs, and crosslink community contacts.

Exhibit 6-5: Costing Methodology

6.3.1 RF Payload Cost Estimation

The RF payload cost drivers have been identified and are listed in Exhibit 6-6. Among all cost drivers, space qualification is the largest unknown factor, owing to a small experience base, and is expected to substantially increase the cost of the first flight units. After fabrication, test, and flight of several units, the space qualification costs are expected to decrease significantly. Payload cost uncertainties are, as expected, smaller for RF than for optical systems.

The parametric RF cost model is summarized in Exhibit 6-7, indicating the key drivers for the antenna and repeater subsystems, and the program management costs that include engineering support. Note that the parametric cost model does not include space qualification cost and launch cost. The key input parameters for the model are antenna diameter, transmitter power, and payload prime power. As discussed in the reference [1], this model is for 60 GHz payloads, and must be appropriately modified to account for relative risks among the various RF implementations.

Exhibit 6-8 shows a detailed RF payload (single-channel, 30-degree, 60-GHz) cost example, indicating the major recurring and non-recurring contributors. Despite the many significant digits, the bottom-line figure is only an approximate payload cost.

Technological risk is one of the key drivers of the final payload cost. Exhibit 6-9 summarizes the relative risks associated with the various RF implementations, and lists the factors that determine risk differences among the various systems. The risk factors are normalized to the single-channel, 30-degree, 32-GHz link, and are used to derive multiplicative factors for the repeater-subsystem recurring and non-recurring cost-estimating equations. Of course, the program management costs are also affected, since the repeater subsystem is one of the elements in the management total costs.

Since the parametric model shown in Exhibit 6-7 is for 60-GHz systems, the following procedure was used to derive the necessary multiplicative factors. The relative risk between the 32-GHz and 60-GHz systems, all else being equal, was estimated at 1.33. The appropriate multiplicative factor was therefore obtained by dividing the risk factors in Exhibit 6-8 by 1.33. The results from the top to bottom in the exhibit are: 0.75, 0.90, 1.10, 1.00.

Other implementations that involve combinations of systems not shown in Exhibit 6-9 are: 2 @ 60-GHz channels with risk factor = 1.50, multiplicative factor = 1.20; and 5 @ 60-GHz channels with risk factor = 1.75, multiplicative factor = 1.33.

The normalized RF payload costs <u>including</u> risk is presented in Exhibit 6-10.

Using the same model but with unmodified repeater subsystem equations from the reference, relative payload costs <u>excluding</u> risk are summarized in Exhibit 6-11. This gives a relative cost after each

- High TWTA transmitter power.
- Transmit/receive antenna and gimbal.
- Multiple-channel FDM communications, including low intermodulation distortion and receiver complexity.
- Payload mass and prime power, including reliability requirements.
- Support electronics and microwave components for wideband communications, high efficiency (low loss), and compact payload design.
- Additional terminal support functions, including microprocessors, thermal control, power conditioning, signal conditioning, and TT&C.
- RF ISL implementation risks -- 32 GHz vs 60 GHz.
- Space qualification.
- Program management.
- Launch cost @ about $50 K per pound, including solar cells @ 0.3 to 0.5 lb/W.

Exhibit 6-6: RF ISL Communications Cost Drivers

- Antenna subsystem
  - Recurring cost = $1.60\ (1.71 + 5.33 \times 10^{-6} \times M_{ANT}^{2})$
  - Non-recurring cost = $1.60\ (-1.23 + 0.788 \times M_{ANT}^{0.5})$

  where $M_{ANT} = (14 + 3.3\ D_{ANT}^{2.2})$ kg, D_{ANT} = antenna diameter in meters

- Repeater subsystem (including electrical power conditioner)
  - Recurring cost = $1.28\ (0.012\ M_{REPS}^{1.3})$
  - Non-recurring cost = $1.50\ (0.626\ M_{REPS}^{0.65})$

  where $M_{REPS} = (23 + 0.08\ P_{ISL} + 1.75\ P_{RF}^{0.227}$

  P_{ISL} = payload prime power in W

  P_{RF} = RF transmitter power in W

- Upper bound of program management cost
  - Recurring cost = 0.488 (Antenna + Repeater Recurring costs)
  - Non-recurring cost = 0.494 (Antenna + Repeater Non-recurring costs)

- Summing the above factors gives the Total Program Cost

Exhibit 6-7: Parametric Cost Model for RF ISL Payload

RF COST MODEL	
Antenna Subsystem	
Antenna diameter (m)	1.5
Antenna mass (kg)	22.1
Recurring cost ($M)	2.783
Non-recurring cost ($M)	3.970
Repeater Subsystem	60 GHz
Transmitter power (W)	9.7
Payload prime power (W)	105
Repeater mass (kg)	34.3
Repeater risk factor	1.00
Recurring cost ($M)	1.528
Non-recurring cost ($M)	9.381
RF ISL Payload	
Recurring cost ($M)	4.310
Non-recurring cost ($M)	13.351
Program Management	
Recurring cost ($M)	2.105
Non-recurring cost ($M)	6.594
Total Terminal Cost ($M, 1986 dollars)	26.360
Inflation (percent)	5
Total Terminal Cost ($M, 1990 dollars)	32.041

* Cost estimate is for a single-channel, 1 Gbps/30-deg, 60 GHz link

Exhibit 6-8: RF Payload Costs

Implementation	Relative Risk Elements	Transceiver Risk Factor	Multiplicative Factor
1 @ 1000 Mbps, 32-GHz QPSK	------	1.00	0.75
2 @ 1000 Mbps, 32-GHz QPSK	Two-channel FDM communications, including intermodulation distortion/TWTA back-off considerations and low-noise receiver complexity, High TWTA power	1.20	0.90
5 @ 1000 Mbps, 32-GHz QPSK	Five-channel FDM communications, Link bandwidth-to-carrier frequency ratio near 15-percent, High TWTA power	1.50	1.10
1 @ 1000 Mbps, 60-GHz QPSK	Technical maturity at component and payload levels, including reliability; More-stringent pointing/tracking requirements than at 32 GHz; Reliable low-noise, wide-bandwidth receiver front ends	1.33	1.00

Exhibit 6-9: Normalized Risk Factors of RF Links

Link	32-GHz QPSK	60-GHz QPSK
1 @ 1000 Mbps/30-deg	1.00	1.09
5 @ 1000 Mbps/30-deg	1.78	1.68
1 @ 625 Mbps/50-deg	1.00	1.16
1 @ 1000 Mbps/125-deg	1.22	1.27
2 @ 1000 Mbps/125-deg	1.41	1.62

Exhibit 6-10: Normalized RF Payload Costs Including Risk

Link	32-GHz QPSK	60-GHz QPSK
1 @ 1000 Mbps/30-deg	1.00	0.92
5 @ 1000 Mbps/30-deg	1.36	1.13
1 @ 625 Mbps/50-deg	1.00	0.97
1 @ 1000 Mbps/125-deg	1.22	1.07
2 @ 1000 Mbps/125-deg	1.28	1.19

Exhibit 6-11: Normalized RF Payload Costs Excluding Risk

technology is equally developed and implementation difficulties are removed. Costs are then driven solely by such key spacecraft parameters as payload weight and prime power. Comparison between Exhibit 6-10 and 6-11 indicates that a large amount of the cost penalty associated with multiple-channel operation results from the difficult implementation.

Conclusions from the RF cost modeling are listed Exhibit 6-12. In summary, technological risks drive relative costs. However, careful evaluation of the relative cost factors in the two previous tables indicates that, except for the multiple-channel links, the differences among the various systems are not that extreme. Reliability concerns were only qualitatively included in these estimates when the key link parameters were selected. A quantitative account of the reliability impact on cost demands completion of an in-depth payload reliability assessment. The impact could be large, since redundancy requirements are likely to surface for some of the more-expensive components (e.g., the high-power TWTA transmitter), and this is a stronger concern at 60 GHz than at 32 GHz. The example payload cost estimate (normalized) is closed to the value calculated from the parametric model, and this is evidence of the reasonably high confidence level in the RF cost equations. A stronger experience base would enhance this confidence level and increase the credibility and accuracy of the RF cost-estimating model.

- When including relative transceiver risks, the 32-GHz implementations are cheapest for all but the five-channel, short-range FDM link. High payload prime power drives the 32-GHz cost for the exception.
- When excluding risk the 60-GHz implementations are always cheapest, owing to a more-favorable link budget – All other parameters being equal, the link budget scales as the square of the carrier frequency.
- Multiple-channel operation significantly increases payload cost, particularly as the number of channels grows, owing to associated increases in transmitter/receiver complexities and link bandwidth.
- Reliability concerns will increase payload cost, and the cost differential is expected to be larger at 60 GHz than at 32 GHz because of a less-mature technology. Detailed payload reliability assessments are required before an accurate cost impact can be determined.
- The single-channel, 1000-Mbps, 30-deg, 32-GHz payload cost is estimated at $30 M to $35 m ($1990). The parametric model carries a reasonably high confidence level because of a relatively strong experience base.

Exhibit 6-12: RF Cost Modeling Conclusions

6.3.2 Optical Payload Cost Estimation

Cost drivers for optical payload are listed in Exhibit 6-13. As is the case for RF, the optical model includes all but the space qualification and launch costs. Space qualification is a very large unknown for optical systems, owing to a very small experience base, and is expected to significantly increase the cost of the first few flight units. After fabrication, test, and flight of several units, the space qualification costs are expected to decrease significantly. A key optical cost driver that does not affected RF system is the need for submicroradian fine pointing and tracking to allow the use of narrow transmit beams that conserve limited laser power. Laboratory experiments have successfully demonstrated such precise pointing and tracking for lasercom system, but it must be duplicated in space and maintained over a long-life mission. Other space systems (e.g., Hubble Space Telescope) had also demonstrated the feasibility of extremely fine pointing subsystem.

Exhibit 6-14 shows cost breakdowns for a laser communications terminal. These estimates are based on a laboratory development model that was designed, fabricated, and tested by Ball Aerospace in the late 1980's. As shown, payload costs are determined by six major program activities: analysis, design, fabrication, integration, test, and management. Recurring cost factors such as fabrication, integration, test, and associated management are estimated at about 58% of the program total. Non-recurring cost factors such as analysis, design, preliminary fabrication, and associated management are estimated at about 42% of the program total.

The parametric optical cost model is summarized in Exhibit 6-15 [1], [22], indicating the key drivers for the antenna, repeater, and thermal/structural subsystems, and the program management costs that include engineering support. Note again that the key input parameters are aperture diameter, transmitter power, and payload prime power. As described in the references 4 and 5, this model is for a DD/QPPM, AlGaAs laser system, and must be appropriately modified to account for relative risks among the various optical implementations. The modification procedure is described later. Finally, because of an extremely small (to nonexistent) flight experience base, this model should be viewed as a qualitative trend indicator of the optical payload costs.

Exhibit 6-16 shows a detailed optical cost example, indicating the major recurring and non-recurring contributors. Despite the many significant digits, the bottom-line figure is only an approximate payload cost.

Exhibit 6-17 summarizes the relative risks associated with the various optical implementations, and lists the factors that determine risk differences among the various systems. The factors are normalized to the single-channel, 30-degree, DD/QPPM link, and are used as a multiplicative factor in the repeater subsystem recurring and non-recurring cost estimating equations. As is the case of RF system, the program management costs are also affected, since the repeated subsystem is one of the factors in the management total.

- Gimballed telescope (coarse pointing subsystem) -- strong function of aperture diameter and primary-mirror wavefront quality.
- Fine steering mirror and servo-control electronics -- Precise, made-to-order hardware.
- Laser transmitter -- strong function of power output
- Multiple-channel communications and system bandwidth.
- Payload mass and prime power, including reliability requirements.
- Support electronics and optical components for acquisition, tracking, and communications, high efficiency (low loss), and compact payload design.
- Additional terminal support functions, including microprocessors, thermal control, power conditioning, signal conditioning, and TT&C.
- Optical ISL implementation risks -- AlGaAs vs Nd:YAG, Direct- vs heterodyne- vs homodyne-detection.
- Space qualification -- big unknown for optical systems owing to lack of heritage.
- Program management
- Launch cost @ about $50 K per pound, including solar cells @ 0.3 to 0.5 lb/W.

Exhibit 6-13: Optical ISL Communications Cost Drivers

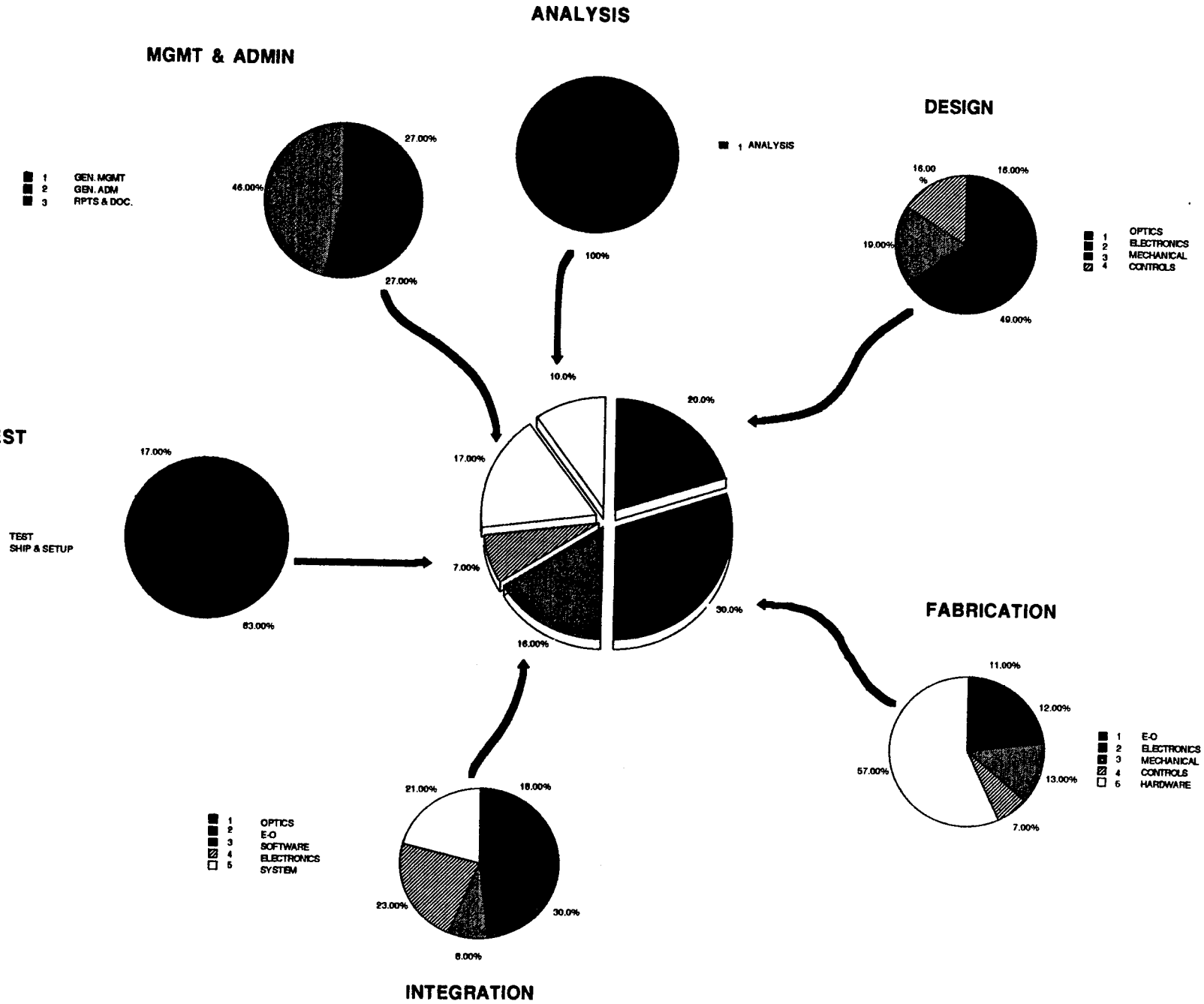

Exhibit 6-14: Laser Communication Terminal Cost

- Antenna subsystem
  - Recurring cost = $0.847 + 13.1\ D^{1.5}$
  - Non-recurring cost = 2 x Antenna Recurring Cost
- Repeater subsystem (including electrical power conditioner)
  - Recurring cost = $0.0132\ M_{REPS}^{1.3}$
  - Non-recurring cost = $0.689\ M_{REPS}^{0.65}$

  where $M_{REPS} = (12.3 + 0.08\ P_{TOT} + 15.3\ P_L^{1.3})$ kg

  P_{TOT} = payload prime power in W

  P_L = laser power in W
- Thermal Control/Structural Subsystem
  - Recurring cost = $0.0187\ M_{T/S}^{0.95}$
  - Non-recurring cost = $0.0034\ M_{T/S}^{1.5}$

  where $M_{T/S} = 0.1\ P_{TOT}$
- Upper bound of program management cost
  - Recurring cost = 0.444 (Antenna + Repeater + Thermal/Structural Recurring costs)
  - Non-recurring cost = 0.449 (Antenna + repeater + Ther./Struc. Non-recurring costs)
- Summing the above factors gives the Total Program Cost

Exhibit 6-15: Parametric Cost Model for Optical ISL Payload

OPTICAL COST MODEL	
Antenna Subsystem	
Antenna diameter (cm)	20.5
Gimballed telescope mass (kg)	14.6
Recurring cost ($M)	2.059
Non-recurring cost ($M)	4.118
Repeater Subsystem	AlGaAs
Laser power (mW)	150
Payload prime power (W)	121
Repeater mass (kg)	23.7
Repeater risk factor	1.00
Recurring cost ($M)	0.809
Non-recurring cost ($M)	5.391
Thermal Control/Structural Subsystem	
Thermal/structural mass (kg)	12.1
Recurring cost ($M)	0.200
Non-recurring cost ($M)	0.143
Optical ISL Payload	
Recurring cost ($M)	3.068
Non-recurring cost ($M)	9.653
Program Management	
Recurring cost ($M)	1.362
Non-recurring cost ($M)	4.334
Total Terminal Cost ($M, 1986 dollars)	18.417
Inflation (percent)	5
Total Terminal Cost ($M, 1990 dollars)	22.386

* Cost estimates is for a single-channel, 625-Mbps/30-deg, DD/QPPM Link

Exhibit 6-16: Optical Payload Costs

Implementation	Relative Risk Elements	Transceiver Risk Factor
1 @ 625 Mbps, DD/QPPM	------	1.00
3 @ 625 Mbps, DD/QPPM	Three-channel WDM co-alignment and stability, 0.5-W per transmit channel	1.25
8 @ 625 Mbps, DD/QPPM	Eight-channel WDM co-alignment and stability, Interchannel interference	1.33
1 @ 625 Mbps, DD/SIM	Wideband subcarrier frequency modulation to enhance receiver sensitivity, 0.25-W transmitter power	1.10
1 @ 625 Mbps, HET/QFSK	Receiver pointing, Receiver frequency acquisition and tracking, Receiver Doppler correction, Transmitter frequency stability, Heterodyne spatial tracking	1.33
1 @ 625 Mbps, HOM/BPSK	Nd:YAG laser complexity, External modulator, 9-photon/symbol homodyne PSK receiver, Receiver pointing, Receiver frequency acquisition and tracking, Receiver Doppler correction, Transmitter frequency stability, Heterodyne spatial tracking	1.60

Exhibit 6-17: Normalized Risk Factors of Optical Links

Relative optical payload costs are summarized in Exhibit 6-18, where the repeater subsystem equations were modified to account for relative risks. Note again the significant cost penalties associated with multiple-channel operation.

Using the unmodified equations from the references, relative cost excluding risks are presented in Exhibit 6-19. This gives a measure of relative cost after each technology is equally developed and implementation difficulties are removed. Cost are then driven solely by such spacecraft parameters as payload weight and prime power.

Comparison between Exhibit 6-18 and 6-19 indicates that, unlike for the RF links, sizable penalties are still experienced for multiple-channel operation. Two reasons for this are the lower data rate per channel in the optical systems that demands more channels to support a given throughput, and the sizable MUX/DEMUX losses associated with the WDM approach.

Conclusions from the optical cost modeling are listed in Exhibit 6-20. These conclusions are similar to those of the RF costing. However, for the optical systems, the normalized payload cost estimate differs significantly from the value calculated from the parametric optical model. This is due to the fairly low confidence level in the optical cost equations that results from lack of heritage. A much stronger experience base is required before accurate cost predictions for optical payloads can be obtained from a parametric model.

Link	DD/QPPM	DD/SIM	HET/QFSK	HOM/BPSK
1 @ 625 Mbps/30-deg	1.00	1.16	1.04	1.23
8 @ 625 Mbps/30-deg	1.94	2.55	2.34	7.02
1 @ 625 Mbps/50-deg	1.13	1.32	1.11	1.26
1 @ 625 Mbps/125-deg	1.32	1.64	1.27	1.32
3 @ 625 Mbps/125-deg	1.95	2.36	1.84	2.48

Exhibit 6-18: Normalized Optical Payload Costs Including Risk

Link	DD/QPPM	DD/SIM	HET/QFSK	HOM/BPSK
1 @ 625 Mbps/30-deg	1.00	1.11	0.88	0.89
8 @ 625 Mbps/30-deg	1.62	2.00	1.57	2.81
1 @ 625 Mbps/50-deg	1.13	1.27	0.94	0.91
1 @ 625 Mbps/125-deg	1.26	1.52	1.10	0.97
3 @ 625 Mbps/125-deg	1.71	2.02	1.38	1.49

Exhibit 6-19: Normalized Optical Payload Costs Excluding Risk

- When including relative transceiver risks, the DD/QPPM implementation is cheapest for 30-deg separation, and loses favor to the HET/QFSK system at 50-deg and 125-deg separations. The high heterodyne receiver sensitivity, efficient diode laser source, and lower risk compared to the homodyne system drives the long-range preference.

- When excluding risk, the HET/QFSK implementations are always cheapest, owing to the combination of a high sensitivity and high transmitter efficiency.

- DD/SIM is inefficient for analog traffic because it uses subcarrier modulation. Heterodyne or homodyne systems offer improved analog communications performance.

- Multiple-channel operation significantly increases payload cost, particularly as the number of channels grows, owing to associated increases in transmitter/receiver complexities and link bandwidth. Nd:YAG lasers are not well-suited to the multiple-channel systems.

- Reliability concerns will increase payload cost, and the cost differential is expected to be significant for optical systems (may be some 25 to 40 percent). Detailed reliability assessments are required before an accurate cost impact can be determined.

- The single-channel, 625-Mbps, 30-deg, DD/QPPM payload cost is estimated at $35 M to $50 M ($1990). The parametric model carriers a very low confidence level because of lacking heritage.

Exhibit 6-20: Optical Cost Modeling Conclusions

6.4 OPTIMIZED ISL LINK PARAMETERS AND ENVELOPE PARAMETERS

With inputs from payload optimization and channelization, the optimized link parameters (required transmit power and antenna aperture size) for all 6 implementations are selected and listed in Exhibit 6-21a, 6-21b, and 6-21c for architectures 1, 2, and 3, respectively.

The payload envelope parameters (aperture size, weight, and power) for all implementations and architectures are given in Exhibit 6-22. The values presented in this exhibit will be mapped into number scores for ISL evaluation in Section 7.

Freq.	# Channels	Data Rate Per Channel	XMTR Implementation	Total Req. Peak XMIT Power (W)	XMTR/RCVR Aperture (m)
32 GHz	5	1 Gbps	1 TWTA/Channel	114	1.75
60 GHz	5	1 Gbps	1 TWTA/Channel	86	1.5
DD-QPPM	8	625 Mbps	1 Diode/Channel	1.2	0.24
DD-SIM	8	625 Mbps	1 Diode/Channel	2	0.29
HET-QFSK	8	625 Mbps	1 Diode/Channel	0.8	0.16
HOM-BPSK	8	625 Mbps	1 Nd:YAG/Channel	8	0.08

Exhibit 6-21a: Optimized Link Parameters for ISL Implementations: Architecture 1

Freq.	# Channels	Data Rate Per Channel	XMTR Implementation	Total Req. Peak XMIT Power (W)	XMTR/RCVR Aperture (m)
32 GHz	1	625 Mbps	1 TWTA/Channel	2.1	1.75
60 GHz	1	625 Mbps	1 TWTA/Channel	1.6	1.5
DD-QPPM	1	625 Mbps	2 Diodes/Channel	0.15	0.26
DD-SIM	1	625 Mbps	2 Diodes/Channel	0.25	0.31
HET-QFSK	1	625 Mbps	2 Diodes/Channel	0.1	0.17
HOM-BPSK	1	625 Mbps	1 Nd:YAG/Channel	1	0.09

Exhibit 6-21b: Optimized Link Parameters for ISL Implementations: Architecture 2

Freq.	# Channels	Data Rate Per Channel	XMTR Implementation	Total Req. Peak XMIT Power (W)	XMTR/RCVR Aperture (m)
32 GHz	2	1 Gbps	1 TWTA/Channel	28	3.25
60 GHz	2	1 Gbps	1 TWTA/Channel	24	3
DD-QPPM	3	625 Mbps	2 Diodes/Channel	1.5	0.31
DD-SIM	3	625 Mbps	2 Diodes/Channel	1.5	0.41
HET-QFSK	3	625 Mbps	2 Diodes/Channel	0.3	0.26
HOM-BPSK	3	625 Mbps	1 Nd:YAG/Channel	3	0.14

Exhibit 6-21c: Optimized Link Parameters for ISL Implementations: Architecture 3

ISL ARCHITECTURE	LINK	32-GHz QPSK			60-GHz QPSK			DD/QPPM			DD/SIM			HET/QFSK			HOM/BPSK		
	Data Rate (Mbps)/ Separation (deg)	Cost ($M)	Payload Weight (LB)	Payload Power (W)	Cost ($M)	Payload Weight (LB)	Payload Power (W)	Cost ($M)	Payload Weight (LB)	Payload Power (W)	Cost ($M)	Payload Weight (LB)	Payload Power (W)	Cost ($M)	Payload Weight (LB)	Payload Power (W)	Cost ($M)	Payload Weight (LB)	Payload Power (W)
1	1000/30 RF 625/30 Optical	32	191	147	35	171	126	22	198	133	25.5	218	146	23	169	140	27	164	153
	Multiple Channels for 5 Gbps	57	407	500	54	366	423	43	818	349	56	900	384	51.5	811	523	154	842	945
2	625/50 RF and Optical	32	182	151	37	165	136	24.4	222	120	29	244	132	24.4	175	136	28	163	171
3	1000/125 RF 625/125 Optical	39	284	258	41	246	239	29	244	145	36	268	160	28	210	151	29	165	154
	Multiple Channels for 1.8 Gbps	45	380	430	52	316	410	43	454	225	52	499	248	40.5	417	289	54.6	366	418

Exhibit 6-22: RF and Optical P/L Envelope Parameters

SECTION 7: EVALUATION OF ISL IMPLEMENTATIONS

As stated in Section 1, the objective of this study is to compare and evaluate the suitability of the six RF and optical implementations for each of the three ISL architectures. A set of evaluation criteria based on system weight/size/power/cost, complexity, and technological risk is established. With inputs from link budget analysis, technology assessment, weight/size/power/cost estimations, and system optimizations, number scores are assigned to each evaluation criteria for all implementations in each architecture. A preferred implementation for each ISL architecture is then selected. The approach to ISL implementation evaluation is depicted in Exhibit 7-1.

In Exhibit 7-2, estimates of antenna/telescope aperture size, payload weight, and payload power for all implementations in each architecture are presented. The system cost, complexity, and technology risk are more qualitative than quantitative and therefore are not listed in the table. As discussed in Section 6, the estimated payload costs are highly uncertain due to the lack of flight experience base and the immaturity of technology (especially in the case of optical systems.) Antenna/telescope aperture size is used as one of the evaluation criteria since it is the driver of the total payload size. The size/weight/power estimates are then ranked according to the following algorithm:

$$\text{Score} = \text{INT}\,[(X_{max} - X_{in}) * (N - 1) / (X_{max} - X_{min}) + 0.5] - 3$$

where X_{max} and X_{min} are the maximum and minimum values of the payload estimate, respectively; X_{in} is the actual payload estimate and N is the number of ranking levels. For example, $X_{max} = 900$ and $X_{min} = 100$ for payload weight evaluation. N is set at a value of 7 since the estimates are mapped into the following seven number scores: -3, -2,-1,0,1,2,3. The INT[x] is an integer function which transforms real numbers into integers.

The resulting scores are presented in Exhibit 7-3, 7-4, and 7-5 for ISL architecture 1, 2, and 3, respectively. From these results, the following observations can be made:

- In general, RF systems perform better than optical systems in all three ISL architectures.
  - The difference is driven mainly by technical maturity.
  - However, 32-GHz multiple-channel operation requires 8 PSK modulation which results in highly complex system.
- For long crosslink with single or few channels, heterodyne QFSK system and DD/QPPM system both look like viable alternative to RF systems.

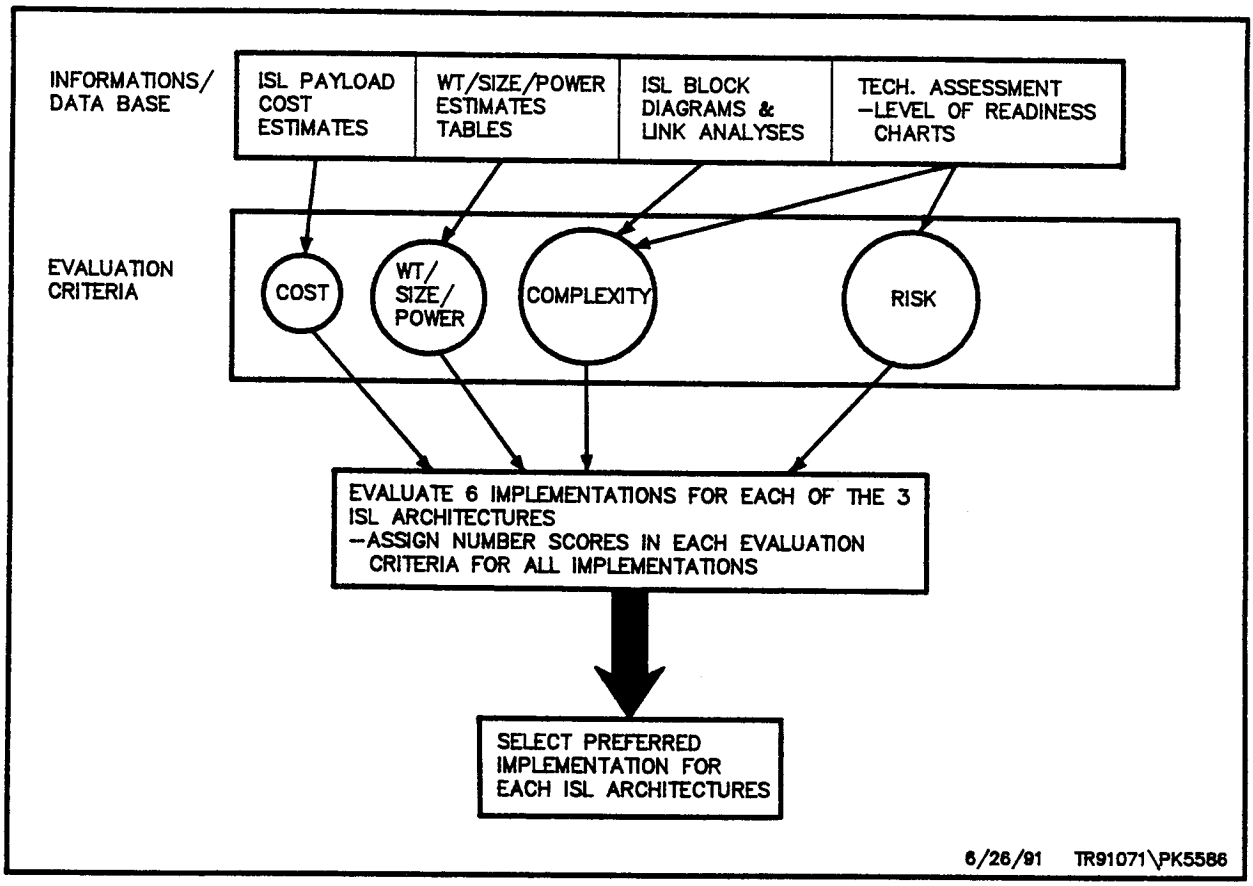

Exhibit 7–1: Approach to ISL Implementations Evaluation

* Envelope Data Rate = 5 Gbps
* Range = 30 Degree

Weighed Performance Index / ISL Implementations		Evaluation Criteria							
		Weight	Size	Power	Cost	Risk	System Complexity	Total Score	Comments
32 GHz	(1 channel)	2	0	2	2	2	3	11	* Relatively mature technology
	(5 channels)	0	0	-1	0	0	-1	-2	* Bandwidth limitation increases multiple-channel system complexity
60 GHz	(1 channel)	3	0	3	1	1	3	11	* Less mature technology base than 32-GHz
	(5 channels)	1	0	1	0	0	1	3	
DD-QPPM	(1 channel)	2	3	3	0	0	1	9	* Ground and flight demo programs exist (GSFC FSDD; SILEX)
	(8 channels)	-2	3	1	-1	-1	-1	-1	
DD-SIM	(1 channel)	2	2	3	-1	-1	-1	4	* No identifiable program
	(8 channels)	-3	2	1	-2	-2	-3	-7	
HET-FSK	(1 channel)	2	3	3	0	0	-1	7	* Ground demonstration program exists (MIT-LL)
	(8 channels)	-2	3	0	-1	-2	-2	-4	
HOM-PSK	(1 channel)	3	3	3	-2	-2	-2	3	* High Technology risk and cost
	(8 channels)	-3	3	-3	-3	-3	-3	-12	* Nd:YAG has very limited tunability

* Weighed Performance Index: -3 = worst, 0=neutral, 3 = Best

Exhibit 7-2: Evaluation of ISL Implementations: Architecture 1

* Envelope Data Rate = 625 Mbps
* Range = 50 Degree

Weighed Performance Index / ISL Implementations	Evaluation Criteria							
	Weight	Size	Power	Cost	Risk	System Complexity	Total Score	Comments
32 GHz (1 channel)	2	-1	3	2	2	3	11	* Relatively mature technology
60 GHz (1 channel)	2	1	2	1	1	3	10	* Less mature technology base than 32-GHz
DD-QPPM (1 channel)	2	3	3	0	0	1	9	* Ground and flight demo programs exist (GSFC FSDD; SILEX)
DD-SIM (1 channel)	2	3	3	-1	-1	0	6	* No identifiable program
HET-FSK (1 channel)	2	3	3	0	0	-1	7	* Ground demonstration program exists (MIT-LL)
HOM-PSK (1 channel)	3	3	2	-2	-1	-1	4	* High Technology risk and cost * Nd:YAG has very limited tunability

* Weighed Performance Index: -3 = worst, 0=neutral, 3 = Best

Exhibit 7-3: Evaluation of ISL Implementations: Architecture 2

* Envelope Data Rate = 1.8 Gbps
* Range = 125 Degree

Weighed Performance Index / ISL Implementations	Evaluation Criteria: Weight	Size	Power	Cost	Risk	System Complexity	Total Score	Comments
32 GHz (1 channel)	2	-3	2	2	2	3	**8**	* Relatively mature technology
(2 channels)	1	-3	2	1	1	2	**4**	
60 GHz (1 channel)	2	-1	2	1	1	3	**8**	* Less mature technology base than
(2 channels)	2	-1	1	0	0	2	**4**	32-GHz
DD-QPPM (1 channel)	2	3	3	0	0	1	**9**	* Ground and flight demo programs
(3 channels)	0	3	2	-1	0	-1	**3**	exist (GSFC FSDD; SILEX)
DD-SIM (1 channel)	2	2	3	-1	-1	0	**5**	* No identifiable program
(3 channels)	0	2	2	-2	-1	-1	**0**	
HET-FSK (1 channel)	2	3	3	0	0	0	**8**	* Ground demonstration program
(3 channels)	1	3	2	-1	-1	-1	**3**	exists (MIT-LL)
HOM-PSK (1 channel)	3	3	3	-2	-2	-2	**3**	* High Technology risk and cost
(3 channels)	1	3	1	-3	-3	-2	**-3**	* Nd:YAG has very limited tunability

* Weighed Performance Index: -3 = worst, 0=neutral, 3 = Best

Exhibit 7-4: Evaluation of ISL Implementations: Architecture 3

- Optical homodyne BPSK system is the least favorable implementation due to high technology risk in its key components (1997 is too early for homodyne).
  - Successful demo of the european testbed program may reduce the risk.
  - Homodyne system potentially can deliver great benefits in a later date.

Since some of the evaluation criterions are rather qualitative, these results should only be viewed as general trend indicators rather than absolute discriminators for selecting a particular implementation for each ISL architecture.

APPENDIX A: LINK BUDGETS AND ASSOCIATED EQUATIONS

LINK BUDGET ITEM	EQUATIONS	REMARKS
(1) XMIT GAIN (G_T)	$G_T = \eta \left(\frac{\pi f D_T}{c}\right)^2$ η = ANTENNA EFFICIENCY f = CARRIER FREQUENCY (Hz) D_T = ANTENNA APERTURE DIAMETER (m) $c = 3 \times 10^8$ m/s	• ASSUME CIRCULAR APERTURE • $\eta = .55$
(2) EFFECTIVE ISOTROPIC RADIATED POWER (EIRP)	EIRP = $P_T G_T$ P_T = CARRIER POWER AT ANTENNA FEED	
(3) XMITTER POINTING LOSS	• TYPICAL LOSS = 0.2–0.5 dB	• ASSUME APERTURE DISTRIBUTION (ILLUMINATION) IS PARABOLIC • HALF–POWER BEAMWIDTH IS $72.7 \left(\frac{c}{fD_T}\right)$ DEGREES
(4) XMITTER LINE LOSS	• TYPICAL VALUE = 1.5 dB	• LOSSES INCLUDE WAVEGUIDE, COUPLER, POLARIZER ---- ETC.
(5) SPACE LOSS	$L_s = \left(\frac{c}{4\pi fr}\right)^2$ r = RANGE BETWEEN THE TWO GEO–GEO PLATFORMS (m)	RANGE IS RELATED TO SATELLITES SPACING ANGLE (θ) BY $r = 59626950 \sqrt{1 - \cos\left(\theta \frac{\pi}{180}\right)}$ 6/26/91 TR91071\PK5585

Exhibit A–1: RF ISL Budget Equations

LINK BUDGET ITEM	EQUATIONS	REMARKS
(6) RECEIVES ANTENNA GAIN	$G_R = \eta \left(\frac{\pi f D_R}{c}\right)^2$ D_R = RCVR ANTENNA APERTURE DIAMETER (m)	• ASSUME CIRCULAR APERTURE • η = .55
(7) SYSTEM NOISE TEMPERATURE	$T = \frac{T_A}{L} + \left(\frac{L-1}{L}\right)T_o + T_e$ T_A = ANTENNA NOISE TEMPERATURE (K) L = LINE LOSS T_o = AMBIENT TEMPERATURE = 290 K T_e = PREAMP NOISE TEMPERATURE (K) = (F−1) T_o WHERE F = NOISE FIGURE	• $T_A \simeq$ 10 K (DARK BACKGROUND) $T_A \simeq$ 5200 K (SUN BACKGROUND) • T_e = 290 K FOR F=3 dB T_e = 360 K FOR F=3.5 dB • L = 1.41 (1.5 dB)
(8) RCVR POINTING LOSS	• SIMILAR TO XMITTER POINTING LOSS	
(9) RCVR LINE LOSS	• SIMILAR TO XMITTER LINE LOSS	
(10) IMPLEMENTATION LOSS	• 1.5–2 dB NOMINAL	
(11) REQUIRED E_b/N_o FOR COMMUNICATION	• MODULATION SCHEME & BER DEPENDENT: – UNCODED QPSK → 10.5 dB – RATE 1/2, K=7 CONVOLUTIONAL CODED DATA, SOFT DECISION → 4.9 dB	• ASSUME BER = 10^{-6}

07/01/91 TR91071\PK2150

Exhibit A–2: RF ISL Link Budget Equations (Cont'd)

LINK BUDGET ITEM	EQUATIONS	REMARKS
(1) XMIT GAIN (G_o)	$G_o = \left(\frac{\pi D_T}{\lambda}\right)^2$ D_T = TRANSMITTER APERTURE DIAMETER λ = OPTICAL SIGNAL WAVELENGTH	• ON–AXIS GAIN OF AN CIRCULAR, UNIFORMLY ILLUMINATED APERTURE WITH PLANAR WAVEFRONT
(2) XMIT OBSCURATION AND TRUNCATION LOSS	$g_T(\alpha,\gamma) = \frac{2}{\alpha}\left[e^{-2\alpha^2} + e^{-2\alpha^2\gamma^2} - 2e^{-\alpha^2(\gamma^2+1)}\right]$ $\gamma = \frac{\text{RADIUS OF SECONDARY MIRROR}}{\text{RADIUS OF PRIMARY MIRROR}} = \frac{b}{a}$ α = SHAPE PARAMETER OF XMIT BEAM WITH GAUSSIAN INTENSITY DISTRIBUTION ACROSS XMIT APERTURE	• ASSUME $\gamma = 0.3$ • ASSUME ZERO WAVEFRONT CURVATURE AT XMIT APERTURE • REFERS TO DEGRADATION OF BORE–SIGHT GAIN (i.e., Θ = OFFPOINTING ANGLE = 0) • $\alpha \simeq 1.12 - 1.3\gamma^2 + 2.12\gamma^4$ MAXIMIZES BORESIGHT GAIN
(3) OPTICS ATTENUATION (REFLECTANCE/ TRANSMITTANCE)	TYPICAL VALUE: 0.4–0.5 dB	• LOSS DUE TO NON–IDEAL TRANSMITTANCE/REFLECTANCE BY THE MIRROR AND LENSES IN XMITTER
(4) WAVEFRONT PHASE ABERRATIONS (α_S)	$\alpha_S = \exp\left[-(2\pi\Phi_{rms})^2\right]$ Φ_{rms} = RATIO OF rms PHASE DISTORTION TO TRANSMITTED WAVELENGTH (1/10 TO 1/20 ARE TYPICAL)	• APPROXIMATION FOR WAVEFRONT OPERATING NEAR THE DIFFRACTION LIMIT

06/26/91 TR91071\PK4724

Exhibit A–3: Optical ISL Link Budget Equations

LINK BUDGET ITEM	EQUATIONS	REMARKS
(5) XMIT OFF–POINTING LOSS	XMIT OFF–POINTING ANGLE DEPENDENT $L_P \simeq 0.3$ dB FOR $\left\{ \frac{\text{rms JITTER}}{\text{BEAMWIDTH}} = \frac{\sigma D_T}{\lambda} = 0.11 \right.$ ASSUMING ZERO POINTING BIAS	• COMPOSITE OFF–POINTING ANGLE IS RICIAN DISTRIBUTED TIME DEPENDENT RANDOM PROCESS
(6) SPACE LOSS	$L_s = \left(\frac{\lambda}{4\pi r}\right)^2$ λ = OPTICAL SIGNAL WAVELENGTH r = RANGE	
(7) RECEIVER GAIN	$G_R = \left(\frac{\pi D_R}{\lambda}\right)^2$ D_R = RECEIVER APERTURE DIAMETER	
(8) RECEIVER OBSCURATION LOSS	$L_{OBS} = 1-\gamma^2$; $\gamma = \frac{b}{d}$	
(9) OPTICS ATTENUATION (REFLECTANCE/TRANSMITTANCE)	TYPICAL VALUE : 0.4–0.5 dB	
(10) NARROWBAND OPTICAL FILTER ATTENUATION (UNIQUE TO DD)	TYPICAL LOSS : 0.46 dB	• 70% – 90% TRANSMITTANCE DEPENDING UPON OPTICAL BW
(11) WAVEFRONT MISMATCH (UNIQUE TO HETERODYNE AND HOMODYNE DETECTIONS)	$\simeq$ 1.6 dB	• MIT–LL LITE PROGRAM

06/26/91 TR91071\PK4723

Exhibit A–4: Optical ISL Link Budget Equations *(Cont'd)*

LINK BUDGET ITEM	EQUATIONS	REMARKS
(12) PHASE NOISE AT BER = 10^{-6} $\Delta_f T_s$ = 0.03, AND $\nu_d T_s$ = 1	$\simeq$ 0.8 dB	Δ_f = IF LINE WIDTH (SUM OF SIGNAL AND LO LASERS LINEWIDTH) ν_d = FSK TONE SPACING T_s = FSK SYMBOL DURATION ASSUME A DOUBLE BALANCE MIXER IS USED (MIT–LL MODEL).
(13) INSERTION LOSS (UNIQUE TO HOMODYNE)	1–2 dB	• DUE TO EXTERNAL MODULATOR 6/26/91 TR91071\PK5584

Exhibit A–5: Optical ILS Link Budget Equations *(Cont'd)*

DETECTION METHOD	PROBABILITY OF BIT ERROR EQUATIONS	REMARKS
RF QPSK (UNCODED)	$P_E = Q\left(\sqrt{\frac{2E_b}{N_o}}\right)$ WHERE $Q(\alpha) = \frac{1}{\sqrt{2\pi}} \int_{\alpha}^{\infty} e^{-\frac{X^2}{2}} dx$	• FIND THE E_b/N_o THAT GIVES A $P_E = 10^{-6}$: UNCODED ⟶ 10.5 dB $r = \frac{1}{2}$, K = 7 SOFT DECISION CONVOLUTIONAL CODED ⟶ 4.9 dB
OPTICAL DIRECT DETECTION BPPM	$P_E = Q\left(\sqrt{\rho}\right)$ WHERE ρ = SNR OF APD-BASED PPM RECEIVER $= \frac{G^2K_s^2}{G^2F\left(K_s + 2K_B + 2\frac{I_bT_s}{e}\right) + 2\frac{I_sT_s}{e} + 2K_{th}^2}$ K_s = SIGNAL PHOTON COUNT K_b = BACKGROUND PHOTON COUNT I_b = GAIN DEPENDENT DARK CURRENT I_s = GAIN INDEPENDENT DARK CURRENT T_s = PPM SLOT DURATION G = MEAN APD GAIN $F = kG + (2 - \frac{1}{G})(1 - k)$ k = EFFECTIVE IONIZATION RATIO K_{th}^2 = THERMAL NOISE = $2K_BT_{eq}T_s/R_Le^2$	• ASSUME APD OUTPUT IS GUASSIAN DISTRIBUTED • PARAMETER NOMINAL VALUES: I_b = 1 pA I_s = 10 nA $G \doteq 200$ $F \doteq 2.8$ k = 0.006 – 0.02 6/26/91 TR91071\PK5583

Exhibit A–6: BER Equations for RF and Optical Signal Detection

DETECTION METHOD	PROBABILITY OF BIT ERROR EQUATIONS	REMARKS
OPTICAL HETERODYNE BFSK	$P_E = \frac{1}{2} e^{-\frac{\beta}{2}}$ where $\beta = \frac{2\eta P_R T_S}{h\nu}$ η = QUANTUM EFFICIENCY OF DETECTOR P_R = RECEIVED OPTICAL POWER T_S = SYMBOL DURATION h = PLANCK'S CONSTANT ν = OPTICAL FREQUENCY	• ASSUME IDEAL DETECTION • NONCOHERENT (ASYNCHRONOUS) ENVELOPE DETECTION • ASSUME LO POWER IS MUCH LARGER THAN SIGNAL AND BACKGROUND POWER
OPTICAL HOMODYNE BPSK	$P_E = Q\left(\sqrt{\frac{4\eta P_R T_S}{h\nu}}\right)$	• ASSUME ZERO PHASE ERROR AND THE RECEIVED OPTICAL SIGNAL IS ENTIRELY USED FOR DATA RECOVERY
OPTICAL SUBCARRIER INTENSITY MODULATION	$(S/N)_{out} = \frac{m^2 e^2 P^2 G^2}{2B_m D}$ where $D = 2eFG^2(\rho P_s + I_D) + 2eI_{DG} + 4kT_{eff}/R_{DL} + \rho^2 P_s^2 m^2 / 2B_m (S/N)_{in}$ F = APD EXCESS NOISE FACTOR B_m = IF SIGNAL BW P_S = RECEIVED SIGNAL POWER ρ = APD RESPONSIVITY m = OPTICAL INTENSITY MODULATION INDEX	• IF SIGNAL QUALITY IS MEASURED IN TERMS OF OUTPUT SNR RATHER THAN P_E

07/17/91 TR91071\PK7897

Exhibit A–7: BER Equations for RF and Optical Signal Detection (Cont'd)

PARAMETERS		
Carrier Frequency (GHz)	32	60
RF Wavelength (m)	0.009375	0.005
Number of channels	5	5
Single Channel Data Rate (Mbps)	1000	1000
Transmitter Power (W)	68	86
Xmit Antenna Diameter (m)	2	1.5
Xmit Antenna Efficiency	0.55	0.5
Xmit Half-Power Beamwidth (degrees)	0.34	0.24
Receive Antenna Diameter (m)	2	1.5
Receive Antenna Efficiency	0.55	0.5
Receive Half-Power Beamwidth (degrees)	0.34	0.24
ISL Arc Angle (degree)	30	30
Range (km)	21824.98	21824.98
Receive Antenna Noise Temperature (K)	10.00	10.00
Pre-amplifier Noise Figure (dB)	3.00	3.50
Pre-amplifier Noise Temperature (K)	288.63	359.23
Line Loss	1.41	1.41
System Noise Temperature (K)	380.40	451.00
Data Quality (BER)	1.00E-06	1.00E-06
Modulation Type	Uncoded QPSK	Uncoded QPSK

Transmit Antenna Gain (dB)	53.93	56.48
Transmitter EIRP (dBW)	72.25	75.82
Transmitter Pointing Loss (dB)	0.50	0.50
Multiplexing/Combining Loss (dB)	2.50	2.50
Transmit Line Loss (dB)	1.50	1.50
Path Loss (dB)	209.32	214.78
Receive Antenna Gain (dB)	53.93	56.48
Receiver G/T (dB/K)	28.13	29.93
Feed Loss (dB)	0.60	0.60
Receive Line Loss (dB)	1.50	1.50
Boltzmann's Constant (dB-Hz/K)	-228.60	-228.60
C/N0 (dB-Hz/K)	113.05	112.97
Total Data Rate (dB-bps)	96.99	96.99
Eb/N0 into demodulator (dB)	16.07	15.98
Implementation Loss (dB)	2.50	2.50
Power Required for Communication (dB)	10.50	10.50
Link Margin (dB)	3.07	2.98

Exhibit A-8a: RF Link Budget for Architecture 1

PARAMETERS		
Carrier Frequency (GHz)	32	60
RF Wavelength (m)	0.009375	0.005
Single Channel Data Rate (Mbps)	625	625
Transmitter Power (W)	21.4	16
Xmit Antenna Diameter (m)	1.75	1.5
Xmit Antenna Efficiency	0.55	0.5
Xmit Half-Power Beamwidth (degrees)	0.39	0.24
Receive Antenna Diameter (m)	1.75	1.5
Receive Antenna Efficiency	0.55	0.5
Receive Half-Power Beamwidth (degrees)	0.39	0.24
ISL Arc Angle (degree)	50	50
Range (km)	35637.39	35637.39
Receive Antenna Noise Temperature (K)	10.00	10.00
Pre-amplifier Noise Figure (dB)	3.00	3.50
Pre-amplifier Noise Temperature (K)	288.63	359.23
Line Loss	1.41	1.41
System Noise Temperature (K)	380.40	451.00
Data Quality (BER)	1.00E-06	1.00E-06
Modulation Type	Uncoded QPSK	Uncoded QPSK

Transmit Antenna Gain (dB)	52.77	56.48
Transmitter EIRP (dBW)	66.07	68.52
Transmitter Pointing Loss (dB)	0.50	0.50
Transmit Line Loss (dB)	1.50	1.50
Path Loss (dB)	213.58	219.04
Receive Antenna Gain (dB)	52.77	56.48
Receiver G/T (dB/K)	26.97	29.93
Feed Loss (dB)	0.60	0.60
Receive Line Loss (dB)	1.50	1.50
Boltzmann's Constant (dB-Hz/K)	-228.60	-228.60
C/N0 (dB-Hz/K)	103.96	103.91
Data Rate (dB-bps)	87.96	87.96
Eb/N0 into demodulator (dB)	16.00	15.95
Implementation Loss (dB)	2.50	2.50
Power Required for Communication (dB)	10.50	10.50
Link Margin (dB)	3.00	2.95

Exhibit A-8b: RF Link Budget for Architecture 2

PARAMETERS		
Carrier Frequency (GHz)	32	60
RF Wavelength (m)	0.009375	0.005
Number of channels	2	2
Single Channel Data Rate (Mbps)	1000	1000
Total Transmitter Power (W)	28.5	16
Xmit Antenna Diameter (m)	3.25	3
Xmit Antenna Efficiency	0.55	0.5
Xmit Half-Power Beamwidth (degrees)	0.21	0.12
Receive Antenna Diameter (m)	3.25	3
Receive Antenna Efficiency	0.55	0.5
Receive Half-Power Beamwidth (degrees)	0.21	0.12
ISL Arc Angle (degree)	125	125
Range (km)	74797.40	74797.40
Receive Antenna Noise Temperature (K)	10.00	10.00
Pre-amplifier Noise Figure (dB)	3.00	3.50
Pre-amplifier Noise Temperature (K)	288.63	359.23
Line Loss	1.41	1.41
System Noise Temperature (K)	380.40	451.00
Data Quality (BER)	1.00E-06	1.00E-06
Modulation Type	Uncoded QPSK	Uncoded QPSK

Transmit Antenna Gain (dB)	58.14	62.50
Transmitter EIRP (dBW)	72.69	74.54
Transmitter Pointing Loss (dB)	0.50	0.50
Multiplexing/Combining Loss (dB)	0.50	0.50
Transmit Line Loss (dB)	1.50	1.50
Path Loss (dB)	220.02	225.48
Receive Antenna Gain (dB)	58.14	62.50
Receiver G/T (dB/K)	32.34	35.95
Feed Loss (dB)	0.60	0.60
Receive Line Loss (dB)	1.50	1.50
Boltzmann's Constant (dB-Hz/K)	-228.60	-228.60
C/N0 (dB-Hz/K)	109.01	109.01
Total Data Rate (dB-bps)	93.01	93.01
Eb/N0 into demodulator (dB)	16.00	16.00
Implementation Loss (dB)	2.50	2.50
Power Required for Communication (dB)	10.50	10.50
Link Margin (dB)	3.00	3.00

Exhibit A-8c: RF Link Budget for Architecture 3

PARAMETERS				
Modulation	DD QPPM	DD SIM	HET QFSK	HOM BPSK
Number of Channel	8	8	8	8
Total Channel Data Rate (Mbps)	5000	5000	5000	5000
Average Laser Output Power (mW)	300	2000	800	8000
Laser Peak Power (mW)	1200		800	8000
Receiver Sensitivity (photons/bit, n = 0.8)	50	3.5X QPPM w/ FM	18	9
Transmitter Aperture (cm)	24.4	28.6	15.5	8.2
Receiver Aperture (cm)	24.4	28.6	15.5	8.2
MPPM Order	4	NA	NA	NA
Data Quality (BER)	1.00E-06	* 23 dB	1.00E-06	1.00E-06
Optical Wavelength (nm)	850	850	850	1064
ISL Arc Angle (degree)	30	30	30	30
Range (km)	21824.98	21824.98	21824.98	21824.98

Laser Module Output Peak Power (dBW)	0.79	3.01	-0.97	9.03
Extinction Ratio Degradation	-0.50	0.00	0.00	0.00
DL Transmitter Gain	119.10	120.48	115.16	107.68
Optics Attenuation (reflectance/transmittance)	-1.50	-1.50	-1.50	-1.50
Obscuration/Truncation Loss (gamma = 0.3)	-2.23	-2.23	-2.23	-2.23
Multiplexing/combining loss	-3.00	-3.00	-3.00	-3.00
Phase Aberration (wavelength/10 rms Surface Deviation)	-1.71	-1.71	-1.71	-1.71
Pointing Loss (rms jitter = .5 urad)	-0.80	-0.80	-0.80	-0.80
External Modulator Loss (Homodyne PSK)	0.00	0.00	0.00	-1.00
Range Loss (wavelength / 4piR)^2	-290.17	-290.17	-290.17	-288.22
Receiver Gain	119.10	120.48	115.16	107.68
Receiver Obscuration Loss (gamma = 0.3)	-0.40	-0.40	-0.40	-0.40
Het/Hom Implementation loss	0.00	0.00	-1.80	-1.80
Receiver Filter Loss	-1.00	-1.00	-0.50	-0.50
Receiver Optics Attenuation (reflectance/transmittance)	-1.00	-1.00	-1.00	-1.00
Received Power at APD	-63.32	-57.84	-73.76	-77.77
Power Required for Communication	-66.31	-60.87	-76.77	-80.75
Link Margin (dB)	2.99	3.03	3.01	2.98

* Data Quality of DD/SIM is in terms of SNR (dB)

Exhibit A-9a: Optical Link Budget for ISL Architecture 1

PARAMETERS				
Modulation	DD QPPM	DD SIM	HET QFSK	HOM BPSK
Number of Channel	1	1	1	1
Total Channel Data Rate (Mbps)	625	625	625	625
Average Laser Output Power (mW)	37.5	125	100	1000
Laser Peak Power (mW)	150	250	100	1000
Receiver Sensitivity (photons/bit)	50	3.5X QPPM w/ FM	18	9
Transmitter Aperture (cm)	27	31.7	17.1	8.7
Receiver Aperture (cm)	27	31.7	17.1	8.7
MPPM Order	4	NA	NA	NA
Data Quality (BER)	1.00E-06	* 23 dB	1.00E-06	1.00E-06
Optical Wavelength (nm)	850	850	850	1064
ISL Arc Angle (degree)	50	50	50	50
Range (km)	35637.39	35637.39	35637.39	35637.39
Laser Module Output Peak Power (dBW)	-8.24	-6.02	-10.00	0.00
Extinction Ratio Degradation	-0.50	0.00	0.00	0.00
DL Transmitter Gain	119.98	121.38	116.01	108.19
Optics Attenuation (reflectance/transmittance)	-1.50	-1.50	-1.50	-1.50
Obscuration/Truncation Loss (gamma = 0.3)	-2.23	-2.23	-2.23	-2.23
Multiplexing/combining loss	-0.50	-0.50	-0.50	0.00
Phase Aberration (wavelength/10 rms Surface Deviation)	-1.71	-1.71	-1.71	-1.71
Pointing Loss (rms jitter = .5 urad)	-0.80	-0.80	-0.80	-0.80
External Modulator Loss (Homodyne PSK)				-1.50
Range Loss (wavelength / 4piR)^2	-294.43	-294.43	-294.43	-292.48
Receiver Gain	119.98	121.38	116.01	108.19
Receiver Obscuration Loss (gamma = 0.3)	-0.40	-0.40	-0.40	-0.40
Phase Mismatch	0.00	0.00	-1.80	-1.00
Receiver Filter Loss	-1.00	-1.00	-0.50	-0.50
Receiver Optics Attenuation (reflectance/transmittance)	-1.00	-1.00	-1.00	-1.00
Received Power at APD	-72.35	-66.84	-82.84	-86.73
Power Required for Communication	-75.34	-69.84	-85.80	-89.79
Link Margin (dB)	2.99	3.00	2.96	3.05

* Data Quality of DD/SIM is in terms of SNR (dB)

Exhibit A-9b: Optical Link Budget for ISL Architecture 2

PARAMETERS				
Modulation	DD QPPM	DD SIM	HET QFSK	HOM BPSK
Number of Channel	3	3	3	3
Total Channel Data Rate (Mbps)	1875	1875	1875	1875
Average Laser Output Power (mW)	375	750	300	3000
Laser Peak Power (mW)	1500	1500	300	3000
Receiver Sensitivity (photons/bit)	50	3.5X QPPM w/ FM	18	9
Transmitter Aperture (cm)	30.7	41	26.3	13.3
Receiver Aperture (cm)	30.7	41	26.3	13.3
MPPM Order	4	NA	NA	NA
Data Quality (BER)	1.00E-06	* 23 dB	1.00E-06	1.00E-06
Optical Wavelength (nm)	850	850	850	1064
ISL Arc Angle (degree)	125	125	125	125
Range (km)	74797.40	74797.40	74797.40	74797.40
Laser Module Output Peak Power (dBW)	1.76	1.76	-5.23	4.77
Extinction Ratio Degradation	-0.50	0.00	0.00	0.00
DL Transmitter Gain	121.10	123.61	119.75	111.88
Optics Attenuation (reflectance/transmittance)	-1.50	-1.50	-1.50	-1.50
Obscuration/Truncation Loss (gamma = 0.3)	-2.23	-2.23	-2.23	-2.23
Multiplexing/combining loss	-1.50	-1.50	-1.50	-1.00
Phase Aberration (wavelength/10 rms Surface Deviation)	-1.71	-1.71	-1.71	-1.71
Pointing Loss (rms jitter = .5 urad)	-0.80	-0.80	-0.80	-0.80
External Modulator Loss (Homodyne PSK)				-1.50
Range Loss (wavelength / 4piR)^2	-300.87	-300.87	-300.87	-298.92
Receiver Gain	121.10	123.61	119.75	111.88
Receiver Obscuration Loss (gamma = 0.3)	-0.40	-0.40	-0.40	-0.40
Phase Mismatch	0.00	0.00	-1.80	-1.00
Receiver Filter Loss	-1.00	-1.00	-0.50	-0.50
Receiver Optics Attenuation (reflectance/transmittance)	-1.00	-1.00	-1.00	-1.00
Received Power at APD	-67.56	-62.03	-78.03	-82.03
Power Required for Communication	-70.57	-65.07	-81.03	-85.01
Link Margin (dB)	3.01	3.04	2.99	2.99

* Receiver Sensitivity of DD/SIM is in terms of SNR (dB)

Exhibit A-9c: Optical Link Budget for ISL Architecture 3

APPENDIX B: PERFORMANCE PARAMETERS & W/S/P TABLES

* ISL ARC ANGLE = 30 DEGREE * 1 Gbps QPSK CHANNELS (UP TO 5 CHANNELS)								
COMPONENT MODULES	PERFORMANCE PARAMETER		WEIGHT (LB)		SIZE (in X in X in)		INPUT POWER (W)	
	32 GHz	60 GHz	32 GHz	60 GHz	32 GHz	60 GHz	32 GHz	60 GHz
ANTENNA	* 1.75 m DIAMETER * GAIN = 60 dB * EFFICIENCY = 0.55	* 1.5 m DIAMETER * GAIN = 62 dB * EFFICIENCY = 0.55	45	41	1.75 m	1.5 m	NA	NA
GIMBAL & GIMBAL DRIVE ELECTRONICS	* SLEW RATE < 1 mrad/sec	* SLEW RATE < 1 mrad/sec	17	12	23X16X16	23X16X16	35	30
AUTOTRACK PROCESSOR	* BW = 1 Hz * TRACKS UP TO 1/20 BEAMWIDTH	* BW = 1 Hz * TRACKS UP TO 1/20 BEAMWIDTH	5	5	6X6X6	6X6X6	10	10
DIPLEXER	* ISOLATION > 20 dB	* ISOLATION > 20 dB	0.5	0.5	6X6X3	6X6X3	NA	NA
HPA * TWTA (Helix)	* OUTPUT POWER = 13 W (1 CHANNEL) = 114 W (5 CHANNELS) * EFFICIENCY = 40%	* OUTPUT POWER = 9.7 W (1 CHANNEL) = 86 W (5 CHANNELS) * EFFICIENCY = 40%	12 66	9 49.5	12X3X3	10X3X3	33 380	24 287
BPF	* PASSBAND = 700 MHz	* PASSBAND = 700 MHz	2	2	2X1X1	2X1X1	NA	NA
LNA	* GAIN > 20 dB * NOISE FIGURE < 3.5 dB * BANDWIDTH = 2 GHz	* GAIN > 20 dB * NOISE FIGURE < 4 dB * BANDWIDTH = 2 GHz	2	2	6X4X2	6X4X2	0.7	0.7
UPCONVERTER	* LOW LOSS	* LOW LOSS	3	3	1X1X3	1X1X2	5	5
DOWN-CONVERTER	* LOW LOSS	* LOW LOSS	4	4	1.8X2X3	1.8X2X2.7	4.8	4.8
MODULATOR	* BANDWIDTH > 2 GHz	* BANDWIDTH > 2 GHz	4	4	3X4X1	3X4X1	7	7
DEMODULATOR	* IMPLEMENTATION LOSS < 1 dB	* IMPLEMENTATION LOSS < 1 dB	4	4	3X6X2	3X6X2	6	6
ELECT. POW COND.	* 80% EFFICIENCY	* 80% EFFICIENCY	13	12			20	17
PRIME POWER WEIGHT	* AT .33 LB/W	* AT .33 LB/W	44 236	38 193	NA	NA	NA	NA
	TOTAL (1 CHANNEL)	10% margin included	171	150			133	115
	TOTAL (5 CHANNELS)	10% margin included	529	452			716	586

Exhibit B-1: WT/Size/Power Estimation: RF ISL Architecture #1

* ISL ARC ANGLE = 50 DEGREE * 625 Mbps QPSK CHANNEL								
COMPONENT MODULES	PERFORMANCE PARAMETER		WEIGHT (LB)		SIZE (in X in X in)		INPUT POWER (W)	
	32 GHz	60 GHz	32 GHz	60 GHz	32 GHz	60 GHz	32 GHz	60 GHz
ANTENNA	* 2 m DIAMETER * GAIN = 60 dB * EFFICIENCY = 0.55	* 1.5 m DIAMETER * GAIN = 62 dB * EFFICIENCY = 0.55	45	41	1.75 m	1.5 m	NA	NA
GIMBAL & GIMBAL DRIVE ELECTRONICS	* SLEW RATE < 1 mrad/sec	* SLEW RATE < 1 mrad/sec	17	12	23X16X16	21X13X13	35	30
AUTOTRACK PROCESSOR	* BW = 1 Hz * TRACKS UP TO 1/20 BEAMWIDTH	* BW = 1 Hz * TRACKS UP TO 1/20 BEAMWIDTH	5	5	6X6X6	6X6X6	10	10
DIPLEXER	* ISOLATION > 20 dB	* ISOLATION > 20 dB	0.5	0.5	6X6X3	6X6X3	NA	NA
HPA * TWTA (Helix)	* OUTPUT POWER = 21 W (1 CHANNEL) * EFFICIENCY = 45%	* OUTPUT POWER = 16 W (1 CHANNEL) * EFFICIENCY = 40%	14	14	14X3X3	14X3X3	47	40
BPF	* PASSBAND = 400 MHz	* PASSBAND = 400 MHz	2	2	2X1X1	2X1X1	NA	NA
LNA	* GAIN > 20 dB * NOISE FIGURE < 3.5 dB * BANDWIDTH = 2 GHz	* GAIN > 20 dB * NOISE FIGURE < 4 dB * BANDWIDTH = 2 GHz	2	2	6X4X2	6X4X2	0.7	0.7
UPCONVERTER	* LOW LOSS	* LOW LOSS	3	3	1X1X3	1X1X2	5	5
DOWN-CONVERTER	* LOW LOSS	* LOW LOSS	4	4	1.8X2X3	1.8X2X2.7	4.8	4.8
MODULATOR	* BANDWIDTH > 1.3 GHz	* BANDWIDTH > 1.3 GHz	4	4	3X4X1	3X4X1	7	7
DEMODULATOR	* IMPLEMENTATION LOSS < 1 dB	* IMPLEMENTATION LOSS < 1 dB	4	4	3X6X2	3X6X2	6	6
ELECT. POW COND.	* 80% EFFICIENCY	* 80% EFFICIENCY	15	14			23	21
PRIME POWER WEIGHT	* AT .33 LB/W	* AT .33 LB/W	50	45	NA	NA	NA	NA
	TOTAL (1 CHANNEL)	10% margin included	182	165			151	136

Exhibit B-2: WT/Size/Power Estimation: RF ISL Architecture #2

* ISL ARC ANGLE = 125 DEGREE * 1 Gbps QPSK CHANNELS (UP TO 2 CHANNELS)								
COMPONENT MODULES	PERFORMANCE PARAMETER		WEIGHT (LB)		SIZE (in X in X in)		INPUT POWER (W)	
	32 GHz	60 GHz	32 GHz	60 GHz	32 GHz	60 GHz	32 GHz	60 GHz
ANTENNA	* 3.25 m DIAMETER * GAIN = 60 dB * EFFICIENCY = 0.55	* 3 m DIAMETER * GAIN = 62 dB * EFFICIENCY = 0.55	86	77	3.25 m	3 m	NA	NA
GIMBAL & GIMBAL DRIVE ELECTRONICS	* SLEW RATE < 1 mrad/sec	* SLEW RATE < 1 mrad/sec	66	55	23X16X16	23X16X16	86	75
AUTOTRACK PROCESSOR	* BW = 1 Hz * TRACKS UP TO 1/20 BEAMWIDTH	* BW = 1 Hz * TRACKS UP TO 1/20 BEAMWIDTH	5	5	6X6X6	6X6X6	10	10
DIPLEXER	* ISOLATION > 20 dB	* ISOLATION > 20 dB	0.5	0.5	6X6X3	6X6X3	NA	NA
HPA * TWTA (Helix)	* OUTPUT POWER = 14 W (1 CHANNEL) = 28 W (2 CHANNELS) * EFFICIENCY = 40%	* OUTPUT POWER = 12 W (1 CHANNEL) = 24 W (2 CHANNELS) * EFFICIENCY = 40%	16 32	14 28	18X4X4	16X4X4	35 70	30 60
BPF	* PASSBAND = 700 MHz	* PASSBAND = 700 MHz	2	2	2X1X1	2X1X1	NA	NA
LNA	* GAIN > 20 dB * NOISE FIGURE < 3.5 dB * BANDWIDTH = 2 GHz	* GAIN > 20 dB * NOISE FIGURE < 4 dB * BANDWIDTH = 2 GHz	2	2	6X4X2	6X4X2	0.7	0.7
UPCONVERTER	* LOW LOSS	* LOW LOSS	3	3	1X1X3	1X1X2	5	5
DOWN-CONVERTER	* LOW LOSS	* LOW LOSS	4	4	1.8X2X3	1.8X2X2.7	4.8	4.8
MODULATOR	* BANDWIDTH > 2 GHz	* BANDWIDTH > 2 GHz	4	4	3X4X1	3X4X1	7	7
DEMODULATOR	* IMPLEMENTATION LOSS < 1 dB	* IMPLEMENTATION LOSS < 1 dB	4	4	3X6X2	3X6X2	6	6
ELECT. POW COND.	* 80% EFFICIENCY	* 80% EFFICIENCY	20	18			31	28
PRIME POWER WEIGHT	* AT .33 LB/W	* AT .33 LB/W	67 93	60 83	NA	NA	NA	NA
	TOTAL (1 CHANNEL)	10% margin included	308	274			203	182
	TOTAL (2 CHANNELS)	10% margin included	363	326			281	253

Exhibit B-3: WT/Size/Power Estimation: RF ISL Architecture #3

* ISL ARC ANGLE = 30 DEGREE * 625 Mbps CHANNELS (UP TO 8 CHANNELS)			
COMPONENT MODULES	PERFORMANCE PARAMETERS		
	DD QPPM / DD SIM	HETERODYNE QFSK	HOMODYNE BPSK
TELESCOPE	*24 cm DIAMETER (QPPM) *29 cm DIAMETER (SIM)	* 15 cm DIAMETER	* 7.8 cm DIAMETER
	* RMS WAVEFRONT DISTORTION < WAVELENGTH/10		
COARSE POINTING OPTICS & GIMBAL & DRIVE ELECTRONICS	* SLEW RATE < 1 mrad/sec		
OPTICAL BENCH	* ALIGNMENT < 1 microradian * RMS WAVEFRONT DISTORTION = WAVELENGTH/30		
ACQ/TRK SUBSYSTEM	* ACQUISITION TIME < 1 min * SUB-MICRORADIAN TRACKING * BANDWIDTH = 5000 Hz		
LASER XMITTER	* POWER = 1.2 W (TOTAL) * POWER (SIM) = 2 W (TOTAL) * EFFICIENCY > 50%	* POWER = 800 mW (TOTAL) * EFFICIENCY > 50% * LASER LINEWIDTH < 5 MHz	* POWER = 8 W (TOTAL) * DIODE-PUMP EFFICIENCY > 50% * END-TO-END EFFICIENCY > 20%
LASER DRIVER/ MODULATOR AND EQUALIZER (HET ONLY)	* HIGH CURRENT CAPABILITY (> 100 mA) * BW > 1 GHz	* HIGH CURRENT CAPABILITY (> 100 mA) * BW > 1 GHz	NA
EXTERNAL MODULATOR	NA	NA	* BW > 500 MHz * INSERTION LOSS < 1 dB * INPUT POWER << 100 W
MIXER & LOCAL OSCILLATOR & FREQ./ PHASE TRACKER	NA	* LASER LINEWIDTH < 5 MHz * IMP. LOSS < 2 dB	* LASER LINEWIDTH < 10 KHz * IMP. LOSS < 2 dB
PHOTODETECTOR & AMPLIFIER	* QE > 80% * APD EXCESS NOISE FACTOR < 4.5 dB * ADP GAIN < 300 * BW > 1 GHz	* QE > 80% * BW > 1 GHz	* QE > 50% * BW > 1 GHz
DEMODULATOR	* IMPLEMENTATION LOSS < 1 dB	* IMPLEMENTATION LOSS < 1 dB	* IMPLEMENTATION LOSS < 1 dB

Exhibit B-4a: Performance Parameters: Optical ISL Architecture #1

* ISL ARC ANGLE = 30 DEGREE * 625 Mbps CHANNELS (UP TO 8 CHANNELS)									
COMPONENT	WEIGHT (LB)			SIZE (in X in X in)			POWER (W)		
MODULES	DD	HET	HOM	DD	HET	HOM	DD	HET	HOM
TELESCOPE (1 channel) (8 channels)	33 41	16 20	7 8	21 cm (DIA.) 24 cm (DIA.)	13 cm (DIA.) 15 cm (DIA.)	6.8 cm (DIA.) 8 cm (DIA.)	NA NA	NA NA	NA NA
COARSE POINTING OPTICS & GIMBAL & DRIVE ELECTRONICS	22	9	9	8X8X6	7X7X6	7X7X6	43	41	41
OPTICAL BENCH	20	20	20	24X24X8	24X24X8	24X24X8	15	15	15
ACQ/TRK SUBSYSTEM	17	17	17	12X6X2	12X6X2	12X6X2	20	20	20
LASER XMITTER	5	6.1	10	10X6X4	7.4X6.3X6.8	9.3X3.5X3	5	5	10
LASER DRIVER/ MODULATOR AND EQUALIZER (HET ONLY)	6	6	3	4X2X4	3X1X1	4X4X2	1.3	5	10
EXTERNAL MODULATOR	NA	NA	14	NA	NA	5X13X12	NA	NA	25
MIXER & LOCAL OSCILLATOR & FREQ./ PHASE TRACKER	NA	10	10	NA	3X4X2	3X4X2	NA	10	15
PHOTODETECTOR & AMPLIFIER	7	8	8	1.25X2X3	2X3X5	3X3X5	7	10	10
DEMODULATOR	16	15	15	18X16X6	16X15X4	16X15X4	10	10	10
ELECTR. POWER COND.	10	10	10				20	21	23
PRIME POWER WEIGHT AT .33 LB/W	44	46	50	NA	NA	NA	NA	NA	NA
TOTAL (SINGLE CHANNEL)	198	169	164				133	140	153
TOTAL (8 CHANNELS)	818	811	842				349	523	945

* Total weight/power estimates include 10% margin

Exhibit B-4b: WT/Size/Power Estimations: Optical ISL Architecture #1

* ISL ARC ANGLE = 50 DEGREE * 625 Mbps CHANNEL			
COMPONENT MODULES	PERFORMANCE PARAMETERS		
	DD QPPM / DD SIM	HETERODYNE QFSK	HOMODYNE BPSK
TELESCOPE	*27 cm DIAMETER (QPPM) *32 cm DIAMETER (SIM)	* 17 cm DIAMETER	* 8.7 cm DIAMETER
	* RMS WAVEFRONT DISTORTION < WAVELENGTH/10		
COARSE POINTING OPTICS & GIMBAL & DRIVE ELECTRONICS	* SLEW RATE < 1 mrad/sec		
OPTICAL BENCH	* ALIGNMENT < 1 microradian * RMS WAVEFRONT DISTORTION = WAVELENGTH/30		
ACQ/TRK SUBSYSTEM	* ACQUISITION TIME < 1 min * SUB-MICRORADIAN TRACKING * BANDWIDTH = 5000 Hz		
LASER XMITTER (2 DIODES/CHANNEL FOR SIM)	* POWER = 150 mW (TOTAL) * POWER (SIM) = 250 mW (TOTAL) * EFFICIENCY > 50%	* POWER = 100 mW (TOTAL) * EFFICIENCY > 50% * LASER LINEWIDTH < 5 MHz	* POWER = 1 W * DIODE-PUMP EFFICIENCY > 50% * END-TO-END EFFICIENCY > 20%
LASER DRIVER/ MODULATOR AND EQUALIZER (HET ONLY)	* HIGH CURRENT CAPABILITY (> 100 mA) * BW > 1 GHz	* HIGH CURRENT CAPABILITY (> 100 mA) * BW > 1 GHz	NA
EXTERNAL MODULATOR	NA	NA	* BW > 500 MHz * INSERTION LOSS < 1 dB * INPUT POWER << 100 W
MIXER & LOCAL OSCILLATOR & FREQ./ PHASE TRACKER	NA	* LASER LINEWIDTH < 5 MHz * IMP. LOSS < 2 dB	* LASER LINEWIDTH < 10 KHz * IMP. LOSS < 2 dB
PHOTODETECTOR & AMPLIFIER	* QE > 80% * APD EXCESS NOISE FACTOR < 4.5 dB * ADP GAIN < 300 * BW > 1 GHz	* QE > 80% * BW > 1 GHz	* QE > 50% * BW > 1 GHz
DEMODULATOR	* IMPLEMENTATION LOSS < 1 dB	* IMPLEMENTATION LOSS < 1 dB	* IMPLEMENTATION LOSS < 1 dB

Exhibit B-5a: Performance Parameters: Optical ISL Architecture #2

* ISL ARC ANGLE = 50 DEGREE * 625 Mbps CHANNEL									
COMPONENT	WEIGHT (LB)			SIZE (in X in X in)			POWER (W)		
MODULES	DD	HET	HOM	DD	HET	HOM	DD	HET	HOM
TELESCOPE	50	24	9	27 cm (DIA.)	17 cm (DIA.)	8.7 cm (DIA.)	NA	NA	NA
COARSE POINTING OPTICS & GIMBAL & DRIVE ELECTRONICS	41	18	9	8X8X6	8X8X6	8X8X6	44	42	41
OPTICAL BENCH	20	20	20	24X24X8	24X24X8	24X24X8	15	15	15
ACQ/TRK SUBSYSTEM	17	17	17	12X6X2	12X6X2	12X6X2	20	20	20
LASER XMITTER (2 DIODES/CHANNEL)	5	6.1	10	10X6X4	7.4X6.3X6.8	9.3X3.5X3	12	12	10
LASER DRIVER/ MODULATOR AND EQUALIZER (HET ONLY)	6	6	3	4X2X4	3X1X1	4X4X2	1.3	5	10
EXTERNAL MODULATOR	NA	NA	14	NA	NA	5X13X12	NA	NA	25
MIXER & LOCAL OSCILLATOR & FREQ./ PHASE TRACKER	NA	10	10	NA	3X4X2	3X4X2	NA	10	15
PHOTODETECTOR & AMPLIFIER	7	8	8	1.25X2X3	2X3X5	3X3X5	7	10	10
DEMODULATOR	16	15	15	18X16X6	16X15X4	16X15X4	10	10	10
ELECTR. POWER COND.	10	10	10				22	23	23
PRIME POWER WEIGHT AT .33 LB/W	40	45	57	NA	NA	NA	NA	NA	NA
TOTAL (SINGLE CHANNEL)	222	175	163				120	136	171

* Total weight/power estimates include 10% margin

Exhibit B-5b: WT/Size/Power Estimations: Optical ISL Architecture #2

* ISL ARC ANGLE = 125 DEGREE * 625 Mbps CHANNELS (UP TO 3 CHANNELS)			
COMPONENT MODULES	PERFORMANCE PARAMETERS		
	DD QPPM / DD SIM	HETERODYNE QFSK	HOMODYNE BPSK
TELESCOPE	*31 cm DIAMETER (QPPM) *41 cm DIAMETER (SIM)	* 26 cm DIAMETER	* 13 cm DIAMETER
	* RMS WAVEFRONT DISTORTION < WAVELENGTH/10		
COARSE POINTING OPTICS & GIMBAL & DRIVE ELECTRONICS	* SLEW RATE < 1 mrad/sec		
OPTICAL BENCH	* ALIGNMENT < 1 microradian * RMS WAVEFRONT DISTORTION = WAVELENGTH/30		
ACQ/TRK SUBSYSTEM	* ACQUISITION TIME < 1 min * SUB-MICRORADIAN TRACKING * BANDWIDTH = 5000 Hz		
LASER XMITTER (2 DIODES/CHANNEL FOR QPPM and SIM)	* POWER = 1.5 W (TOTAL) * POWER (SIM) = 1.5 W (TOTAL) * EFFICIENCY > 50%	* POWER = 300 mW (TOTAL) * EFFICIENCY > 50% * LASER LINEWIDTH < 5 MHz	* POWER = 3 W (TOTAL) * DIODE-PUMP EFFICIENCY > 50% * END-TO-END EFFICIENCY > 20%
LASER DRIVER/ MODULATOR AND EQUALIZER (HET ONLY)	* HIGH CURRENT CAPABILITY (> 100 mA) * BW > 1 GHz	* HIGH CURRENT CAPABILITY (> 100 mA) * BW > 1 GHz	NA
EXTERNAL MODULATOR	NA	NA	* BW > 500 MHz * INSERTION LOSS < 1 dB * INPUT POWER << 100 W
MIXER & LOCAL OSCILLATOR & FREQ./ PHASE TRACKER	NA	* LASER LINEWIDTH < 5 MHz * IMP. LOSS < 2 dB	* LASER LINEWIDTH < 10 KHz * IMP. LOSS < 2 dB
PHOTODETECTOR & AMPLIFIER	* QE > 80% * APD EXCESS NOISE FACTOR < 4.5 dB * ADP GAIN < 300 * BW > 1 GHz	* QE > 80% * BW > 1 GHz	* QE > 50% * BW > 1 GHz
DEMODULATOR	* IMPLEMENTATION LOSS < 1 dB	* IMPLEMENTATION LOSS < 1 dB	* IMPLEMENTATION LOSS < 1 dB

Exhibit B-6a: Performance parameters: Optical ISL Architecture #3

* ISL ARC ANGLE = 125 DEGREE * 625 Mbps CHANNELS (UP TO 3 CHANNELS)									
COMPONENT	WEIGHT (LB)			SIZE (in X in X in)			POWER (W)		
MODULES	DD	HET	HOM	DD	HET	HOM	DD	HET	HOM
TELESCOPE (1 channel)	53	36	16	28 cm (DIA.)	22 cm (DIA.)	13 cm (DIA.)	NA	NA	NA
(3 channels)	63	47	18	31 cm (DIA.)	26 cm (DIA.)	14 cm (DIA.)	NA	NA	NA
COARSE POINTING OPTICS & GIMBAL & DRIVE ELECTRONICS	45	33	10	8X8X6	8X8X6	8X8X6	44	43	41
OPTICAL BENCH	20	20	20	24X24X8	24X24X8	24X24X8	15	15	15
ACQ/TRK SUBSYSTEM	17	17	17	12X6X2	12X6X2	12X6X2	20	20	20
LASER XMITTER (2 DIODES/CHAN. FOR DD)	10	6.1	10	10X6X4	7.4X6.3X6.8	9.3X3.5X3	12	12	10
LASER DRIVER/ MODULATOR AND EQUALIZER (HET ONLY)	6	6	3	4X2X4	3X1X1	4X4X2	1.3	5	10
EXTERNAL MODULATOR	NA	NA	14	NA	NA	5X13X12	NA	NA	25
MIXER & LOCAL OSCILLATOR & FREQ./ PHASE TRACKER	NA	10	10	NA	3X4X2	3X4X2	NA	10	15
PHOTODETECTOR & AMPLIFIER	7	8	8	1.25X2X3	2X3X5	3X3X5	7	10	10
DEMODULATOR	16	15	15	18X16X6	16X15X4	16X15X4	10	10	10
ELECTR. POWER COND.	10	10	10				22	23	23
PRIME POWER WEIGHT AT .33 LB/W	48	50	51	NA	NA	NA	NA	NA	NA
TOTAL (SINGLE CHANNEL)	244	210	165				145	151	154
TOTAL (3 CHANNELS)	454	417	366				225	289	418

* Total weight/power estimates include 10% margin

Exhibit B-6b: WT/Size/Power Estimations: Optical ISL Architecture #3

REFERENCES

[1] Young S. Lee, "Intersatellite Link (ISL) Application to Commercial Communications Satellites," Final Report, NASA Lewis Research Center, Contract No. NAS3-24884, Jan., 1987.

[2] G.R. Welti and Y.S. Lee, "Study of Intersatellite Links," Task 6 Final Report of Planning Assistance for the 30/20 GHz Program. Contract No. NAS3-22905, Nov., 1981.

[3] Stanford Telecom, "System Engineering Support to the Optical Communication FSDD," Technical Briefing, NASA GSFC, 30 June 1989.

[4] S. Karp and R. Gagliardi, "The Design of Pulse Position Modulated Optical Communication Systems," IEEE Trans. Commun. Technology, Vol. COM-17, No. 6, pp. 670-676, Dec. 1969.

[5] C.C. Chen and C.S. Gardner, "Comparison of Direct and Heterodyne Detection Optical Intersatellite Communication Links, "Univ. of Ill. EOSL Tech. Report UIUL-ENG-87-2548, Mar. 1987.

[6] W.K. Pratt, Laser Communication Systems. New York: Wiley, 1969.

[7] V.W.S. Chen, "Space Coherent Optical Communication System - An Introduction, "Journal of Lightwave Technology, Vol. Lt-5, No. 4, April 1987.

[8] U.A. Johann and H. Sontag, "Free-Space Laser Communications Test-bed Based on Coherent Diode-pumped Nd:YAG Laser Technology," SPIE Proceedings, SPIE Vol. 1218, Free-Space Laser Communication Technologies II (1990), pp. 412-418.

[9] J.W. Hansen, "US TWTs from 1 to 100/GHz," Microwave Journal, 1989 State-of-the-art reference.

[10] Y.C. Stich and H.J. Kuno, "Solid-State Sources from 1 to 100 GHz," Microwave Journal, 1989 State-of-the-art reference.

[11] Ford Aerospace, "60 GHz Intersatellite Communication Link Definition Study," Baseline Document, Sept. 1986.

[12] Vanguard Research, Inc., Titan Systems, Inc. and Stanford Telecom, Inc., "C2/SOIF Technology Roadmap," Vol. 1, March 1989.

[13] T.J. Kane et. al., "Single-frequency Diode-pumped Lasers for Free-Space Communications," SPIE Proceedings, SPIE Vol. 1218, Free-Space Laser Communication Technologies II (1990), pp. 239-249.

[14] INRAD Specifications for Lithium Niobate Phase Modulators, Models 632-040 and 632-090, Short Form Catalog, 1991.

[15] G. Keiser, Optical Fiber Communications New York: McGraw-Hill, 1983.

[16] Stanford Telecom, "FSDD Spatial Acquisition Processing/Implementation Alternatives," Technical Briefing, NASA GSFC, 15 Sept. 1989.

[17] L.L. Jeromin and V.W.S. Chen, "M-ary FSK Performance for Coherent Optical Communication Systems using Semiconductor Lasers," IEEE Trans. Commun., Vol. Com-34, No. 4, pp. 375-381, April 1986.

[18] W.C. Lindsey and M.K. Simon, Telecommunications Systems Engineering, Prentice-Hall, Inc., Englewood Cliffs, N.J. 1973.

[19] A. Viterbi, Principles of Coherent Communication, McGraw-Hill, Inc., New York, N.Y., 1966.

[20] R.E. Ziemen and R.L. Peterson, Digital Communications and Spread Spectrum Systems, Macmillan Publishing Co., New York, N.Y., 1985.

[21] R.G. Marshalek and D.K. Paul, "Mass, Prime Power, and Volume Estimates for Reliable Optical Intersatellite Link Payloads," SPIE Proceedings, SPIE Vol. 1218, Free-Space Laser Communication Technologies II (1990), pp. 40-50.

[22] Y.S. Lee, A.E. Atia, and D.S. Ponchak, "Intersatellite Link Application to Commercial Communications Satellites," COMSAT Technical Review, Vol. 18, No. 2 Fall 1988, pp. 147-189.